

國立交通大學

機械工程學系

碩士論文

晶片快速取放機構之設計

Design of a High Speed Mechanism for Chip's Pick and Place



研究生：張志榮

指導教授：蔡忠杓 教授

中華民國九十四年六月

晶片快速取放機構之設計

Design of a High Speed Mechanism for Chip's Pick and Place

研究生：張志榮

Student : Chee-Yong Teo

指導教授：蔡忠杓

Advisor : Dr. Chung-Biau Tsay

國立交通大學
機械工程學系
碩士論文

A Thesis
Submitted to Department of Mechanical Engineering
College of Engineering

National Chiao Tung University

in Partial Fulfillment of the Requirements

for the Degree of

Master

in

Mechanical Engineering

June 2005

Hsinchu, Taiwan, Republic of China

中華民國九十四年六月

國立交通大學

博碩士論文全文電子檔著作權授權書

(提供授權人裝訂於紙本論文書名頁之次頁用)

本授權書所授權之論文為授權人在國立交通大學工學院機械工程學系
設計製造組 93學年度第二學期取得碩士學位之論文。

論文題目：晶片快速取收機構之設計

指導教授：蔡忠杓 教授

同意 不同意

本人茲將本著作，以非專屬、無償授權國立交通大學與台灣聯合大學系統圖書館：基於推動讀者間「資源共享、互惠合作」之理念，與回饋社會與學術研究之目的，國立交通大學及台灣聯合大學系統圖書館得不限地域、時間與次數，以紙本、光碟或數位化等各種方法收錄、重製與利用；於著作權法合理使用範圍內，讀者得進行線上檢索、閱覽、下載或列印。

論文全文上載網路公開之範圍及時間：

本校及台灣聯合大學系統區域網路	■ 中華民國 94 年 06 月 21 日公開
校外網際網路	■ 中華民國 94 年 06 月 21 日公開

授權人：張志榮

親筆簽名： 張志榮

中華民國 94 年 6 月 21 日

國立交通大學

博碩士論文全文電子檔著作權授權書

(提供授權人裝訂於紙本論文書名頁之次頁用)

本授權書所授權之論文為授權人在國立交通大學工學院機械工程學系
設計製造組 93學年度第二學期取得碩士學位之論文。

論文題目：晶片快速取收機構之設計

指導教授：蔡忠杓 教授

■ 同意

本人茲將本著作，以非專屬、無償授權國立交通大學，基於推動讀者間「資源共享、互惠合作」之理念，與回饋社會與學術研究之目的，國立交通大學圖書館得以紙本收錄、重製與利用；於著作權法合理使用範圍內，讀者得進行閱覽或列印。

本論文為本人向經濟部智慧局申請專利(未申請者本條款請不予理會)的附件之一，申請文號為：_____，請將論文延至_____年_____月_____日再公開。



授權人：張志榮

親筆簽名：_____

中華民國 94 年 6 月 21 日

國家圖書館博碩士論文電子檔案上網授權書

ID:GT009214513

本授權書所授權之論文為授權人在國立交通大學 工學院 機械工程學系 設計製造組 93 學年度第 二 學期取得碩士學位之論文。

論文題目：晶片快速取收機構之設計

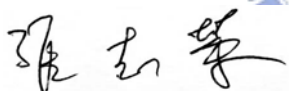
指導教授：蔡忠杓 教授

茲同意將授權人擁有著作權之上列論文全文（含摘要），非專屬、無償授權國家圖書館，不限地域、時間與次數，以微縮、光碟或其他各種數位化方式將上列論文重製，並得將數位化之上列論文及論文電子檔以上載網路方式，提供讀者基於個人非營利性質之線上檢索、閱覽、下載或列印。

※ 讀者基於非營利性質之線上檢索、閱覽、下載或列印上列論文，應依著作權法相關規定辦理。

授 權 人：張志榮

親筆簽名：





民國 94 年 6 月 21 日

1. 本授權書請以黑筆撰寫，並列印二份，其中一份影印裝訂於附錄三之二(博碩士紙本論文著作權授權書)之次頁；另一份於辦理離校時繳交給系所助理，由圖書館彙總寄交國家圖書館。

國立交通大學

論文口試委員會審定書

本校 機械工程 學系碩士班 張志榮 君

所提論文(中文) 晶片快速取放機構之設計

(英文) Design of a High Speed Mechanism for Chip's Pick and Place

合於碩士資格水準、業經本委員會評審認可。

口試委員：

孫可維

吳隆庸

馮展華

指導教授：

蔡忠杓

系主任：

傅武雄

教授

中華民國 94 年 6 月 9 日

晶片快速取放機構之設計

研究生：張志榮

指導教授：蔡忠杓 博士

國立交通大學機械工程學系碩士班

摘要

在半導體製程設備當中，速度是非常重要的考量因素；如何在最短的時間內，生產出最多的產品，一直是所追求的目標。而在半導體後段製程當中，晶片往往需要不斷地傳輸運送；因此晶片的取放是相當關鍵的技術，而晶片快速取放機構也因此扮演著重要的角色。

一般而言，能完成取放動作的機構有很多種，且各有優缺點。除了半導體製設備以外，在其他機械設備當中，也常常利用到取放機構。因此，依照不同要求所做出的設計，其所達成的效果及影響也有所不同。

曲柄搖桿機構在兩個肘節點位置時，曲柄與耦桿皆位在同一直線上；因此對於整體機構所造成之震動較小。將此特性加以利用至取放機構當中，其所造成的震動影響相對減小，精度較易掌控，也因此可減輕設計者的考量因素及負擔。

本論文中，利用機械設計、機動學及材料力學之理論為基礎；同時訂定出設計環境之限制條件；再應用曲柄搖桿機構，設計出晶片快速取放機構。另外利用一組已有的曲柄搖桿晶片快速取放機構作為比較基準，與本論文之設計成果做一比較。在本設計中，利用電腦軟體 ADAMS 作為輔助工具，分析取放機構在整體運動過程中之動態特性，以更快地達成設計目標；同時也利用電腦軟體 Nastran，作為有限元素之分析工具，分析所設計的桿件是否符合強度要求。

Design of a High Speed Mechanism for Chip's Pick and Place

Student : Chee-Yong Teo

Advisor : Dr. Chung-Biau Tsay

Department of Mechanical Engineering

National Chiao Tung University

Abstract

High speed is an important issue in the semiconductor processing equipment. In usual, the chip need to be transferred frequently in the semiconductor back-end processing; therefore the pick and place mechanism plays an important role in the semiconductor processing equipment.

Beside the semiconductor processing equipment, pick and place mechanism is also used in many other areas. Many kinds of mechanism can achieve the purpose of pick and place, but due to the different characteristics, the design result and effects are different.

Crank rocker mechanism has two toggle points, where the crank and coupler are along the same line, small vibration is occurred in the said two toggle points. By using crank rocker as a pick and place mechanism, the vibration can be reduced and precision can be induced; which causes the designer's work much more simple.

In this thesis, the principles of machine design, mechanisms, and mechanics of material are used. The design constraints are carried out, and the crank rocker is used to design a chip's pick and place mechanism. A chip's pick and place mechanism designed by ITRI is also shown in order to compare with the present design. Computer software ADAMS and Nastran are used to assist the design procedures. ADAMS is used to analyze the dynamic performance of mechanism, which can also help to optimize the present design. Nastran is used as a tool to

check the stiffness of each bar and show the finite element result of the chip's pick and place mechanism in the present design.



誌謝

本論文能夠順利完成，首先必須感謝指導教授 蔡忠杓博士；感謝老師您對於學生的指導及幫助，雖然老師非常忙碌，但仍非常用心的給於學生最大的信心與自由，讓學生能夠有更大的空間發揮。而老師在待人處事及做事方面的態度，更是值得學生銘記在心，也受用無窮。

另外也必須感謝曾錦煥 教授對於學生的指點，在學生需要幫助時，總是能給學生提供建議和指引，讓學生在研究上能夠更順利。另外也必需感謝曾老師在學生生活上的幫助，讓學生能夠減輕生活上的壓力。

同時也感謝工研院機械所光電與半導體製程設備部門之各位同仁，尤其是劉俊賢經理、黃國興 先生、徐嘉彬 先生、洪嘉宏 先生、林宏毅 先生等。在我需要協助或是遇到問題時，總是能夠適時地伸出援手，不厭其煩地向我解釋同時提供需多寶貴的實務經驗；讓我能夠更具體的解決問題。

而實驗室的伙伴們：曾瑞堂學長、陳冠宇學長、游明達同學、趙立基同學、黃俊瑜學弟以及蘇政豪學弟，有你們的陪伴、協助以及一起玩樂，我讓在實驗室這兩年能有很多的歡樂。

感謝父母對於我的栽培與養育，給我充分的自由與信任；讓我在唸書及研究過程中，少了許多生活上的煩惱，無須顧慮太多東西。而家人的支持，也是我促使我更加努力的動力來源。

最後，也必需感謝我的女朋友—林秀真 小姐，這些年來的陪伴；謝謝你這些年一直以來的鼓勵及支持，在我心情低落時，能給我適時的關懷，讓我能更快的恢復信心。而我們一起所走過的日子，也將會是我生命當中美好回憶的一部份。

最後，感謝所有在我生命過程中曾給於我幫助的所有人。

Contents

摘要	i
Abstract.....	ii
誌謝	iv
Contents	v
List of Diagram.....	vii
List of Tables	ix
Nomenclature.....	x
Chapter 1 Introduction.....	1
1.1 Foreword.....	1
1.2 Review of Literature.....	2
1.3 Organization	6
Chapter 2 Fundamental Principles.....	7
2.1 Mechanical Design	7
2.1.1 Stress.....	7
2.1.2 Safety Factor.....	7
2.2 Principles of Mechanisms.....	8
2.2.1 Position Analysis	8
2.2.2 Velocity Analysis.....	9
2.2.3 Acceleration Analysis.....	11
2.2.4 Forces and Torques	12
2.3 Optimum Design	15
Chapter 3 Design Constraints.....	17
3.1 Introduction to Pick and Place Action	17
3.2 Dimension Limitation.....	19
3.3 Components	20
3.3.1 Driving Source.....	20
3.3.2 Bearing	22
3.3.3 Pivot Pin	23
3.3.4 Voice Coil Motor	23
3.4 Material and Safety Factor	24
Chapter 4 Present Design	26
4.1 Foreword.....	26
4.2 The Chip's Pick and Place Mechanism Design by ITRI	26
4.3 Design Procedure and Dimensional Synthesis	38
4.4 Structure Design of Bars.....	40
4.5 Sensitivity of Design Variables.....	46

4.6 Result of the Present Design.....	49
4.7 Results of the Optimal Pick and Place Mechanism for Case 6	58
Chapter 5 Conclusions and Future Work.....	68
5.1 Conclusions	68
5.2 Future Works	69
Reference.....	70



List of Diagram

Fig.1.1 Semiconductor mounting apparatus with a chip gripper traveling back and forth (US 6,185,815 [2]).....	2
Fig.1.2 Linear guide with an air bearing having provision for heating a support element of the linear guide to maintain fluid gap (US 6,571,461 [3])	3
Fig.1.3 High speed pick and place apparatus (US6758113 [4])	3
Fig.1.4 Device for fast taking out and putting in (US 6,505,528 [7])	4
Fig.1.5 Industrial use robot with horizontal multiple articulated arms with means to minimize or eliminate interference among driving portions (US 5,151,007 [8]).....	5
Fig.2.1 Position vector loop for a four-bar linkage	9
Fig.2.2 Position vector loop for a four-bar linkage showing velocity vectors for an input angular velocity ω_2	10
Fig.2.3 Position vector loop for a four-bar linkage showing acceleration vectors	11
Fig.2.4 Dynamic force analysis of a four-bar linkage	13
Fig.2.5 Free body diagrams of a four-bar linkage	13
Fig.3.1 Some symbols used in the present design of a four-bar linkage	17
Fig.3.2 Picking position (first toggle point)	18
Fig.3.3 Placing position (second toggle point)	18
Fig.3.4 Requirement of distance for pick and place, and the maximum length of bonding arm	19
Fig.3.5 The input mode of the input mode of AC servo motor in the present design	21
Fig.3.6 Schematic view of bearing used in the present design.....	22
Fig.3.7 Pivot pin used in the present design.....	23
Fig.3.8 A schematic figure of voice coil motor	24
Fig.4.1 Chip's pick and place mechanism designed by ITRI	27
Fig.4.2 Angular velocity and angular acceleration of crank of the chip's pick and place mechanism designed by ITRI.....	29
Fig.4.3 Torque driven by motor of the chip's pick and place mechanism designed by ITRI...	30
Fig.4.4 Shaking force of the chip's pick and place mechanism designed by ITRI	31
Fig.4.5 Shaking torque of the chip's pick and place mechanism designed by ITRI	32
Fig.4.6 Angular ($\theta_2, \theta_3, \theta_4, \gamma$) variations of the chip's pick and place mechanism designed by ITRI	33
Fig.4.7 Maximum stress of the chip's pick and place mechanism designed by ITRI	35
Fig.4.8 Stress distribution on the crank of the chip's pick and place mechanism designed by ITRI at 0.024 seconds.....	36
Fig.4.9 Stress distribution on the coupler of the chip's pick and place mechanism designed by ITRI at 0.024 seconds.....	36

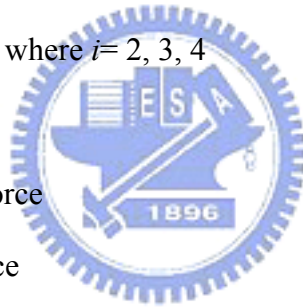
Fig.4.10 Stress distribution on the bonding arm of the chip's pick and place mechanism designed by ITRI at 0.024 seconds	37
Fig.4.11 Procedures of the proposed design.....	38
Fig.4.12 Procedure of dimensional synthesis.....	39
Fig.4.13 Schematic view of the present design- crank.....	41
Fig.4.14 Schematic view of the present design- coupler.....	42
Fig.4.15 Schematic view of the present design- bonding arm.....	43
Fig.4.16 Procedures of building mass-reduced holes on the I-beam of crank, coupler, and rocker.....	45
Fig.4.17 Procedures of building mass-reduced holes on the channel of picking arm.....	45
Fig.4.18 Initial chip's pick and place mechanism in the present design	47
Fig.4.19 Sensitivity of max. torque driven by motor vs. design variables (l_1, l_4, θ_4)	48
Fig.4.20 Sensitivity of crank rotation angle vs. design variables (l_1, l_4, θ_4)	48
Fig.4.21 Sensitivity of max. torque driven by motor vs. VCM's mass	49
Fig.4.22 Variations on design variables, cost function and constraint in case 1	52
Fig.4.23 Variations on design variables, cost function and constraint in case 2	53
Fig.4.24 Variations on design variables, cost function and constraint in case 3	54
Fig.4.25 Variations on design variables, cost function and constraint in case 4	55
Fig.4.26 Variations on design variables, cost function and constraint in case 5	56
Fig.4.27 Variations on design variables, cost function and constraint in case 6	57
Fig.4.28 The optimal chip's pick and place mechanism in the present design (Case 6).....	59
Fig.4.29 Angular velocity and angular acceleration of crank for the optimal chip's pick and place mechanism in the present design (Case 6).....	60
Fig.4.30 Torque driven by motor of the optimal chip's pick and place mechanism in the present design (Case 6)	61
Fig.4.31 Shaking force and shaking torque for the optimal chip's pick and place mechanism in the present design (Case 6).....	62
Fig.4.32 Angular ($\theta_2, \theta_3, \theta_4, \gamma$) variations of the optimal chip's pick and place mechanism in the present design (Case 6).....	63
Fig.4.33 Maximum stress of the optimal chip's pick and place mechanism in the present design (Case 6).....	65
Fig.4.34 Stress distributions for the crank of the optimal chip's pick and place mechanism in the present design (Case 6) at 0.022 seconds.....	66
Fig.4.35 Stress distributions for the coupler of the optimal chip's pick and place mechanism in the present design (Case 6) at 0.022 seconds.....	66
Fig.4.36 Stress distributions for the bonding arm of the optimal chip's pick and place mechanism in the present design - bonding arm (Case 6) at 0.022 seconds.....	67

List of Tables

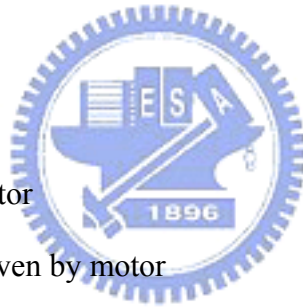
Table 2.1 Recommended safety factor for ductile materials based on yield strength [15].....	8
Table 3.1 Major setting of AC servo motor used in the present design.....	20
Table 3.2 Major specification of the input mode of AC servo motor.....	21
Table 3.3 Major specification of two types of bearing used in the present design.....	22
Table 3.4 Properties of Al 7075-T6 [24].....	24
Table 3.5 Selection of the safety factor	25
Table 4.1 Data of the pick and place mechanism designed by ITRI	26
Table 4.2 ADAMS simulation results of the pick and place mechanism designed by ITRI	28
Table 4.3 FEA settings of the pick and place mechanism designed by ITRI	34
Table 4.4 FEA simulation results of the pick and place mechanism designed by ITRI	34
Table 4.5 Parameters which vary in some specified values	44
Table 4.6 Main parameters for the bars for the initial design of this study	46
Table 4.7 Values of the principle design variables used to check the sensitivity	47
Table 4.8 Parameters changed in the present design (all units are in mm).....	50
Table 4.9 FEA setting in the present design	51
Table 4.10 Summary results for the cases in the present design	58
Table 4.11 Simulation results of the optimal chip's pick and place mechanism in the present design (Case 6) by applying computer software ADAMS.....	59
Table 4.12 FEA results of the optimal pick and place mechanism in the present design (Case 6)	64

Nomenclature

D_{rci}	Distance between two mass-reduced hole center of bar i ; where $i= 2$ (crank), 3(coupler), 4(rocker)
D_{rcPA}	Distance between two mass-reduced hole center of picking arm
D_{ri}	Diameter of mass-reduced hole of bar i ; where $i= 2, 3, 4$
D_{riPA}	Diameter of picking arm's i^{th} mass-reduced hole; where $i= 1^{st}, 2^{nd}, \dots, 8^{th}$
D_{rPA}	Presumed diameter of picking arm's mass-reduced hole
E	Young's modulus
e_{cPA}	Length between the edge of channel and pivot pin, or VCM part of picking arm
e_{il}	Length between the edge of I-beam and motor beam hole, pivot pin hole, or bearing hole of bar i ; where $i= 2, 3, 4$
F_s	Shaking force
F_{sm}	Maximum shaking force
F_{sn}	Norm of shaking force
G_{ri}	Presumed gap between two mass-reduced holes of bar i ; where $i= 2, 3, 4$
G_{rPA}	Presumed gap between two mass-reduced holes of picking arm
G_{ii}	True gap between two mass-reduced holes of bar i ; where $i= 2, 3, 4$
h_{cPA}	Height of the channel of picking arm
h_i	Height of bar i , where $i= 2, 3, 4$
h_{il}	Height of the I-beam of bar i ; where $i= 2, 3, 4$
h_{PV}	Height of VCM part at the end of picking arm
J_{12}	Joint of base and crank
J_{14}	Joint of base and rocker
J_{32}	Joint of crank and coupler



J_{34}	Joint of coupler and rocker
l_{cPA}	Length of the channel of picking arm
l_i	Length of bar i , where $i= 1$ (base), 2 (crank), 3 (coupler), 4 (rocker), $4'$ (picking arm), $4''$ (bonding arm)
l_{iI}	Length of the I-beam of bar i ; where $i= 2, 3, 4$
l_{PV}	Length of VCM part at the end of picking arm
N_{ri}	Number of mass-reduced hole of bar i ; where $i= 2, 3, 4$
N_{rPA}	Number of mass-reduced hole of picking arm
s_{cPA}	Length between the side of channel and the side of picking arm
S_f	Safety factor
s_{iI}	Length between the side of I-beam and the side of bar i ; where $i= 2, 3, 4$
S_u	Ultimate stress
S_y	Yielding stress
T_m	Torque driven by motor
T_{mm}	Maximum torque driven by motor
T_{mn}	Norm of torque driven by motor
T_s	Shaking torque
T_{sm}	Maximum shaking torque
T_{sn}	Norm of shaking torque
VCM	Voice coil motor
w_i	Width of bar i , where $i= 2, 3, 4$
w_{PV}	Width of VCM part at the end of picking arm
α_i	Angular acceleration of bar i , where $i= 2, 3, 4$
α_m	Angular acceleration of motor
γ	Transmission angle, angle between coupler and rocker



γ_f	Final transmission angle
γ_i	Initial transmission angle
θ_{2r}	crank rotation angle in the pick and place motion
θ_i	Angle between bar i and x-axis, where $i= 2, 3, 4$
θ_{if}	Final angle between bar i and x-axis at the second toggle point, where $i= 2, 3, 4$
θ_{ii}	Initial angle between bar i and x-axis at the first toggle point, where $i= 2, 3, 4$
ν	Poisson ratio
ρ	Density
ω_i	Angular velocity of bar i , where $i= 2, 3, 4$
ω_{mf}	Final angular velocity of motor
ω_{mi}	Initial angular velocity of motor



Chapter 1 Introduction

1.1 Foreword

A high speed pick and place apparatus is being widely used in many areas, especially in semiconductor equipments; such as die sorter, die bonder, wire bonder, flip chip and etc.. High speed and accuracy are the most important issues in the process of pick and place, as they would affect the quality and quantity of production. The unit of showing the speed of a semiconductor processing machine is “cycle time”, which represents the time need to complete a full cycle; or sometimes also using the “uph” (unit per hour) to express the unit of dies or chips to be finished in an hour. Usually, a die or chip is picked up from a location, then transfer to and place down on the other specified location. From the above requirement, a pick and place apparatus need to have the functions of sudden stop and high speed transferring. In the process of pick or place, the mechanism needs to stop for a short time, while in the process of high speed transfer, the mechanism need to be fastly moved.

There are many ways can reach the requirement of high speed pick and place, for example by using linkages, gears, ball screws and many others. In general, the distance between the points to be picked and placed is fixed as it would be much easier for design and control. In usual, the process of pick and place is completed by two or more mechanisms; one mechanism controls the motion of pick and place, and the other controls the position of the wafer.

The four-bar linkage is a simple mechanism which is being widely used in many areas as it has many advantages. Four-bar linkage can achieve many special functions by a properly design. Toggle points of a four-bar linkage can be used to carry out the action of pick and place, while rotation of the input bar can drive the output bar to be moved in a certain range of rotation angle.

A crank-rocker mechanism is a typical mechanism which can provide the motion mentioned above. The crank is an input bar which is used as a driving source of the mechanism, it can move or rotate in a full rotation; the rocker is an output bar which is used to perform the specific requirement, it can move or rotate in a specific range; the coupler or connecting rod is an intermediate conveyor which connects the input and output bars.

In this research, a crank-rocker mechanism is designed to work as an apparatus to perform the function of pick and place.

1.2 Review of Literature

Esec SA (Cham, CH) owns some patents which are related to the pick and place apparatus. The patent US 6,185,815 [2] (Fig.1.1) introduces a semiconductor mounting apparatus with a chip gripper traveling back and forth, which is using a crank-slider mechanism.

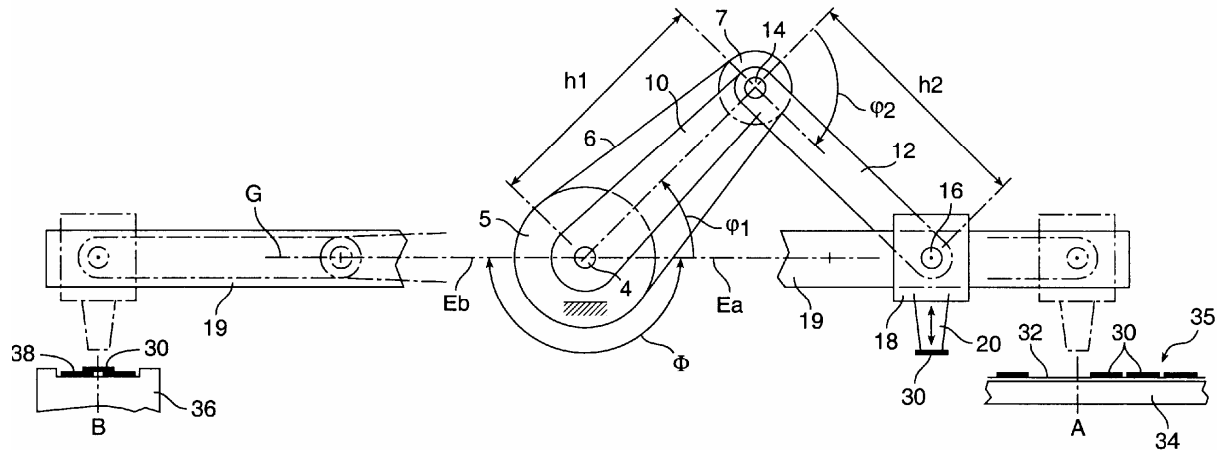


Fig.1.1 Semiconductor mounting apparatus with a chip gripper traveling back and forth (US 6,185,815 [2])

The patent US 6,571,461 [3] (Fig.1.2) introduces a device provided with a linear guide with an air bearing to perform the function of planar transferring motion. While the patent US

6,758,113 [4] (owned by ASM Assembly Automation Limited, Fig.1.3) introduces damping particles 9 used to decrease the vibration occurred by sudden stop. Decrease of vibration improves the settling time, the speed of pick and place can be also highly improved.

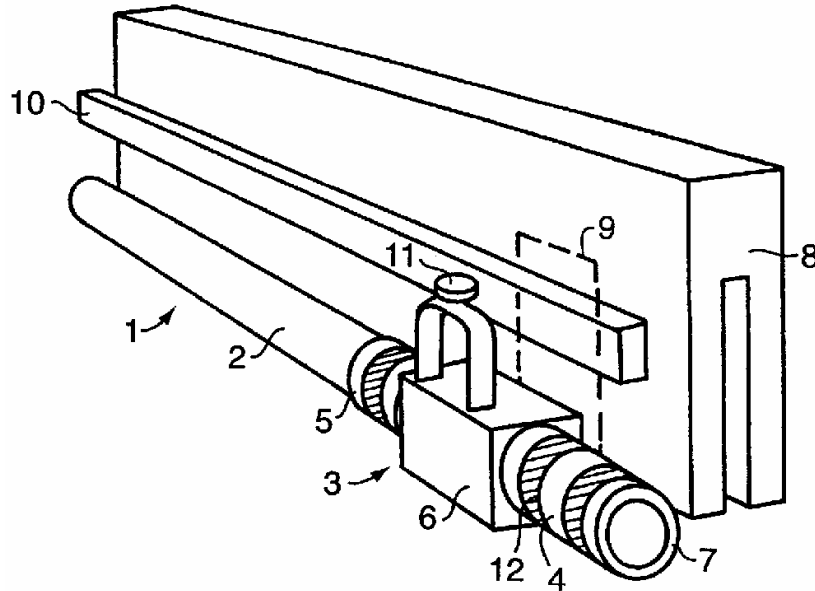


Fig.1.2 Linear guide with an air bearing having provision for heating a support element of the linear guide to maintain fluid gap (US 6,571,461 [3])

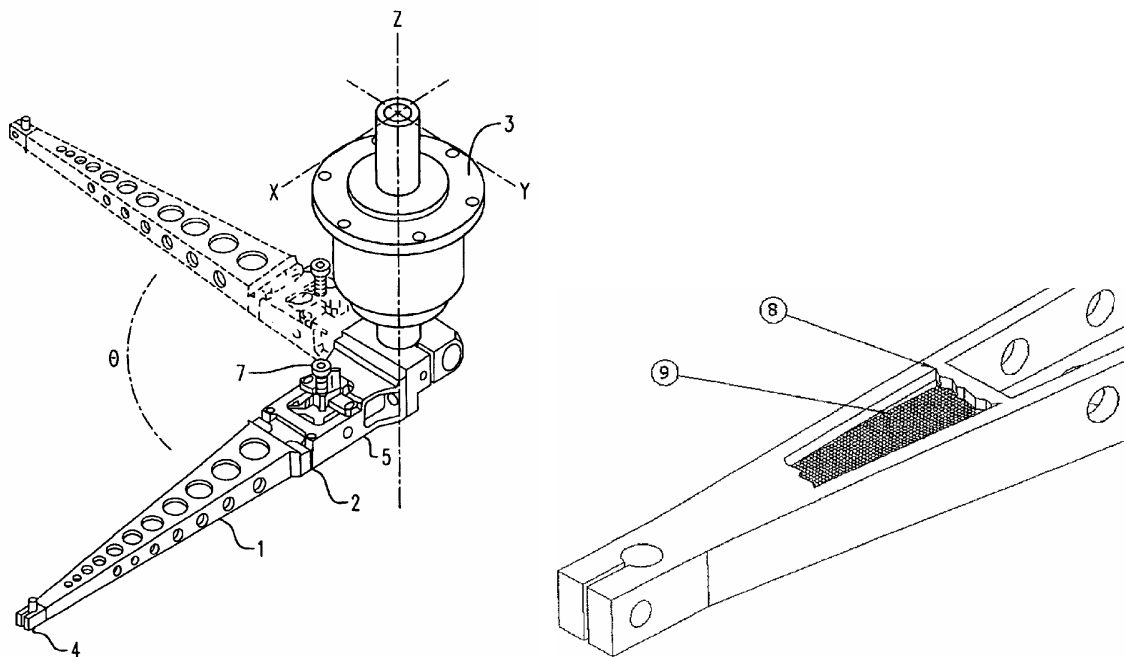


Fig.1.3 High speed pick and place apparatus (US6758113 [4])

ITRI introduces a mechanism provided with a gear set which consists of at least two big gears and one small gear (US 6,505,528 [7], Fig.1.4). The mechanism performs the operations of picking up, placing down and a short distance transferring.

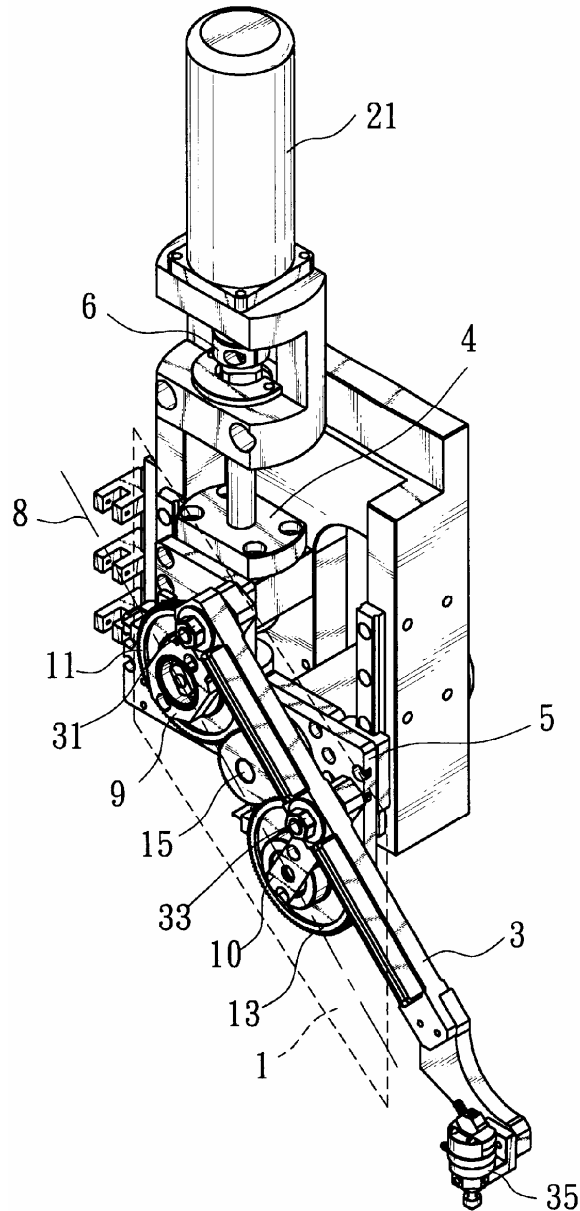


Fig.1.4 Device for fast taking out and putting in (US 6,505,528 [7])

Matsushita Electric Industrial Co., Ltd. introduces extendable arm(s) to overcome the problem of different weighting objects, and movable load(s) to change the position of the center of gravity of arm(s) (US 5,151,007 [8], Fig.1.5).

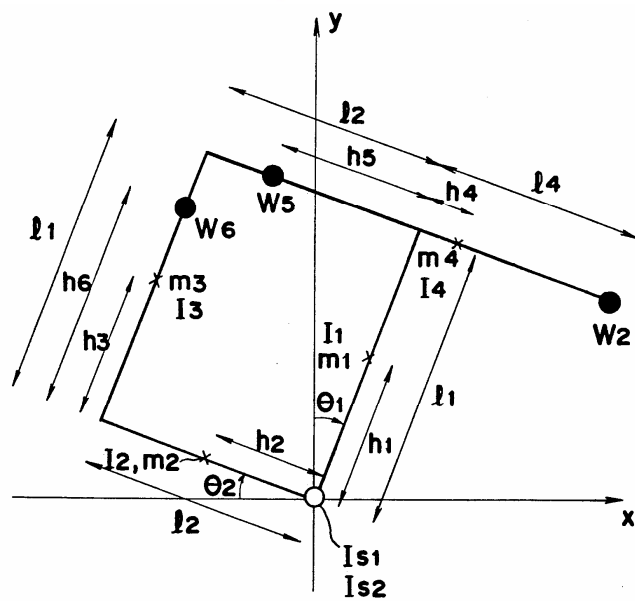
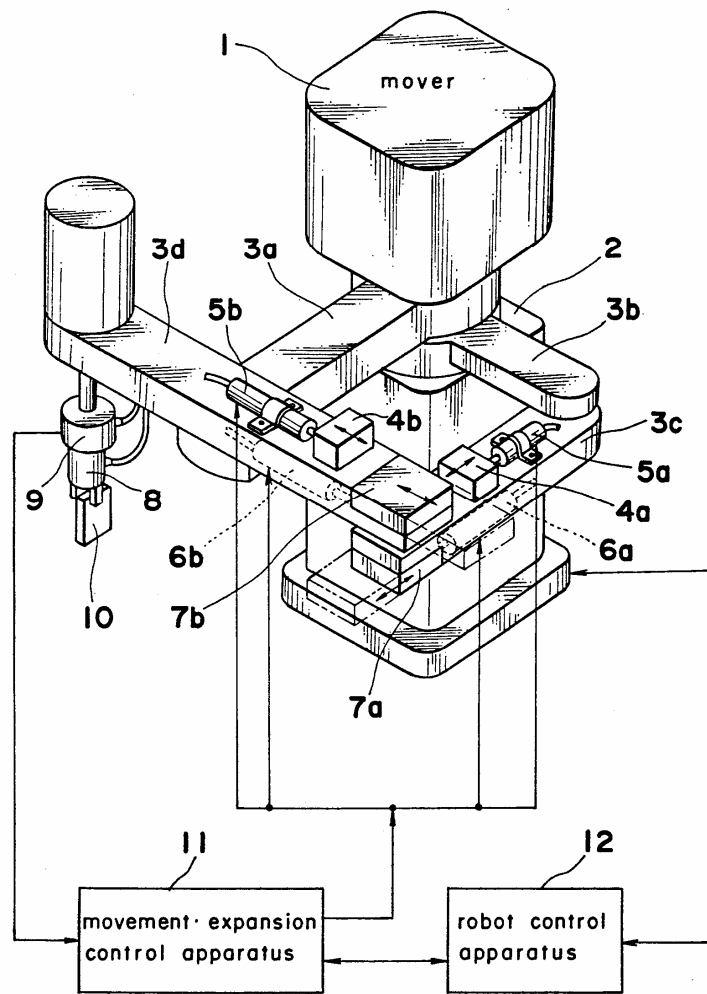


Fig.1.5 Industrial use robot with horizontal multiple articulated arms with means to minimize or eliminate interference among driving portions (US 5,151,007 [8])

1.3 Organization

This research is focus on the planar kinematics of transferring action with a chip's pick and place device. High speed and stiffness are two main targets to be achieved. In Chapter 2, basic principles of mechanisms, mechanics, machine design and optimization which are used in this research are carried out firstly.

In Chapter 3, design constraints which need to be obeyed are shown, such as the dimension limitation and components used in the present design. The dimension limitation limits the ranges of bar dimensions of the four-bar linkage; while the components used in the present design affect the performance of the chip's pick and place mechanism. The design result needs to satisfy the capability of motor, bearings and etc.; while the material of bar, mass of voice coil motor and etc. would affect the design result.

An ITRI model of chip's pick and place mechanism would be shown firstly in Chapter 4, the dynamic performance and finite element analysis (FEA) results are carried out in order to use as a sample of comparison. Design procedures, structure design and sensitivity analysis of design variable are showed after it. Computer softwares: MSC. ADAMS and MSC. Nastran are used in the present design and analysis of this research. An optimization of the chip's pick and place mechanism will be investigated in order to find out the optimum dimension of bars, where FEA is used to check the stiffness of bars. Finally, an optimal chip's pick and place mechanism is carried out, and dynamic performance and FEA result are shown.

Conclusions and future works are also made in Chapter 5.

Chapter 2 Fundamental Principles

2.1 Mechanical Design

The basic principles of mechanical design which is being used in the present design are carried out below.

2.1.1 Stress

Stress can be simply explained as force per unit area. There are two types of stress, called normal stress and shear stress. Normal stress at a point is defined by equation:

$$\sigma(x, y, z) = \lim_{\Delta A \rightarrow 0} \left(\frac{\Delta F}{\Delta A} \right), \quad (1)$$

and shear stress is defined by equation:

$$\tau = \lim_{\Delta A \rightarrow 0} \left(\frac{\Delta V}{\Delta A} \right). \quad (2)$$



2.1.2 Safety Factor

Safety factor is a very important issue in a design process which accommodates uncertainty in material properties and the design process, the consequences of failure, risk to people, and degree of characterization of and control over the service environment. The safety factor is defined as:

$$S_f = \frac{\text{design capacity}}{\text{load}} = \frac{\text{strength}}{\text{stress}} > 1. \quad (3)$$

Safety factor is a ratio greater than 1, which simply showing that the designed load capacity must be greater than real load and strength must be greater than stress.

Recommended values of safety factors for ductile materials are shown in Table 2.1. Safety factors for ductile materials are based on yield strength, while safety factors for brittle

materials are based on ultimate strength and are twice the recommended values for ductile materials.

Table 2.1 Recommended safety factor for ductile materials based on yield strength [15]

Knowledge of Loads	Knowledge of Stress	Knowledge of Materials	Knowledge of Environment	Safety Factor
Accurate	Accurate	Well Known	Controllable	1.2-1.5
Good	Good	Well Known	Constant	1.5-2.0
Good	Good	Average	Ordinary	2.0-2.5
Average	Average	Less Tried	Ordinary	2.5-3.0
Average	Average	Untried	Ordinary	3.0-4.0
Uncertain	Uncertain	Better Known	Uncertain	3.0-4.0

2.2 Principles of Mechanisms

Once a mechanism is synthesized, it must be analyzed; including forces and torques applied on the joints, and situation of the mechanism are the main items concerned. To perform the force and torque analyses, position analysis, velocity analysis and acceleration should be find out firstly.

2.2.1 Position Analysis

For a four-bar linkage, if the link lengths a , b , c , and d are defined, by a given input crank angle θ_2 the position angles of rocker and coupler, θ_3 and θ_4 , can be determined in terms of these parameters as follows:,

$$\theta_3 = f\{a, b, c, d, \theta_2\},$$

$$\text{and } \theta_4 = g\{a, b, c, d, \theta_2\}. \quad (4)$$

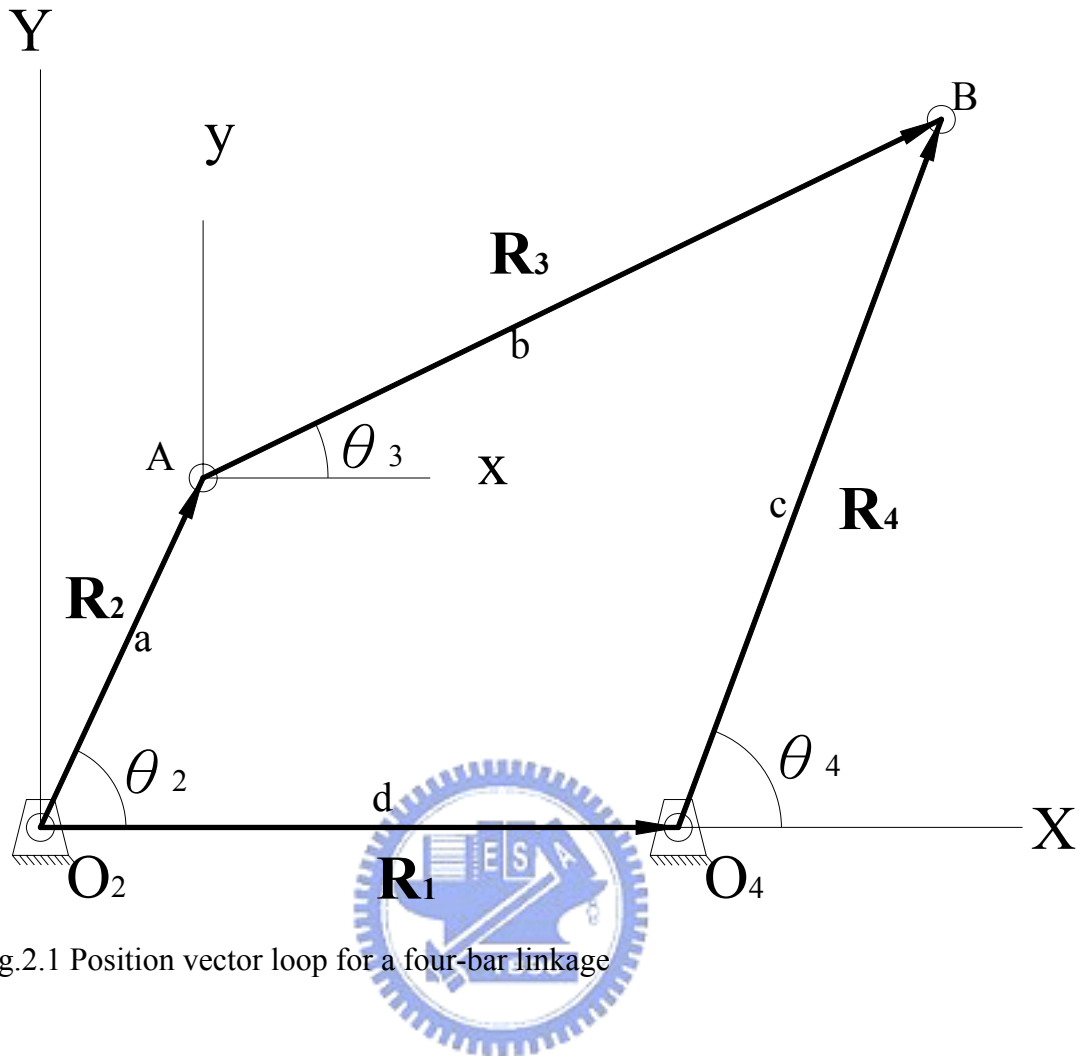


Fig.2.1 Position vector loop for a four-bar linkage

Based on Fig.2.1, the vector loop equation for a four-bar linkage is derived as follow:

$$\mathbf{R}_2 + \mathbf{R}_3 - \mathbf{R}_4 - \mathbf{R}_1 = 0. \quad (5)$$

Substituting the complex number notations for each position vector, Eq. (5) becomes:

$$ae^{j\theta_2} + be^{j\theta_3} - ce^{j\theta_4} - de^{j\theta_1} = 0. \quad (6)$$

By using Euler equivalents for the $e^{j\theta}$ terms, Eq. (6) yields:

$$a(\cos\theta_2 + j\sin\theta_2) + b(\cos\theta_3 + j\sin\theta_3) - c(\cos\theta_4 + j\sin\theta_4) - d(\cos\theta_1 + j\sin\theta_1) = 0. \quad (7)$$

2.2.2 Velocity Analysis

Figure 2.2 shows the position vector loop for a four-bar linkage showing velocity vectors

for an input angular velocity ω_2 . By the position analysis, angular velocities ω_3 and ω_4 can be determined in terms of other design parameters as follows:

$$\omega_3 = f\{a, b, c, d, \theta_2, \theta_3, \theta_4, \omega_2\},$$

$$\text{and } \omega_4 = g\{a, b, c, d, \theta_2, \theta_3, \theta_4, \omega_2\}. \quad (8)$$

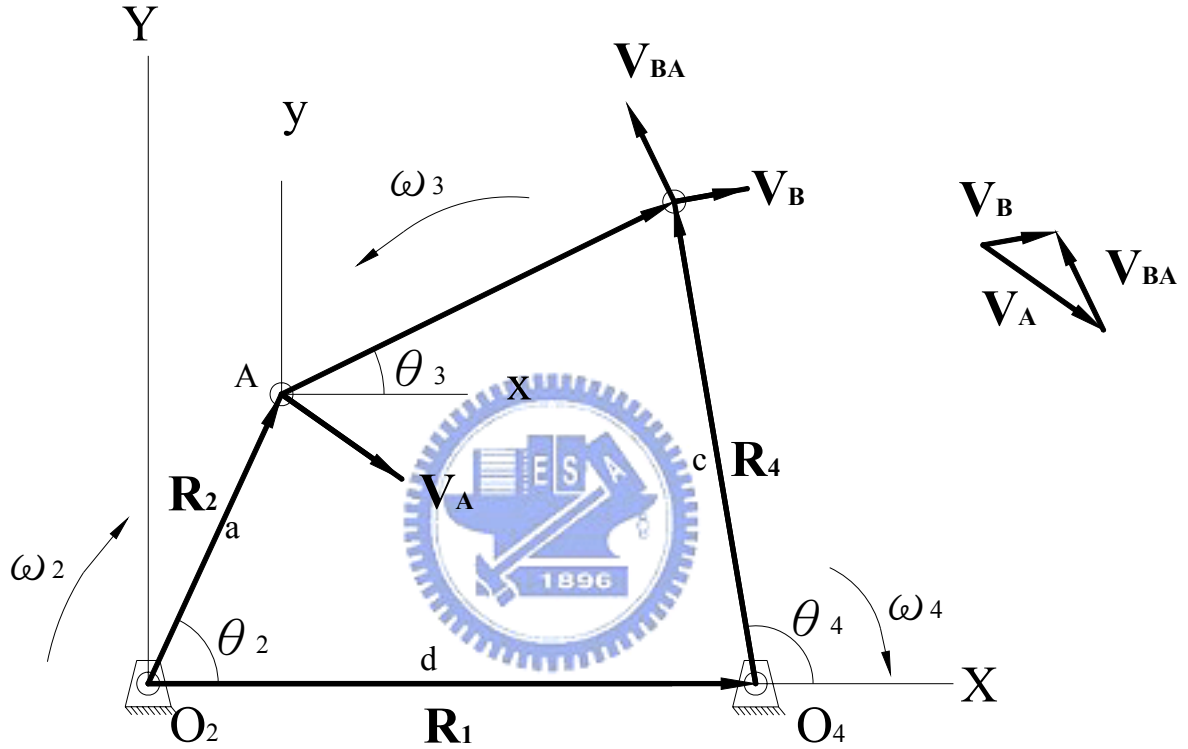


Fig.2.2 Position vector loop for a four-bar linkage showing velocity vectors for an input angular velocity ω_2

The vector loop equation as shown in Eqs.(6) and (7) can be differentiated with respect to time to obtain the equation of velocity as follows:

$$jae^{j\theta_2} \frac{d\theta_2}{dt} + jbe^{j\theta_3} \frac{d\theta_3}{dt} - jce^{j\theta_4} \frac{d\theta_4}{dt} = 0, \quad (9)$$

$$\text{and } ja\omega_2 e^{j\theta_2} + jb\omega_3 e^{j\theta_3} - jc\omega_4 e^{j\theta_4} = 0. \quad (10)$$

$$\text{where } \frac{d\theta_2}{dt} = \omega_2, \quad \frac{d\theta_3}{dt} = \omega_3, \quad \text{and } \frac{d\theta_4}{dt} = \omega_4. \quad (11)$$

The relative velocity between point A and point B, V_{BA} , can be expressed by the equation

$$\mathbf{V}_A + \mathbf{V}_{BA} - \mathbf{V}_B = 0, \quad (12)$$

$$\text{where } \mathbf{V}_A = ja\omega_2 e^{j\theta_2}, \quad \mathbf{V}_{BA} = jb\omega_3 e^{j\theta_3}, \quad \text{and } \mathbf{V}_B = jc\omega_4 e^{j\theta_4}. \quad (13)$$

By using Euler identity, Eq. (10) becomes

$$ja\omega_2(\cos\theta_2 + j\sin\theta_2) + jb\omega_3(\cos\theta_3 + j\sin\theta_3) - jc\omega_4(\cos\theta_4 + j\sin\theta_4) = 0, \quad (14)$$

$$a\omega_2(j\cos\theta_2 + j^2\sin\theta_2) + b\omega_3(j\cos\theta_3 + j^2\sin\theta_3) - c\omega_4(j\cos\theta_4 + j^2\sin\theta_4) = 0, \quad (15)$$

$$\text{and } a\omega_2(-\sin\theta_2 + j\cos\theta_2) + b\omega_3(-\sin\theta_3 + j\cos\theta_3) - c\omega_4(-\sin\theta_4 + j\cos\theta_4) = 0. \quad (16)$$

2.2.3 Acceleration Analysis

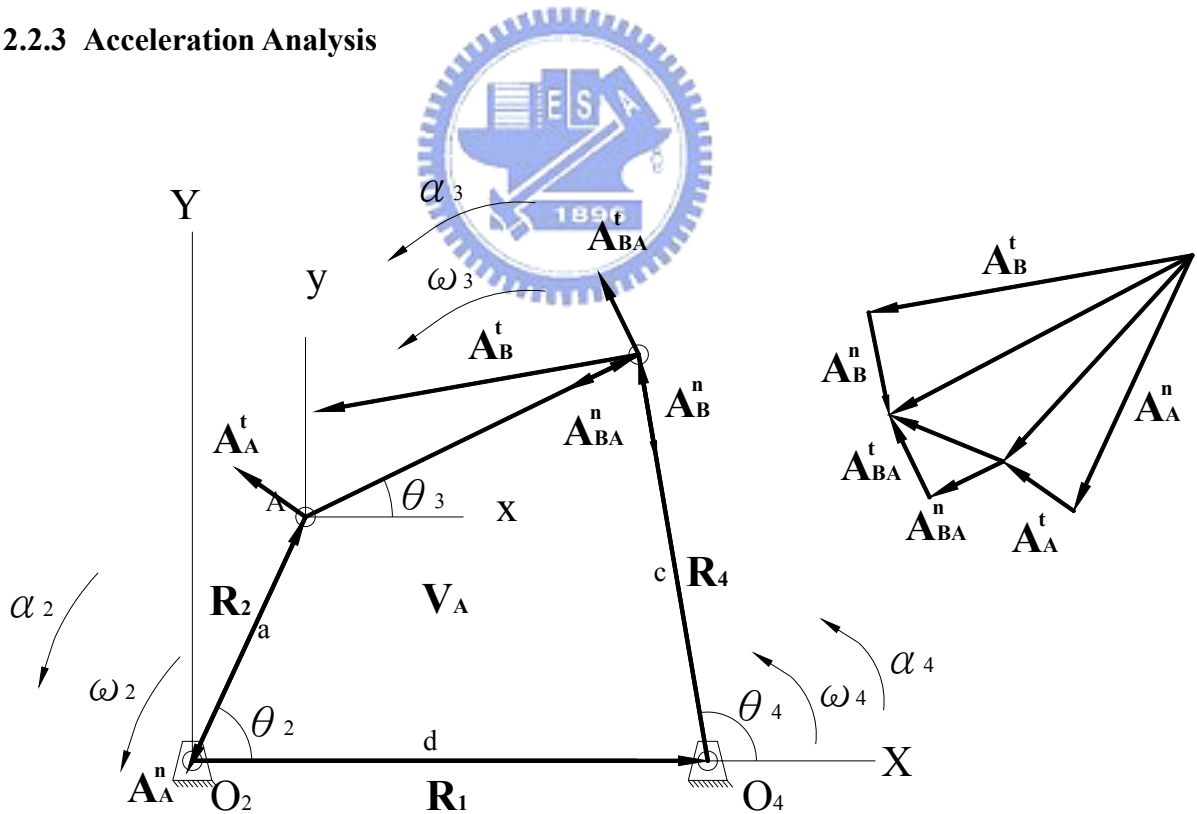


Fig.2.3 Position vector loop for a four-bar linkage showing acceleration vectors

Figure 2.3 shows the position vector loop for a four-bar linkage showing acceleration vectors. After performing the position and velocity analyses, the acceleration of the links can

be determined in terms of the following parameters:

$$\alpha_3 = f\{a, b, c, d, \theta_2, \theta_3, \theta_4, \omega_2, \omega_3, \omega_4, \alpha_2\},$$

$$\text{and } \alpha_4 = g\{a, b, c, d, \theta_2, \theta_3, \theta_4, \omega_2, \omega_3, \omega_4, \alpha_2\}. \quad (17)$$

By differentiating Eq. (10) with respect to time, it results in the acceleration expression for each term in the acceleration equation:

$$\begin{aligned} & (j^2 a \omega_2^2 e^{j\theta_2} + ja\alpha_2 e^{j\theta_2}) + (j^2 b \omega_3^2 e^{j\theta_3} + jb\alpha_3 e^{j\theta_3}) \\ & - (j^2 c \omega_4^2 e^{j\theta_4} + jc\alpha_4 e^{j\theta_4}) = 0, \end{aligned} \quad (18)$$

$$\text{and } \begin{aligned} & (ja\alpha_2 e^{j\theta_2} - a\omega_2^2 e^{j\theta_2}) + (jb\alpha_3 e^{j\theta_3} - b\omega_3^2 e^{j\theta_3}) \\ & - (jc\alpha_4 e^{j\theta_4} - c\omega_4^2 e^{j\theta_4}) = 0. \end{aligned} \quad (19)$$

The relative linear acceleration between point A and point B, \mathbf{A}_{BA} , can be expressed by:

$$\mathbf{A}_A + \mathbf{A}_{BA} - \mathbf{A}_B = 0, \quad (20)$$

$$\text{where } \mathbf{A}_A = (\mathbf{A}_A^t + \mathbf{A}_A^n) = ja\alpha_2 e^{j\theta_2} - a\omega_2^2 e^{j\theta_2},$$

$$\mathbf{A}_{BA} = (\mathbf{A}_{BA}^t + \mathbf{A}_{BA}^n) = jb\alpha_3 e^{j\theta_3} - b\omega_3^2 e^{j\theta_3},$$

$$\text{and } \mathbf{A}_B = (\mathbf{A}_B^t + \mathbf{A}_B^n) = jc\alpha_4 e^{j\theta_4} - c\omega_4^2 e^{j\theta_4}. \quad (21)$$

By using Euler equation, Eq. (19) becomes

$$\begin{aligned} & [a\alpha_2 j(\cos \theta_2 + j \sin \theta_2) - a\omega_2^2(\cos \theta_2 + j \sin \theta_2)] \\ & + [b\alpha_3 j(\cos \theta_3 + j \sin \theta_3) - b\omega_3^2(\cos \theta_3 + j \sin \theta_3)] \\ & - [c\alpha_4 j(\cos \theta_4 + j \sin \theta_4) - c\omega_4^2(\cos \theta_4 + j \sin \theta_4)] = 0. \end{aligned} \quad (22)$$

2.2.4 Forces and Torques

Figure 2.4 shows an external force (\mathbf{F}_p) acts on link 3, and an external torque (\mathbf{T}_4) acts on link 4. To analyze the dynamic forces, the free body diagrams for every link should be drawn, as shown in Fig.2.5.

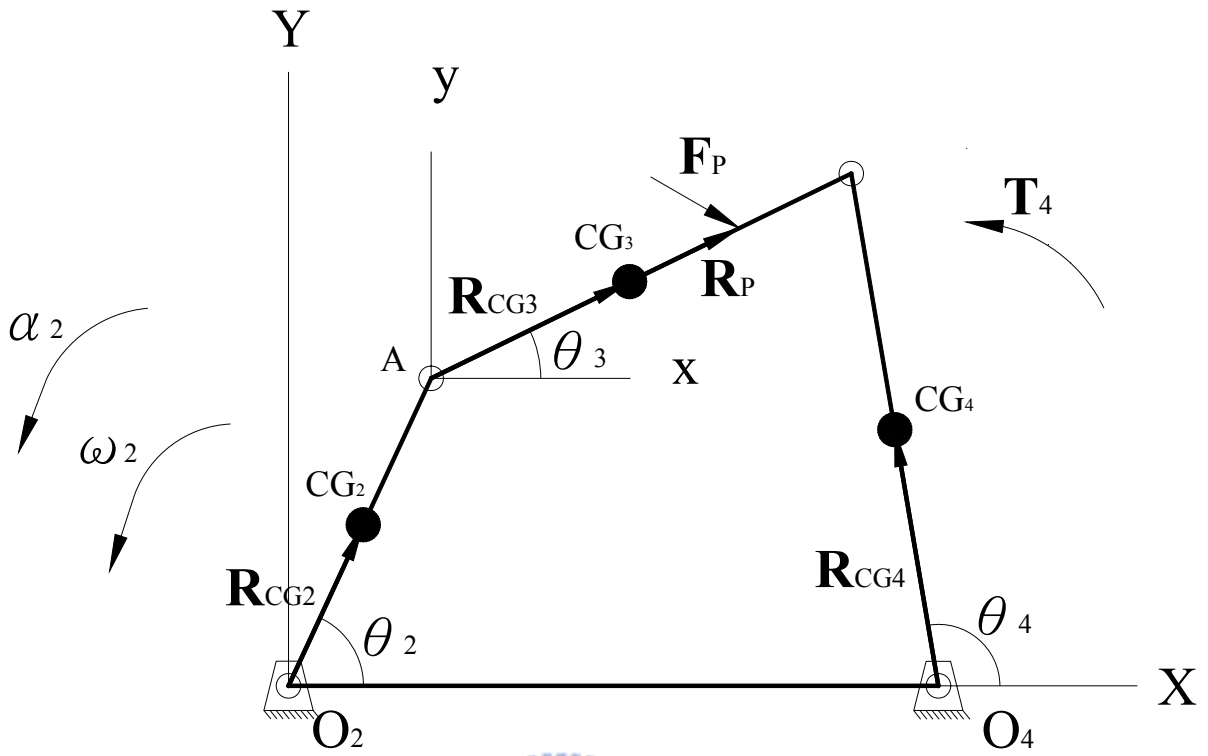


Fig.2.4 Dynamic force analysis of a four-bar linkage

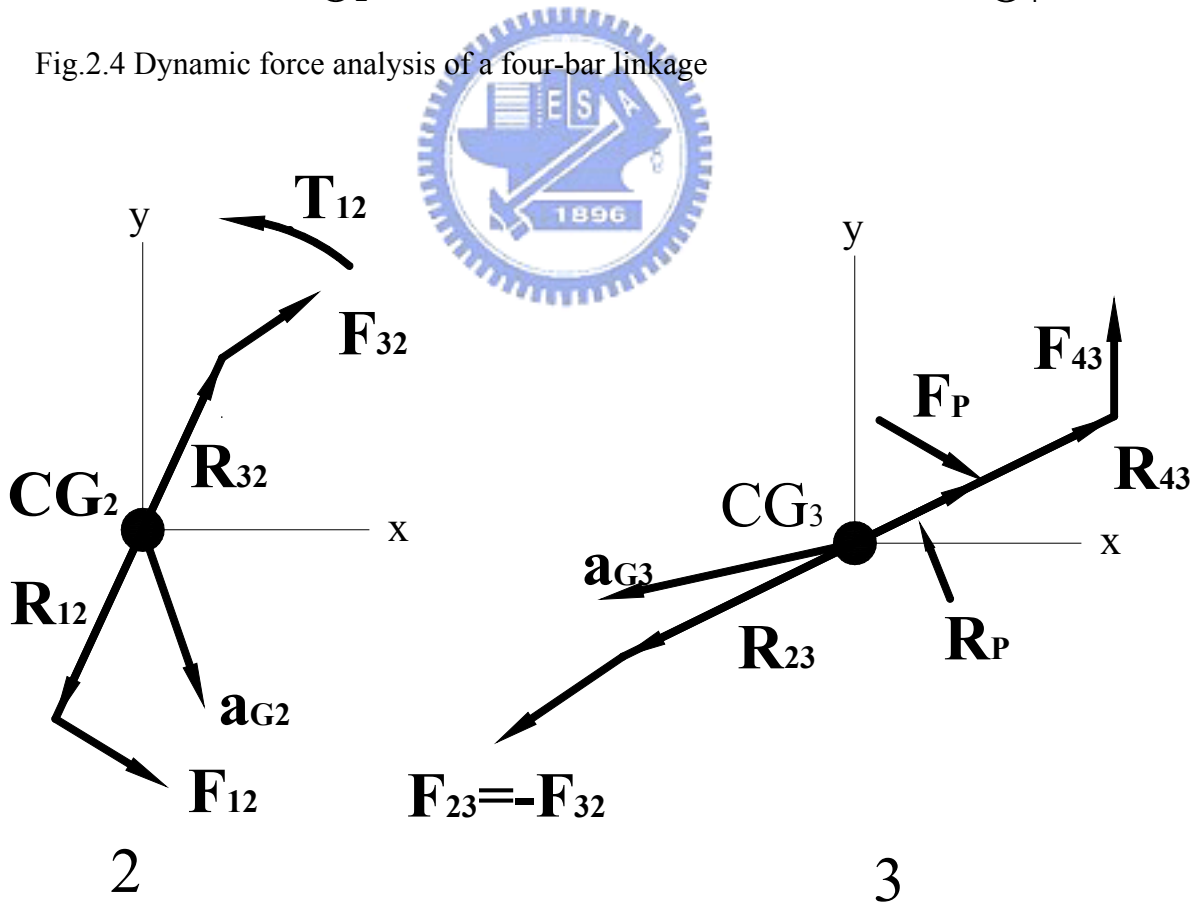


Fig.2.5 Free body diagrams of a four-bar linkage

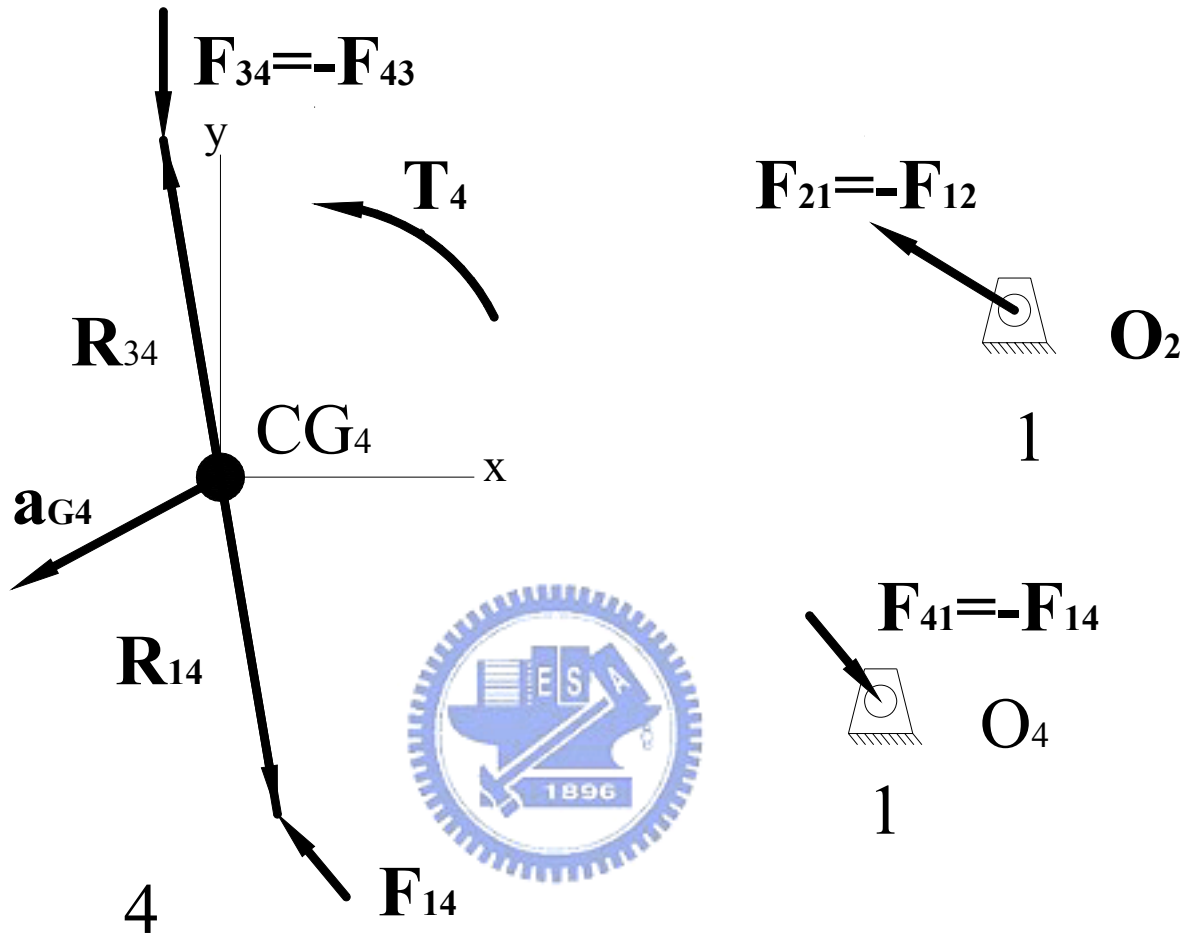


Fig.2.5 Free body diagrams of a four-bar linkage (continued)

From the free body diagrams, a system of nine unknowns (F_{12x} , F_{12y} , F_{32x} , F_{32y} , F_{43x} , F_{43y} , F_{14x} , F_{14y} , T_{12}) with nine equations can be set up as follow:

$$\begin{bmatrix}
1 & 0 & 1 & 0 & 0 & 0 & 0 & 0 & 0 \\
0 & 1 & 0 & 1 & 0 & 0 & 0 & 0 & 0 \\
-R_{12y} & R_{12x} & -R_{32y} & R_{32x} & 0 & 0 & 0 & 0 & 1 \\
0 & 0 & -1 & 0 & 1 & 0 & 0 & 0 & 0 \\
0 & 0 & 0 & -1 & 0 & 1 & 0 & 0 & 0 \\
0 & 0 & R_{23y} & -R_{23x} & -R_{43y} & R_{43x} & 0 & 0 & 0 \\
0 & 0 & 0 & 0 & -1 & 0 & 1 & 0 & 0 \\
0 & 0 & 0 & 0 & 0 & -1 & 0 & 1 & 0 \\
0 & 0 & 0 & 0 & R_{34y} & -R_{34x} & -R_{14y} & R_{14x} & 0
\end{bmatrix}
\begin{bmatrix}
F_{12x} \\
F_{12y} \\
F_{32x} \\
F_{32y} \\
F_{43x} \\
F_{43y} \\
F_{14x} \\
F_{14y} \\
T_{12}
\end{bmatrix}
=
\begin{bmatrix}
m_2 a_{G2x} \\
m_2 a_{G2y} \\
I_{G2} \alpha_2 \\
m_3 a_{G3x} - F_{Px} \\
m_3 a_{G3y} - F_{Py} \\
I_{G3} \alpha_3 - R_{Px} F_{Py} + R_{Py} F_{Px} \\
m_4 a_{G4x} \\
m_4 a_{G4y} \\
I_{G4} \alpha_2 - T_4
\end{bmatrix}
\quad (23)$$

The dynamic force acting on the ground can cause vibrations in a structure which supports the machine. The summation of all the forces acting on the ground plane is called the shaking force (\mathbf{F}_s); the reaction torque reacted to the ground plane is called the shaking torque (\mathbf{T}_s).

In a four-bar linkage, as shown in Fig.2.5, the shaking force can be obtained by the following equation:

$$\mathbf{F}_s = \mathbf{F}_{21} + \mathbf{F}_{41}. \quad (24)$$

However, in a four-bar linkage, the shaking torque is the only torque acts on the ground:

$$\mathbf{T}_s = \mathbf{T}_{21} = -\mathbf{T}_{12}. \quad (25)$$

2.3 Optimum Design

Optimization is a tool that helps the designer to find the most efficient and feasible

solutions to an engineering problem. Optimization model can be described as follow:

Find an n-vector $\mathbf{x} = (x_1, x_2, \dots, x_n)$ of design variables to minimize a cost function

$$f(\mathbf{x}) = f(x_1, x_2, \dots, x_n), \quad (26)$$

subjected to the p equality constraints

$$h_j(\mathbf{x}) = h_j(x_1, x_2, \dots, x_n) = 0; j = 1 \text{ to } p, \quad (27)$$

and the m inequality constraints

$$g_i(\mathbf{x}) = g_i(x_1, x_2, \dots, x_n) = 0; i = 1 \text{ to } m. \quad (28)$$



Chapter 3 Design Constraints

3.1 Introduction to Pick and Place Action

In the present design, some symbols used are shown in Fig.3.1. The bonding arm is the combination of rocker and picking arm; a voice coil motor (VCM) is located at the end of the bonding arm which performs an up-and-down action, in order to “pick” or “place” a chip.

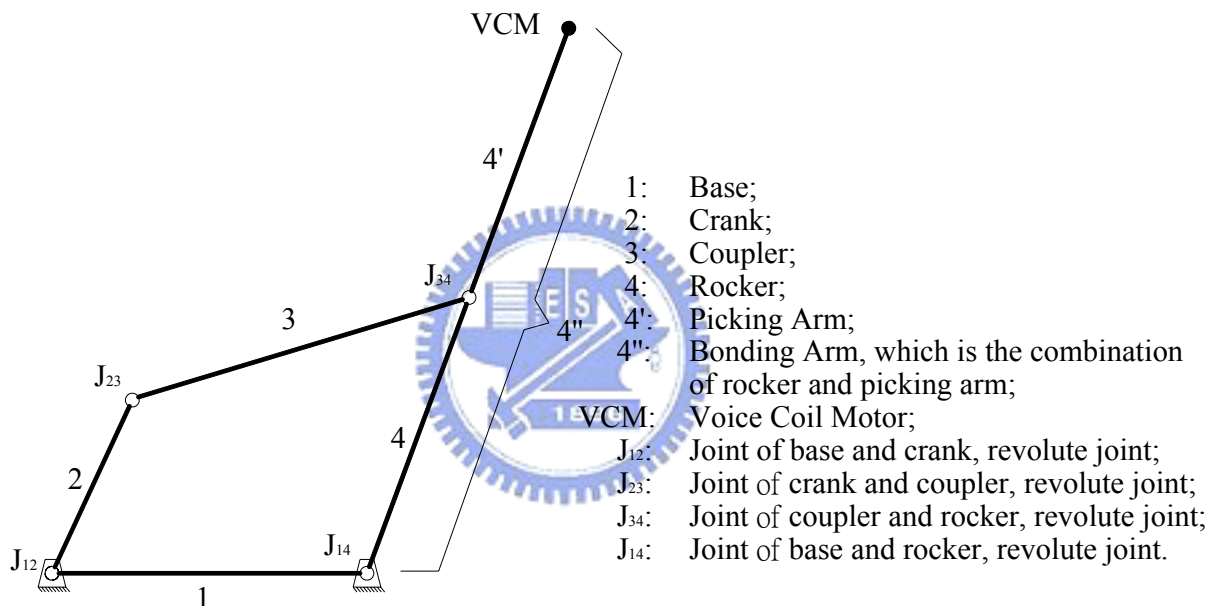


Fig.3.1 Some symbols used in the present design of a four-bar linkage

The picking and placing positions are the first and second toggle points of four-bar linkage, as shown in Figs. 3.2 and 3.3. By using the toggle points to perform the pick and place action, the vibration at the end of bonding arm can be reduced and thus the action of picking and placing can be more stable.

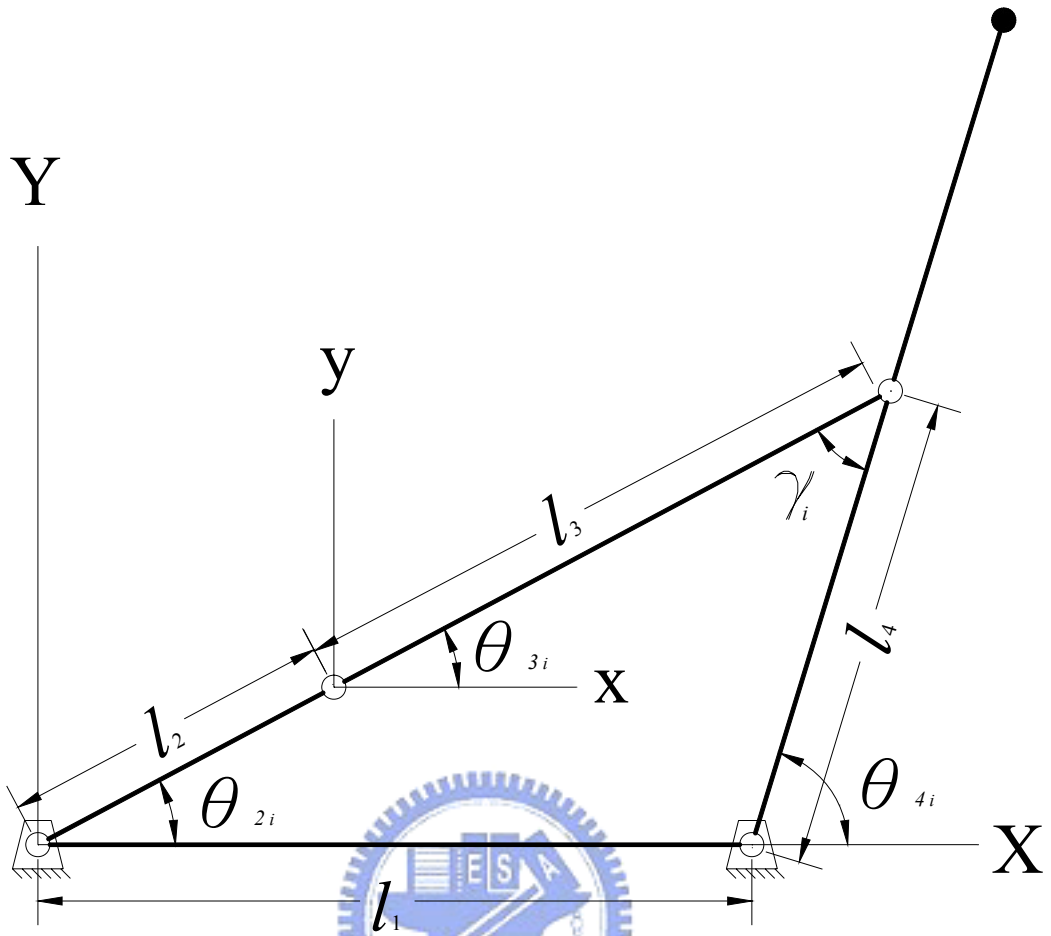


Fig.3.2 Picking position (first toggle point)

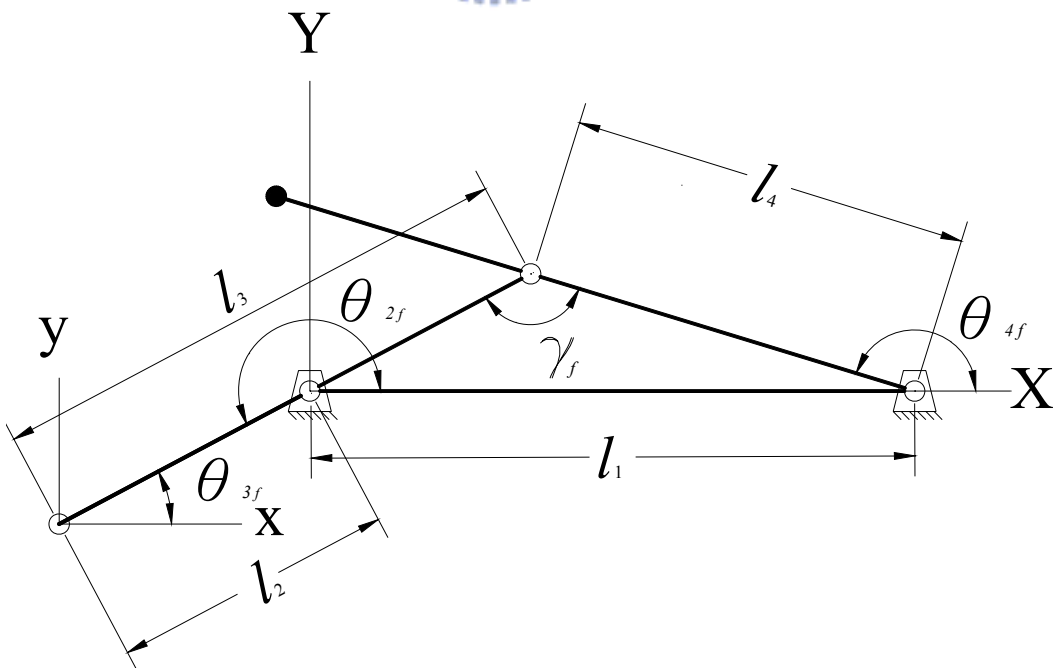


Fig.3.3 Placing position (second toggle point)

3.2 Dimension Limitation

For a 12 inches wafer, the distance between the picking and placing locations is usually larger than 300mm; the distance requirement in the present research is 320mm. For a convenient chips arrangement, the bonding arm (rocker) for picking and placing chips should perform a 90° rotation angle.

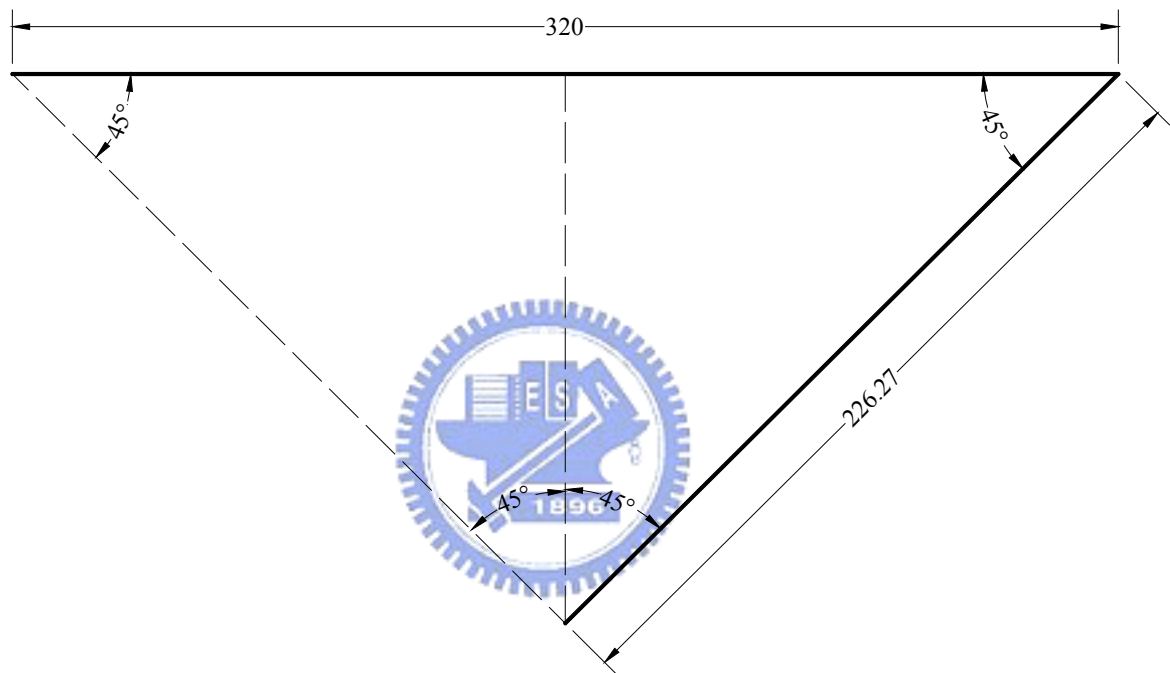


Fig.3.4 Requirement of distance for pick and place, and the maximum length of bonding arm

By referring to Fig.3.4, the length of the bonding arm can be calculated, as follows:

$$l_4'' = \frac{(320/2)}{\sin 45^\circ} \approx 226.27 \text{ (mm)}. \quad (29)$$

By referring to Fig.3.3, to reach the second toggle point, the crank should be shorter than the coupler. It means that the final angle between bonding arm and x-axis lies between 90° and 180°, therefore the initial angle between bonding arm and x-axis should lie between 0° and 90°, it can be expressed as equation:

$$0^\circ \leq \theta_{4_initial} \leq 90^\circ . \quad (30)$$

3.3 Components

To compose a four-bar linkage, four bars need to be jointed together; some standard components are used as joints in the present design, for example bearings, pivot pins and motor. In the present design, the base is fixed, a motor is used to joint the crank and base, where the motor provides the driving source for the crank to rotate. Bearings and pivot pins are used as revolute joints to joint the crank and coupler, coupler and rocker, and base and rocker.

3.3.1 Driving Source

An AC servo motor is used as a driving source to drive the crank. The major setting is listed in Table 3.1.



Table 3.1 Major setting of AC servo motor used in the present design

Rated output		400 W
Voltage		200 V
Encoder Specifications		2500 p/r incremental
With / Without Oil seal		no
With / Without holding brake		no
Torque	Rated	$1.3N \cdot m = 1300N \cdot mm$
	Max	$3.8N \cdot m = 3800N \cdot mm$
Speed	Rated	$3000 \text{ r/min} = 18000 \text{ }^\circ/\text{s}$
	Max	$5000 \text{ r/min} = 30000 \text{ }^\circ/\text{s}$
Weight		1.6 kg

Trapezoid wave is the input mode which used to drive the motor. The unit used here is

pulse; for one rotation (360°) of the servo motor, it needs 30000 pulses. The major specification is listed in Table 3.2.

Table 3.2 Major specification of the input mode of AC servo motor

Rate	50
Acceleration/Deceleration Rate (pulse/sec²)	140000=1.4×10 ⁵
Initial Velocity (pulse/sec)	20
Final Velocity (pulse/sec)	5600

From the data above, the setting of motor can be expressed as follow:

$$\omega_{mi} = 20 \times 50 \times \frac{360}{30000} = 12 \text{ deg./sec}, \quad (31)$$

$$\omega_{mf} = 5600 \times 50 \times \frac{360}{30000} = 3360 \text{ deg./sec}, \quad (32)$$

And $\alpha_m = 140000 \times 50 \times \frac{360}{30000} = 84000 \text{ deg./sec}^2.$ (33)

The input mode can be expressed as shown in Fig.3.5.

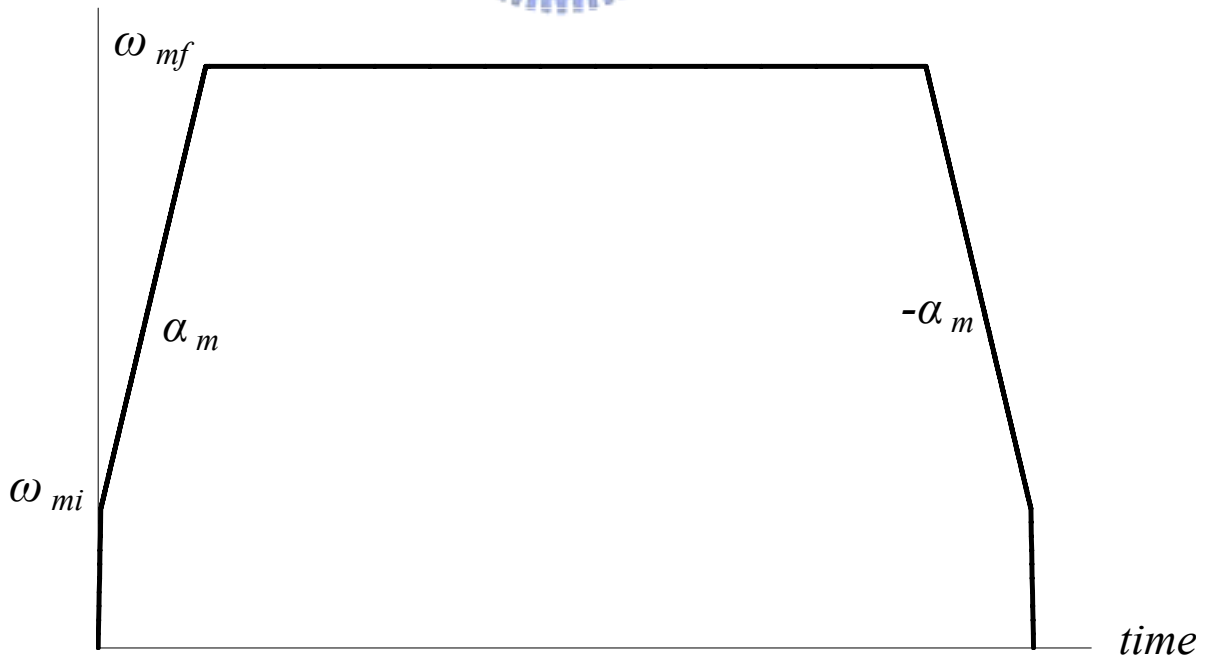


Fig.3.5 The input mode of the input mode of AC servo motor in the present design

3.3.2 Bearing

Bearing is used to connect two bars, which acts as a revolute joint. Two types of bearings are used in the present design, and are shown in Fig.3.6, and their major specifications are listed in Table 3.3.

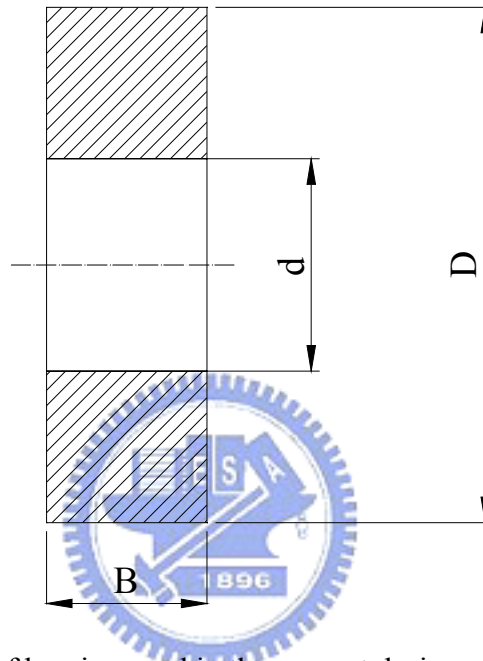


Fig.3.6 Schematic view of bearing used in the present design

Table 3.3 Major specification of two types of bearing used in the present design

	Bearing 1	Bearing 2
Inside Diameter (d)	5 mm	10 mm
Outside Diameter (D)	14 mm	22 mm
Width (B)	4 mm	6 mm
Operating Load	905 N	3000 N
Static Load	304 N	1520 N
Limiting Speed	-	67000rpm = 402000 % _s (grease)
Coefficient of Friction	0.0015	0.0015

3.3.3 Pivot Pin

Pivot pin works together with bearings, and becomes a revolute joint which connect two bars, it is shown in Fig.3.7.



Fig.3.7 Pivot pin used in the present design

3.3.4 Voice Coil Motor

The voice coil motor is widely used in many areas, such as the pick-up head of a CD-ROM. The function of a VCM is to provide the motion for up and down in a very short time. A VCM is used in the present design, as shown in Fig.3.1 where bonding head is assembled by a VCM to pick up or put down the chip. The VCM used in the present design is weighting 20g and is shown in Fig.3.8.

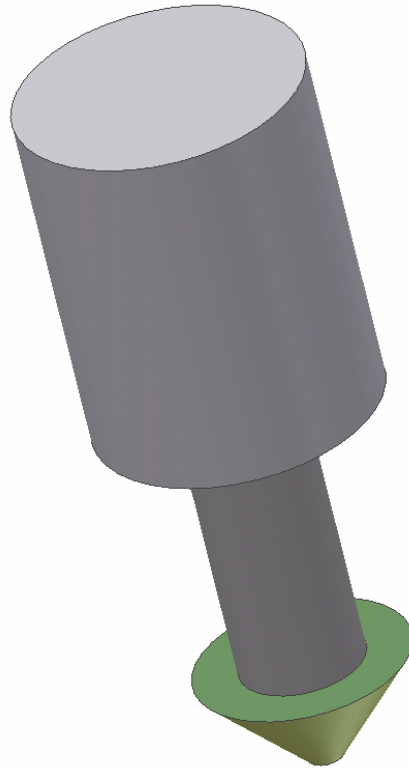


Fig.3.8 A schematic figure of voice coil motor

3.4 Material and Safety Factor

The material Al 7075-T6 is chosen for the four-bar linkage in the present design, the properties of said material is listed in Table 3.4.

Table 3.4 Properties of Al 7075-T6 [24]

Density (ρ)	$2810 \frac{kg}{m^3}$
Yielding Stress (S_y)	503 MPa
Ultimate Stress (S_u)	572 MPa
Modulus of Elasticity (E)	71.7 GPa
Shear Modulus of Elasticity (G)	26.9 GPa
Poissons Ratio	0.33

As for conveniently design discussion, some assumptions have been made as follows:

1. Only the masses of bars and VCM are concerned; compare to bars and VCM, the masses

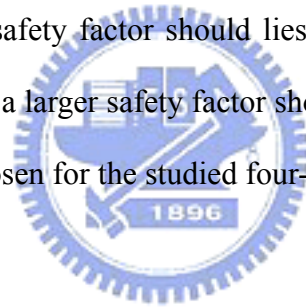
- of bolts, nuts, bearings, and pivot pins are very light and can be ignored.
2. Only the main shapes of bars are concerned, others such as the holes on bars for bolts and nuts are ignored.
 3. Only the planar motion is concerned, the effect of gravity is ignored.

Refer to Table 2.1, selection of the safety factor for the four-bar linkage is listed in Table 3.5.

Table 3.5 Selection of the safety factor

Knowledge of Loads	Knowledge of Stress	Knowledge of Materials	Knowledge of Environment
Average	Average	Average	Constant

Based on Table 3.5, the safety factor should lie between 2.0 to 3.0. According to the assumptions mentioned above, a larger safety factor should be chosen. In the present design, a safety factor of value 3.0 is chosen for the studied four-bar linkage pick and place apparatus.



Chapter 4 Present Design

4.1 Foreword

In this chapter, a chip's pick and place mechanism designed by ITRI will be carried out first, which is used as a sample to compare with the present design. The present design (including procedure, structure design, optimization of mechanism, test of FEA) will also be shown thereafter. Finally, some design cases and comparisons will be carried out.

4.2 The Chip's Pick and Place Mechanism Design by ITRI

In this section, a sample of chip's pick and place mechanism designed by ITRI is shown in Fig.4.1, and Table 4.1 shows the major data of the four bars.

Table 4.1 Data of the pick and place mechanism designed by ITRI

	Length l_i (mm)	Weight (g)	I_{xx} (g-mm ²)	I_{yy} (g-mm ²)	I_{zz} (g-mm ²)
Base (Bar 1)	85.00	-	-	-	-
Crank (Bar 2)	54.81	37.61	3383.52	18903.75	20767.06
Coupler (Bar 3)	103.81	23.52	1133.76	35049.78	35867.87
Rocker (Bar 4)	98.00	-	-	-	-
Bonding arm	226.27	76.71	5107.10	357470.83	359994.85

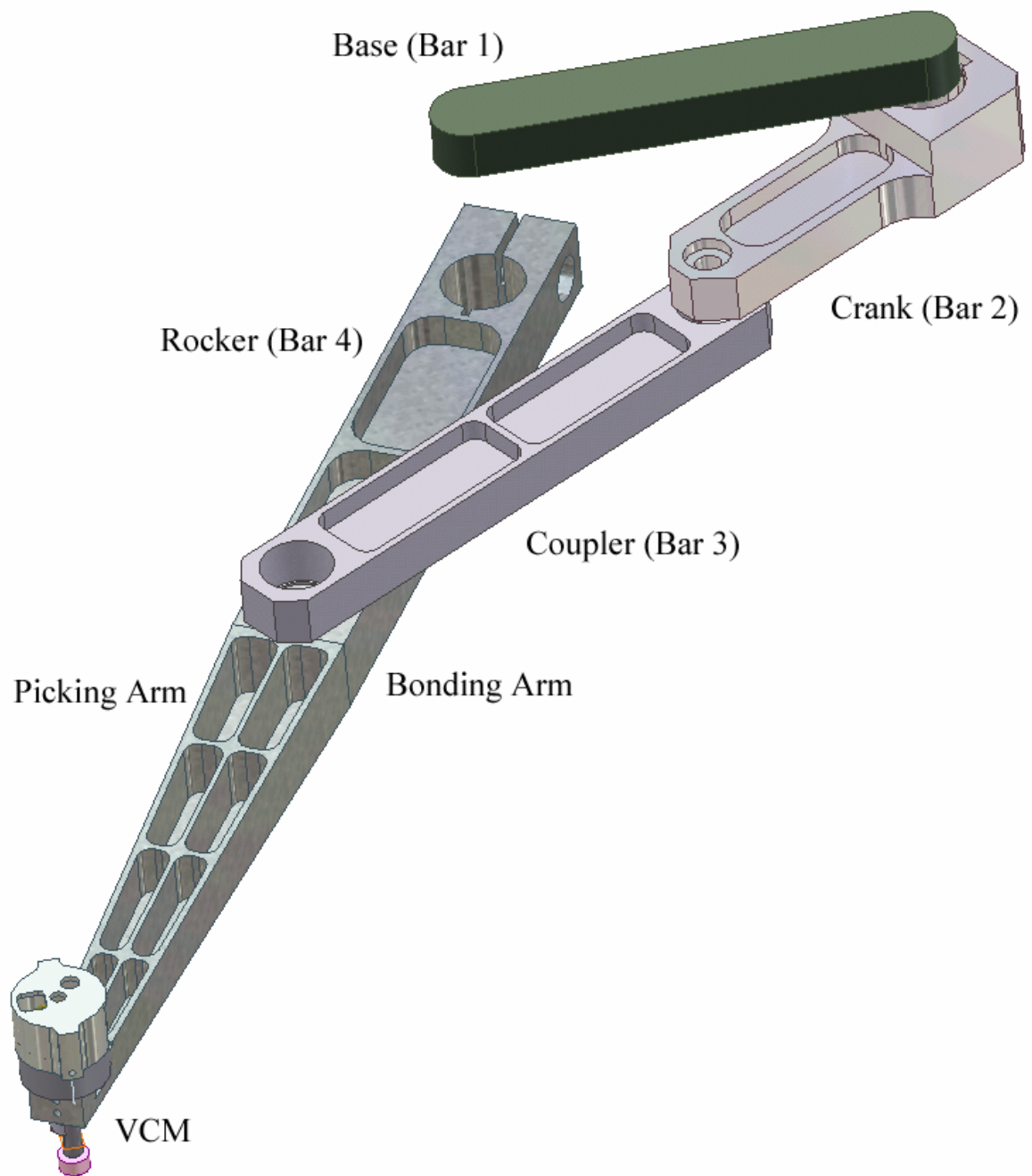


Fig.4.1 Chip's pick and place mechanism designed by ITRI

By using computer software ADAMS, the dynamic performances of the ITRI chip's pick and place mechanism can be simulated and shown in Figs. 4.2 to 4.6. In the ADAMS simulation, the time step is set as 0.0004 seconds.

It is noted that as the input mode of motor is symmetric to the pick-to-place, and place-to-pick actions, the forces, torques, angular velocities, angular acceleration, etc. are also symmetric. The full-cycle time of pick and place motion in this case is 0.2204 seconds, where the half-cycle (pick-to-place or place-to-pick) is 0.1102 seconds. Table 4.2 shows the simulated results of the ITRI chip's pick and place mechanism by using the computer software ADAMS.

Table 4.2 ADAMS simulation results of the pick and place mechanism designed by ITRI

	Time (sec.)	Absolute Extreme Value
T_{mm}	0.0280 / 0.1924	1851.881 / 1852.226 (N-mm)
T_{sm}	0.0248 / 0.1956	4064.177 / 4064.021 (N-mm)
F_{sm}	0.0256 / 0.1948	25.096 / 25.100 (N)

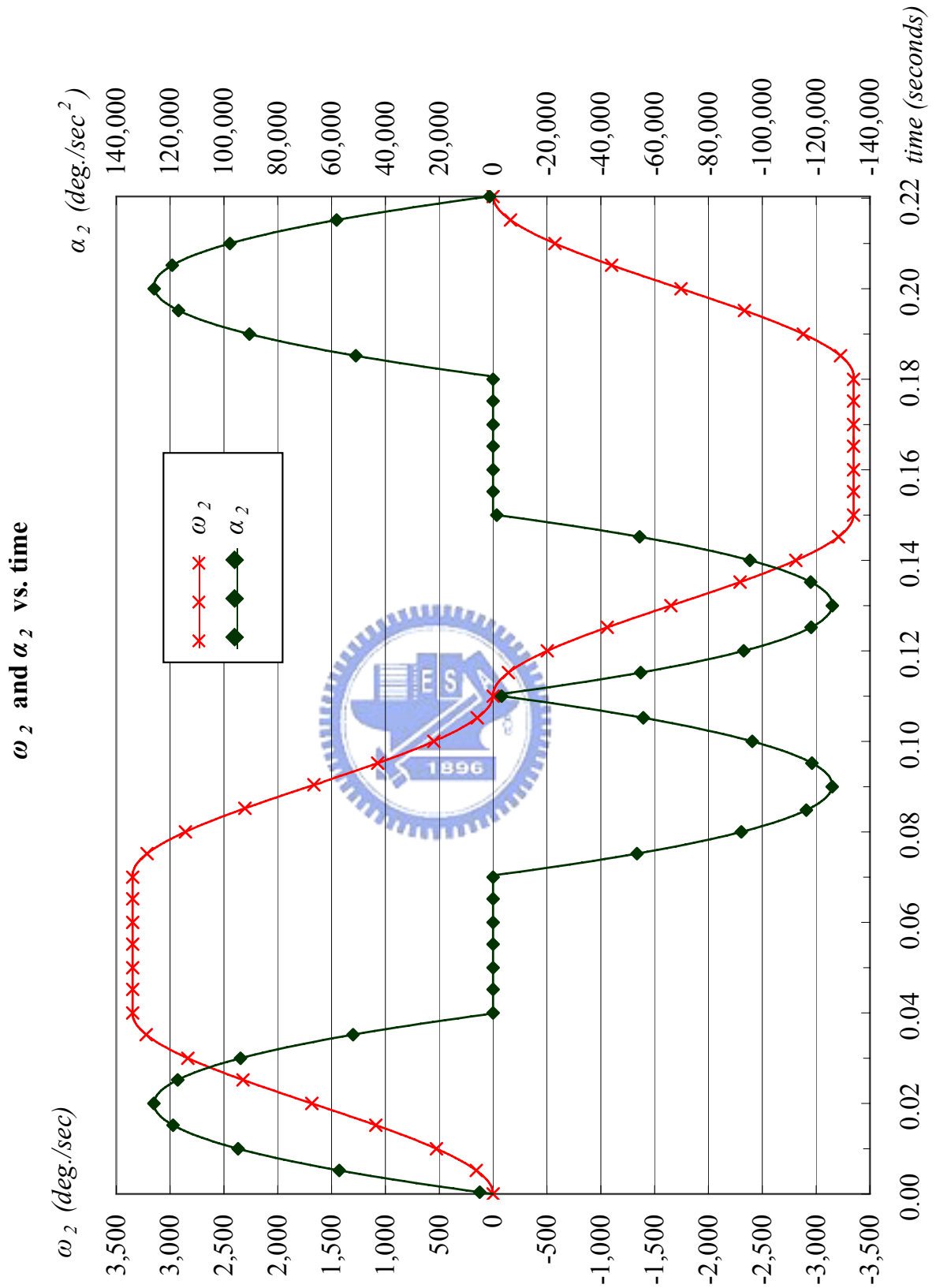


Fig.4.2 Angular velocity and angular acceleration of crank of the chip's pick and place mechanism designed by ITRI

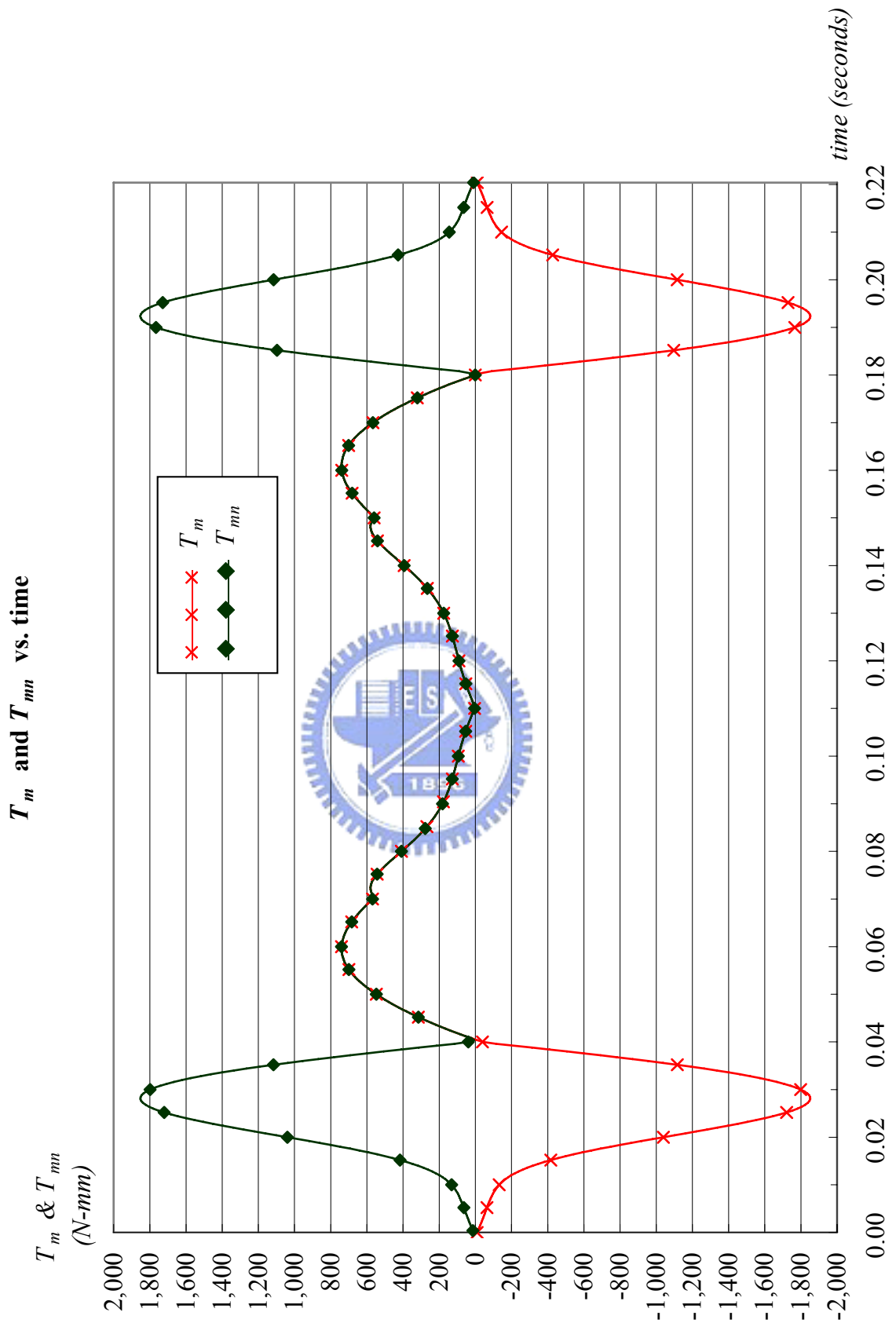


Fig.4.3 Torque driven by motor of the chip's pick and place mechanism designed by ITRI

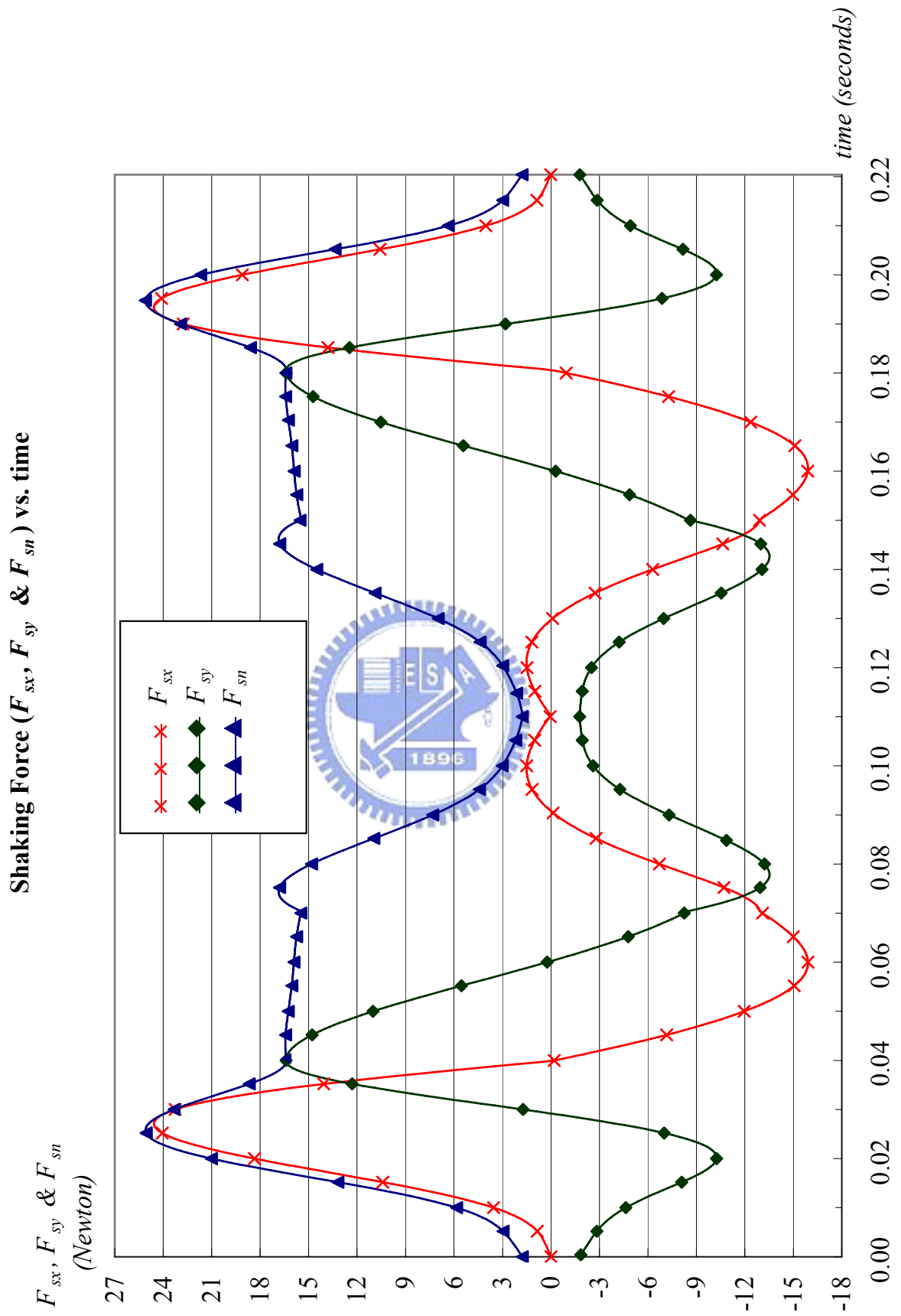


Fig.4.4 Shaking force of the chip's pick and place mechanism designed by ITRI

Shaking Torque (T_s , T_{sn}) vs. time

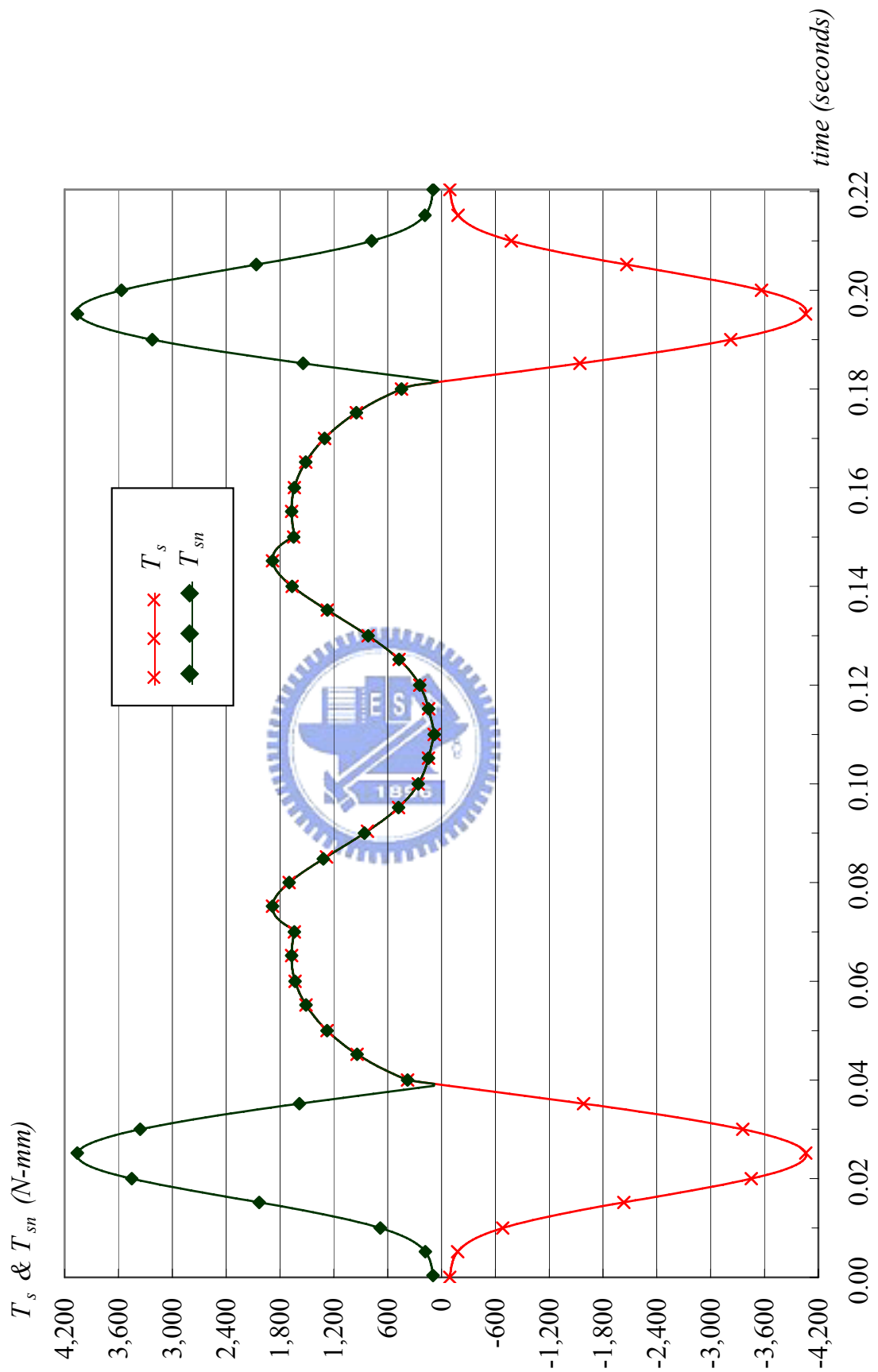


Fig.4.5 Shaking torque of the chip's pick and place mechanism designed by ITRI

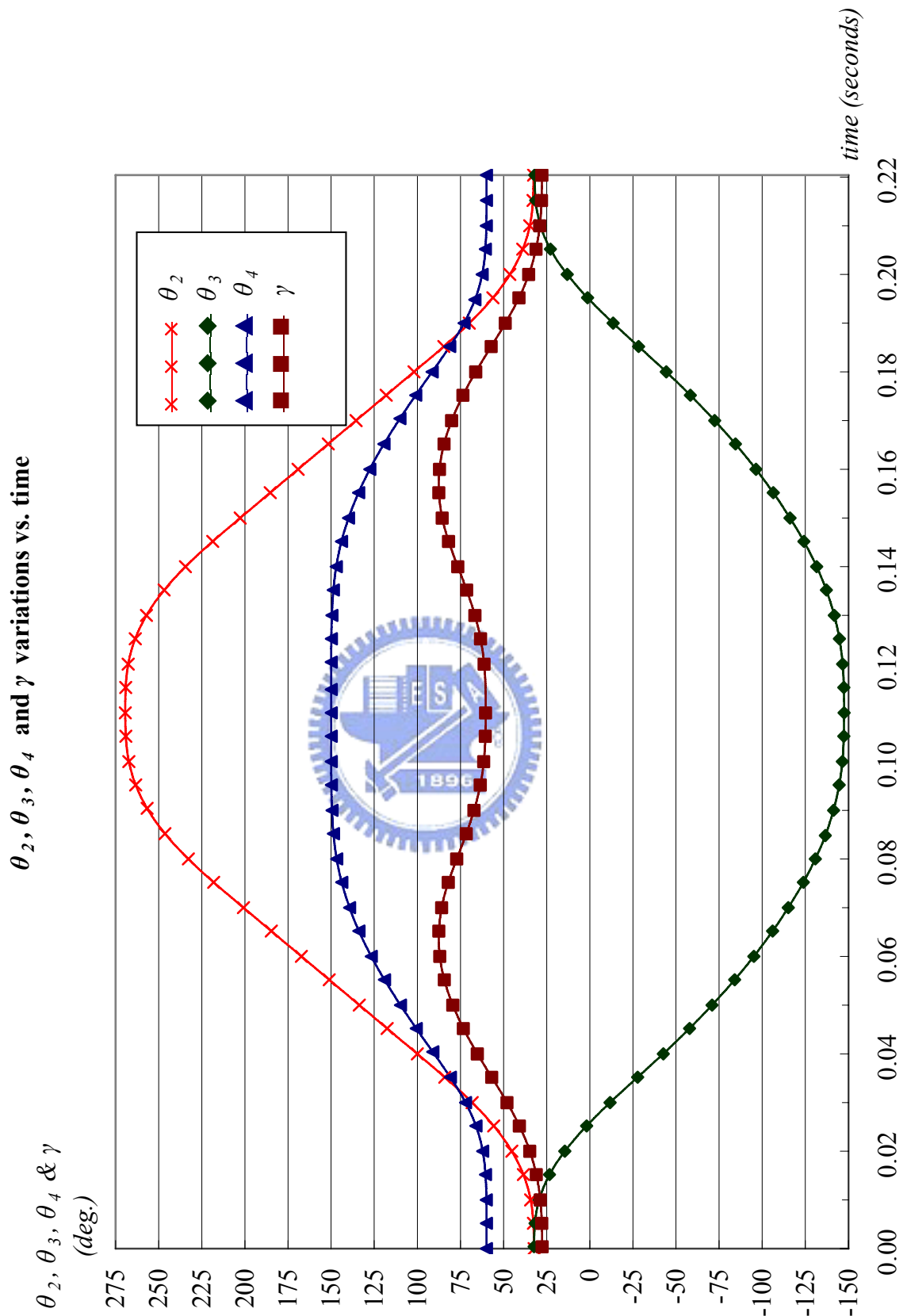


Fig.4.6 Angular ($\theta_2, \theta_3, \theta_4, \gamma$) variations of the chip's pick and place mechanism designed by ITRI

In general, the finite element analysis (FEA) is run at a static condition, while the chip's pick and place mechanism is run in a continuous motion in the present design. Therefore the FEA need to run at some specified positions or intervals in this continuous motion. Computer software Nastran is chosen to run the FEA in the present research. Due to the performance of personal computer, the simulation time step for the FEA in the present research is set as 0.002 seconds, which is five times larger than the time step size set in ADAMS.

Table 4.3 shows the Nastran FEA settings of nodes and elements for three bars (crank, coupler and bonding arm) of the chip's pick and place mechanism designed by ITRI; while Fig.4.7 and Table 4.4 show the FEA results based on the of Nastran simulations. Figures 4.8 to 4.10 show the stresses distributions on crank, coupler and bonding arm, respectively.

It is also noted that the simulated results are symmetric to the pick-to-place and place-to-pick actions.



Table 4.3 FEA settings of the pick and place mechanism designed by ITRI

	Mesh Size (mm)	Nodes	Elements
Crank	2.5	9707	5462
Coupler	2.5	11146	5706
Bonding Arm	2.5	31603	16921

Table 4.4 FEA simulation results of the pick and place mechanism designed by ITRI

	Time (sec.)	Max. Stress (MPa)	Min. Safety Factor
Crank	0.024 / 0.198	10.8 / 10.7	46.6 / 47.1
Coupler	0.024 / 0.198	12.6 / 12.4	39.8 / 40.6
Bonding Arm	0.024 / 0.198	43.7 / 43.7	11.7 / 11.7

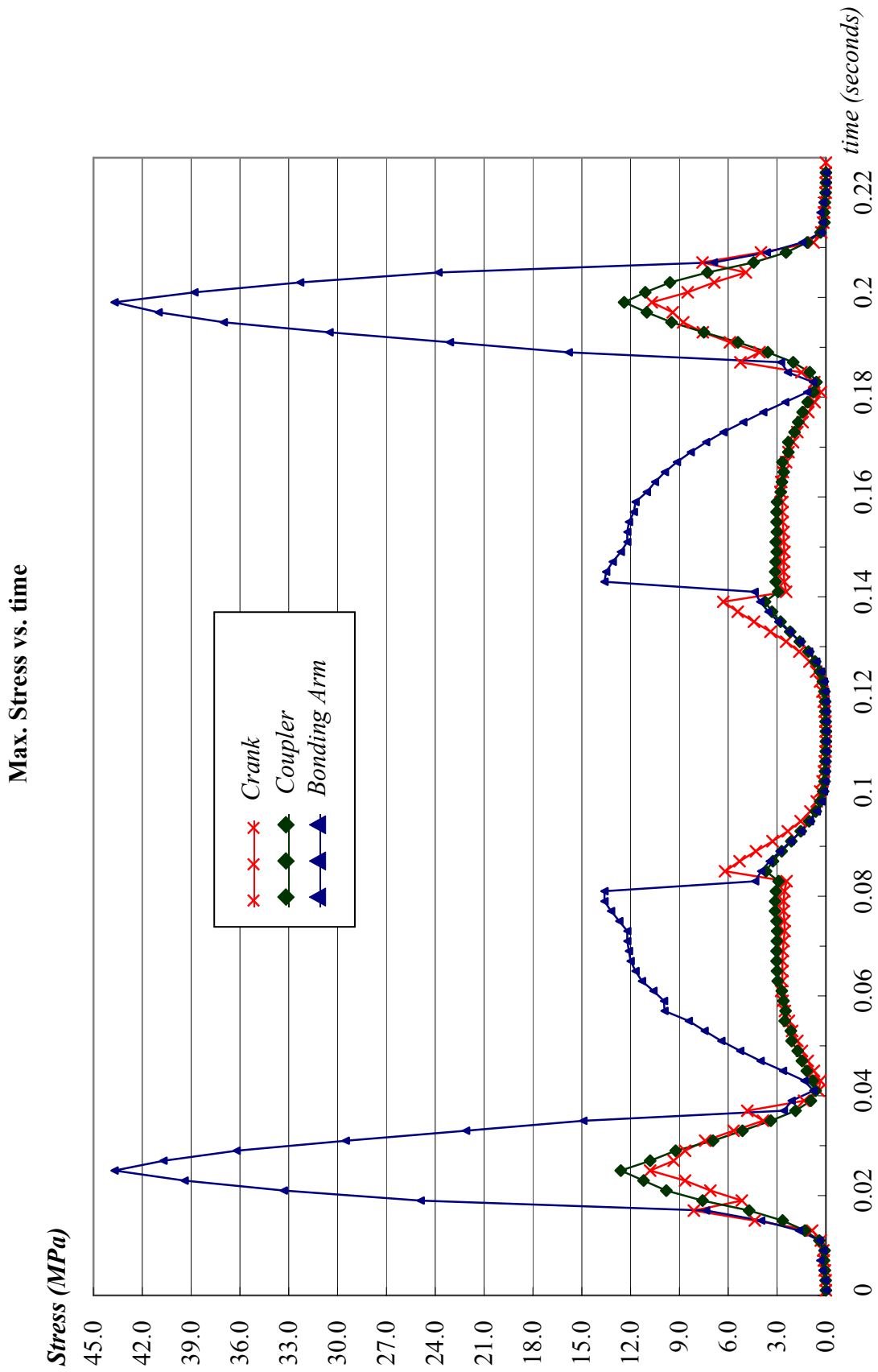


Fig.4.7 Maximum stress of the chip's pick and place mechanism designed by ITRI

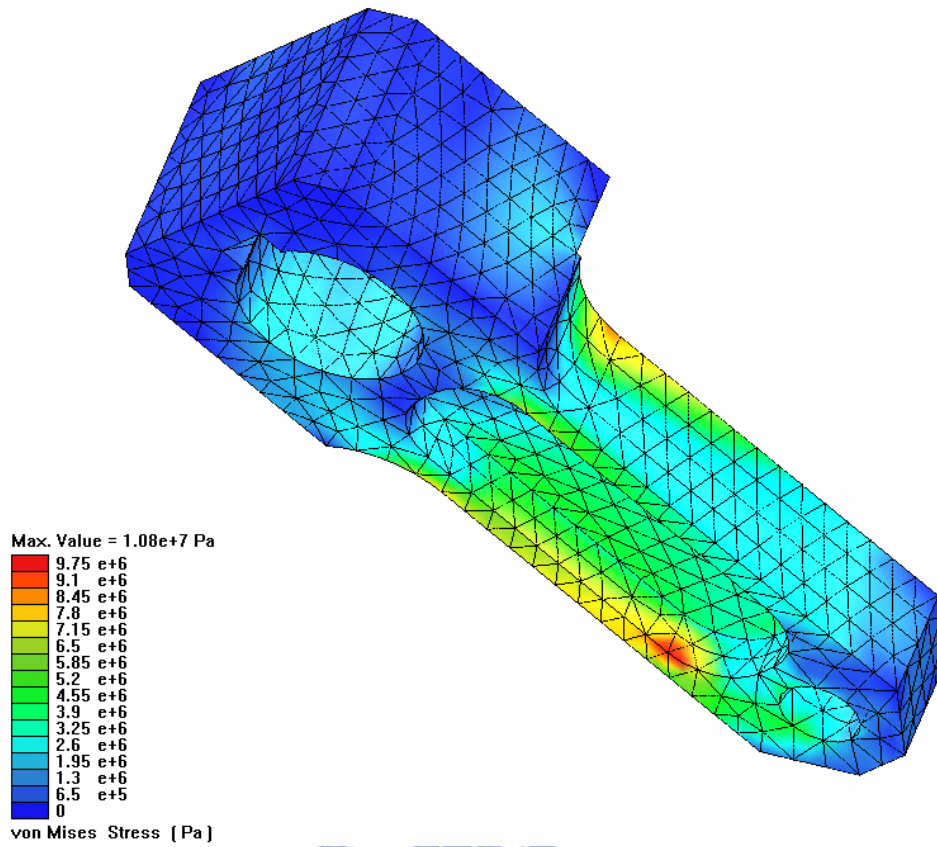


Fig.4.8 Stress distribution on the crank of the chip's pick and place mechanism designed by ITRI at 0.024 seconds

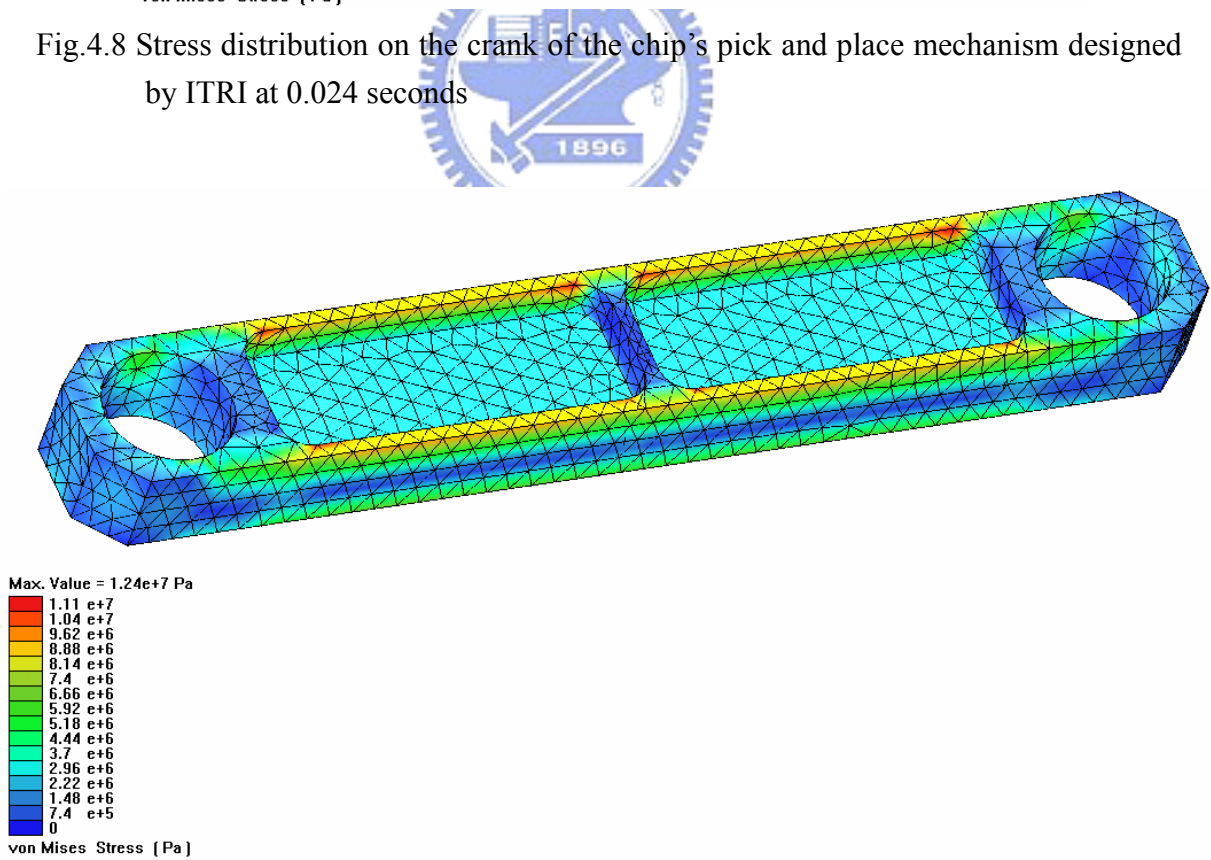


Fig.4.9 Stress distribution on the coupler of the chip's pick and place mechanism designed by ITRI at 0.024 seconds

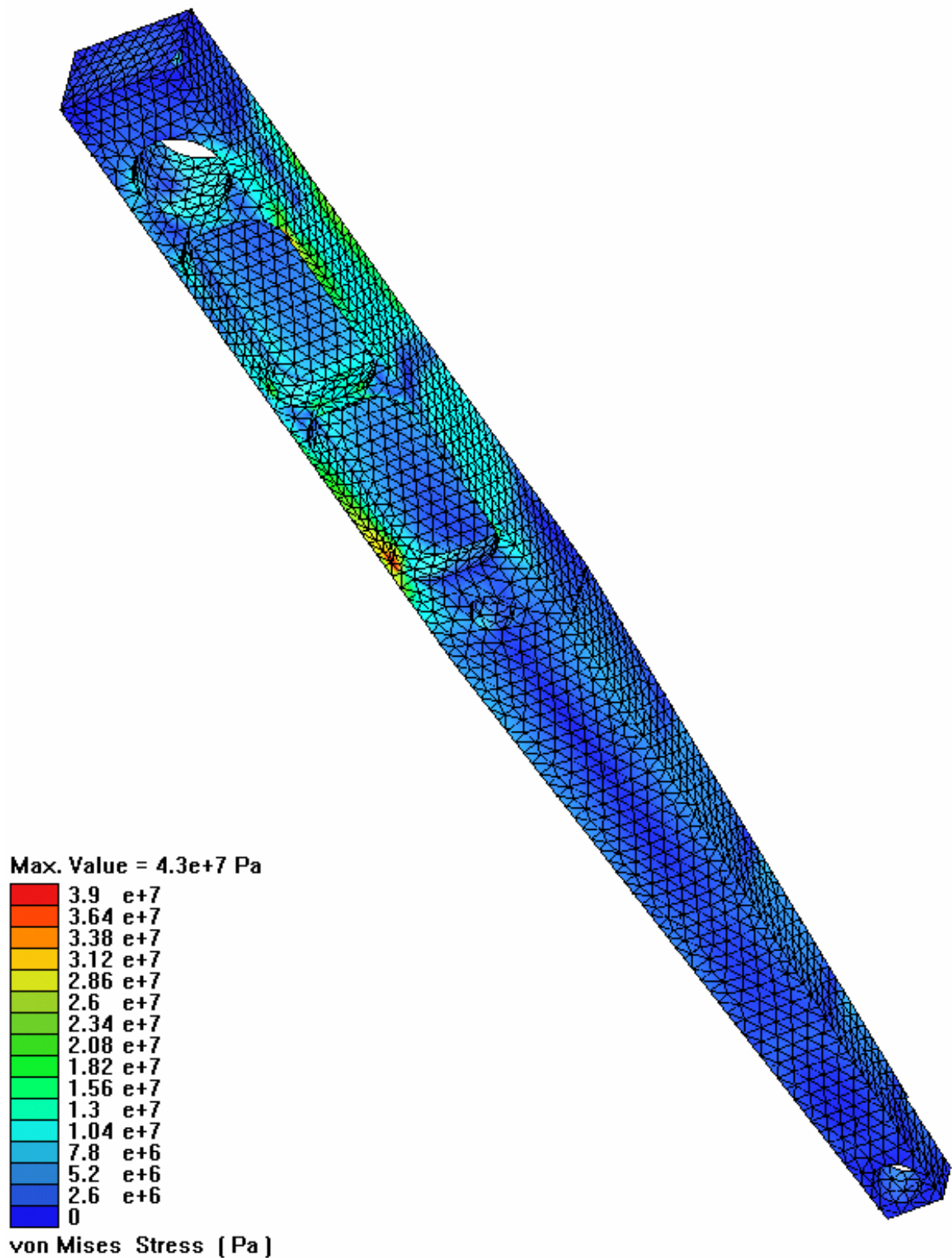


Fig.4.10 Stress distribution on the bonding arm of the chip's pick and place mechanism designed by ITRI at 0.024 seconds

4.3 Design Procedure and Dimensional Synthesis

In the present design, the main target is to achieve a design for high speed pick and place mechanism, while the torque driven by motor can be maintained in an acceptable range. The torque driven by motor is an issue in the analysis of mechanism process, which will be affected by the mass and moment of inertia of the mechanism structure. In this study, the optimization of mechanism is performed by computer software ADAMS, while Nastran is used as a tool to check the stresses induced by bars. Figure 4.11 shows the design procedures of the present design.

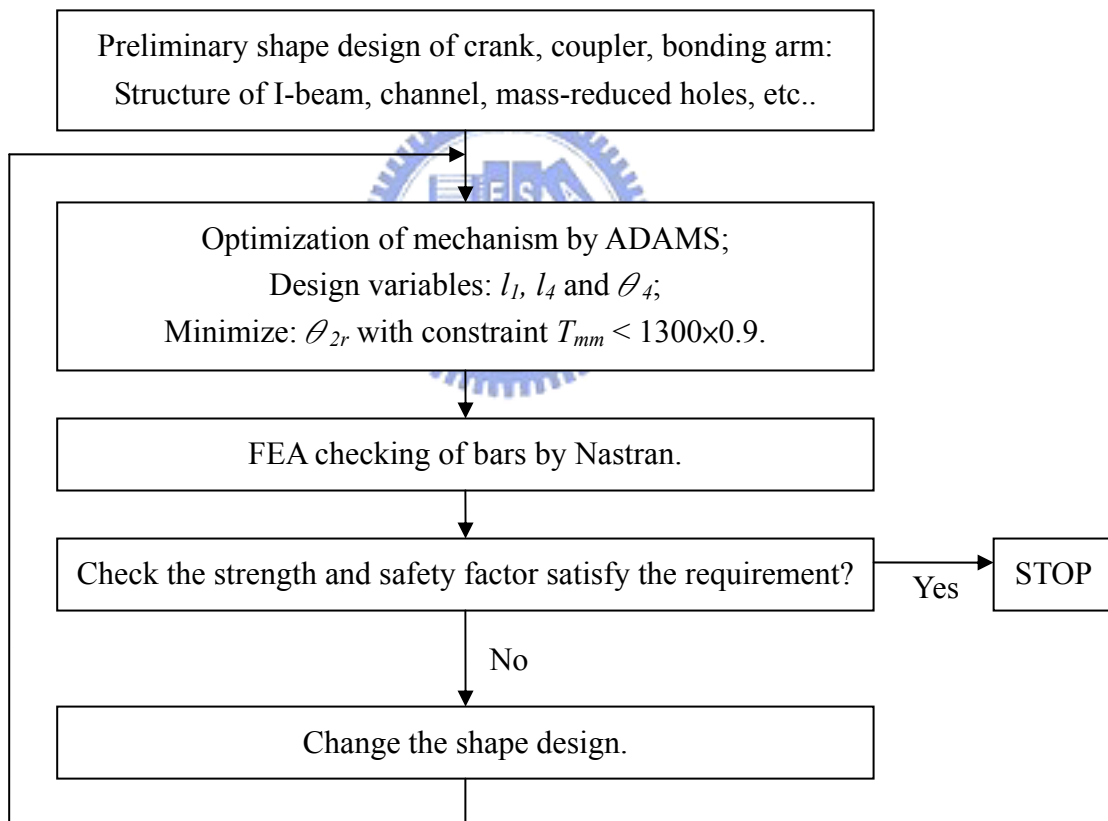


Fig.4.11 Procedures of the proposed design

There are two approaches that can achieve the actions of pick and place; one is that the crank keeps rotating in a same direction (i.e. crank has a 360° rotation), the other is that the crank rotates back and forth between the two positions of pick and place (i.e. crank has a

back-and-forth rotation). In the proposed design, the latter approach is used.

variables : $l_1, l_2, l_3, l_4, \theta_{2i}, \theta_{3i}, \theta_{4i}, \theta_{2f}, \theta_{3f}, \theta_{4f}, \gamma_i$, and γ_f

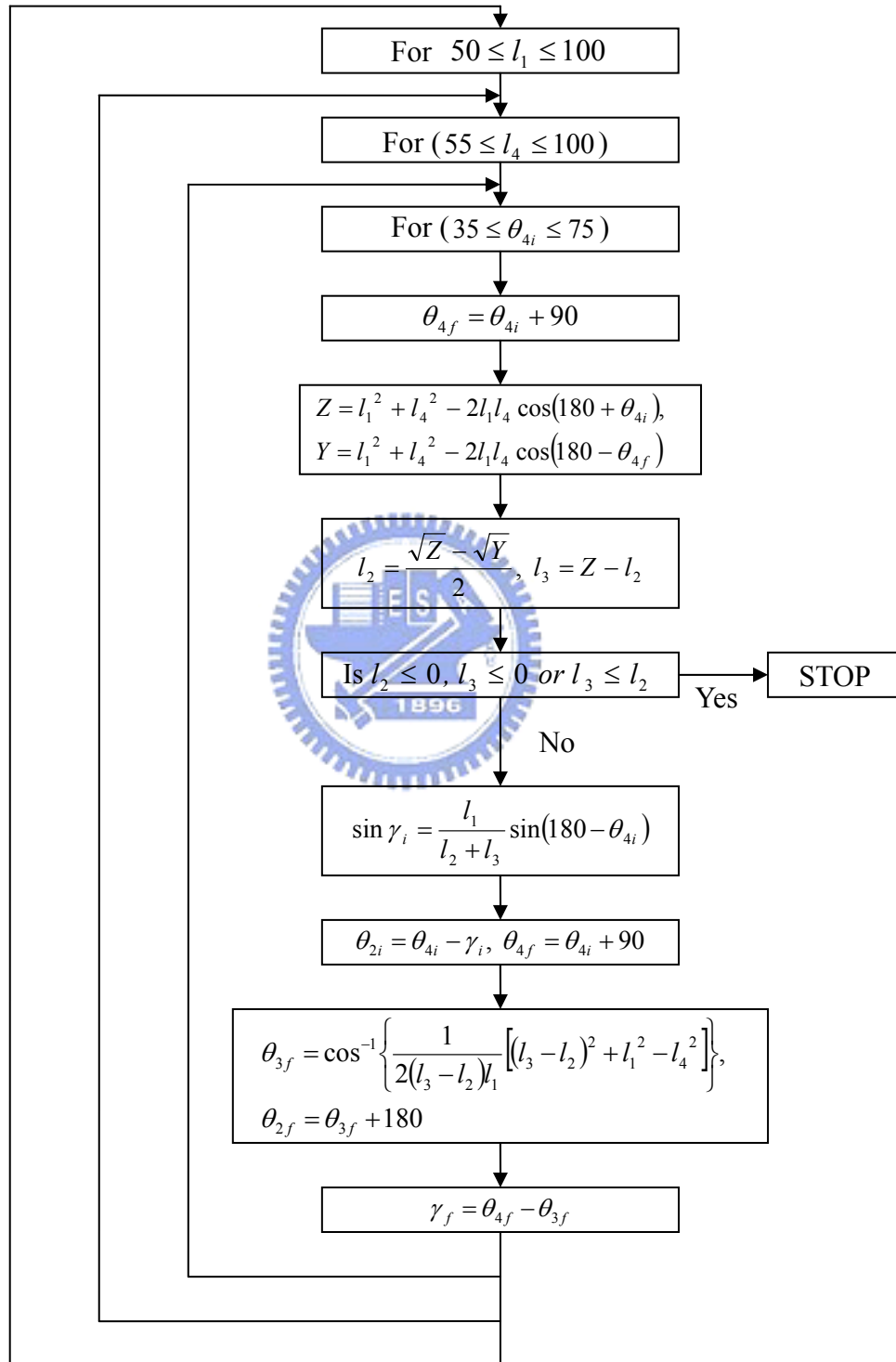


Fig.4.12 Procedure of dimensional synthesis

With the requirements the mechanism is designed to perform pick and place action (refer to Figs. 3.2 and 3.3) at the first and second toggle points. Figure 4.12 shows the procedure of dimensional synthesis.

There are three main parameters (l_1 , l_4 , and θ_{4i} in the proposed design) which are used to find the dimensions of the four-bar linkage. Due to the space for motor installation, avoiding the huge vibration at the end of bonding arm, and avoiding the interference of space; the dimensions of these parameters are set to lie in the range as follows:

$$50mm \leq l_1 \leq 100mm , \quad (34)$$

$$55mm \leq l_4 \leq 100mm , \quad (35)$$

$$\text{and } 35^\circ \leq \theta_{4i} \leq 75^\circ . \quad (36)$$

4.4 Structure Design of Bars

The structure designs of the bars are shown in Figs.4.13 to 4.15. In order to assemble with the bearings, pivot pins and VCM, the dimension of width and height of the bars are fixed; the widths and heights of crank, coupler and rocker are chosen by:

$$w_2 = w_3 = 18mm , \quad (37)$$

$$w_4 = 20mm , \quad (38)$$

$$h_2 = h_3 = 6mm , \quad (39)$$

$$\text{and } h_4 = 10mm . \quad (40)$$

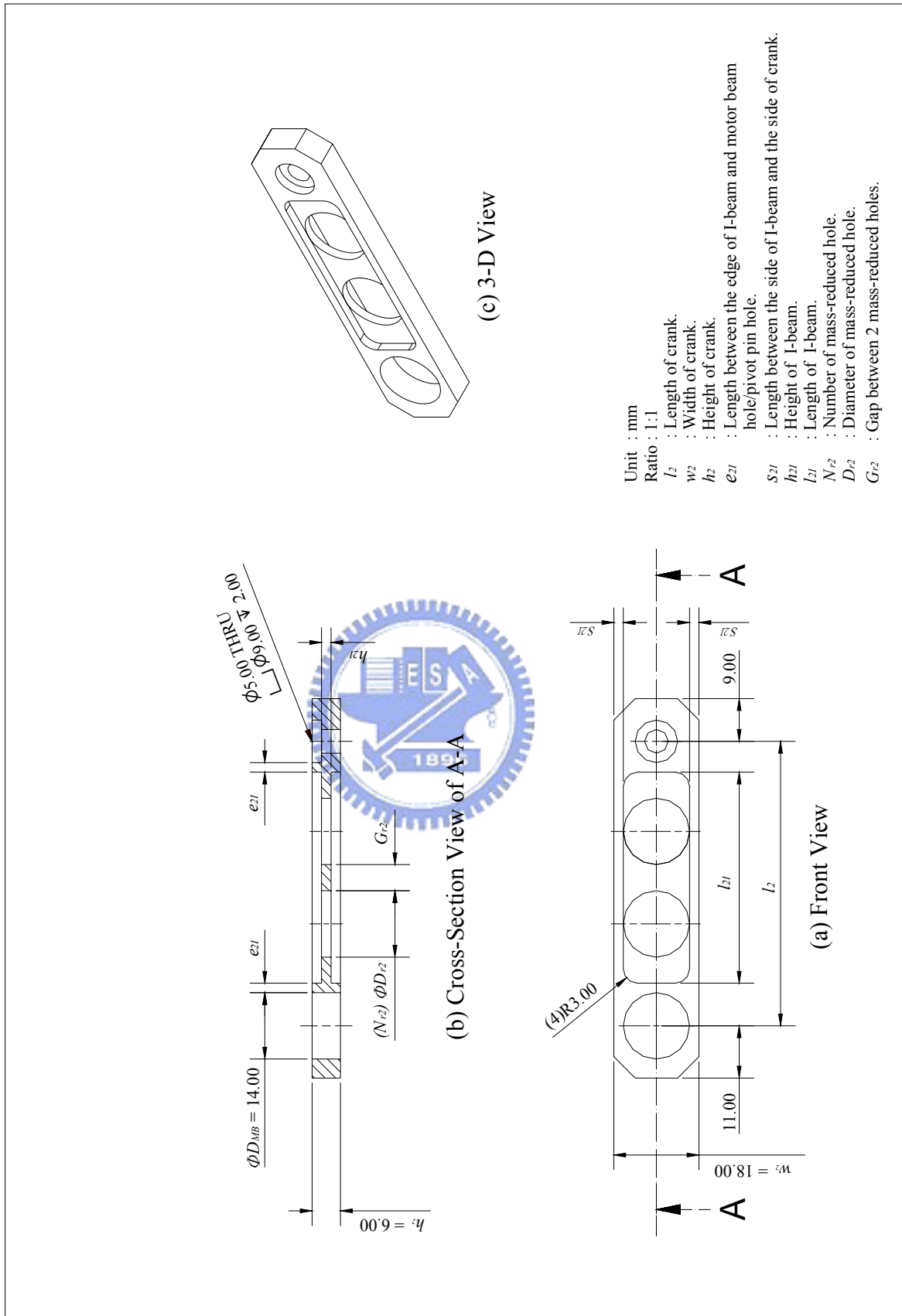


Fig.4.13 Schematic view of the present design- crank

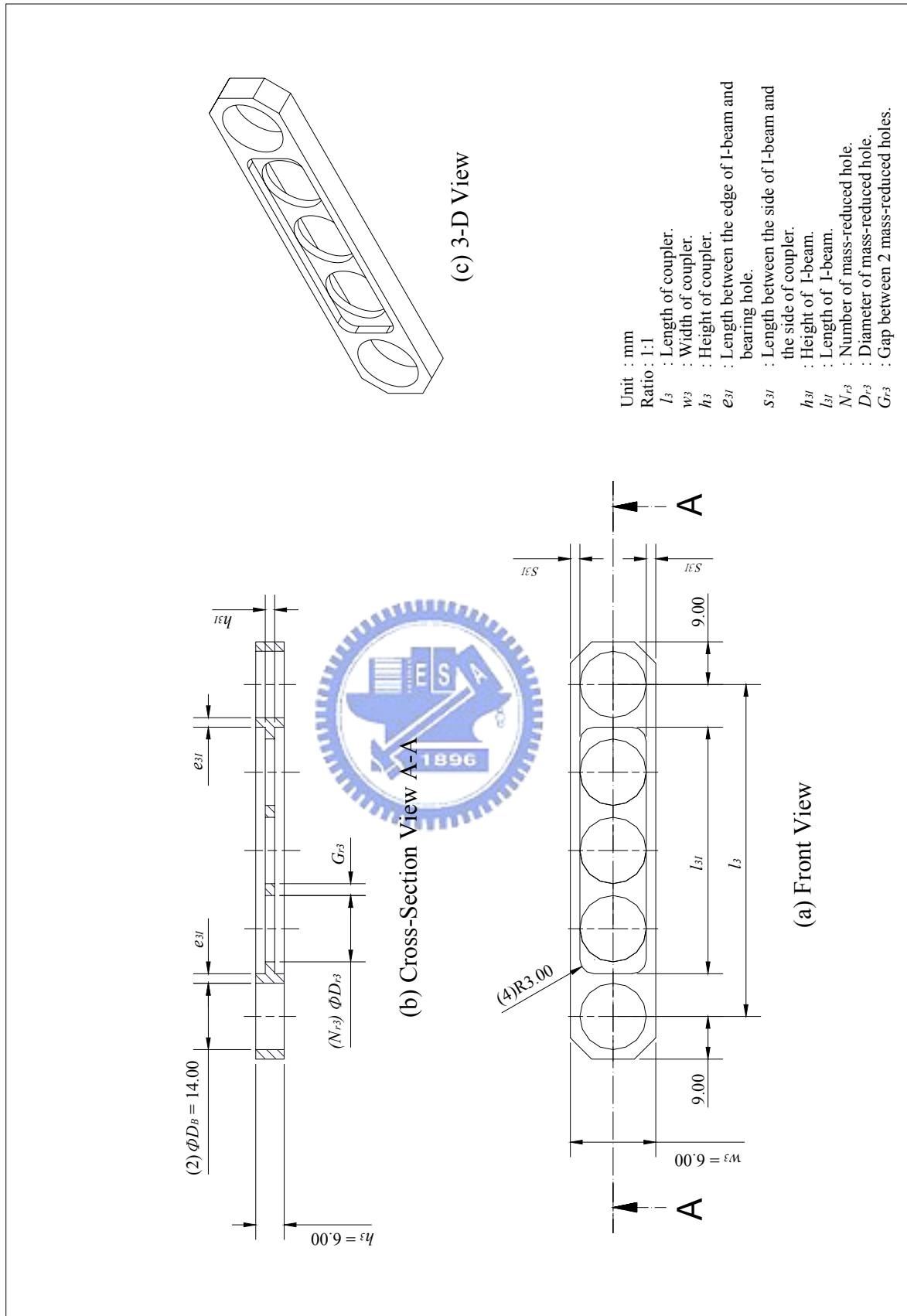


Fig.4.14 Schematic view of the present design- coupler

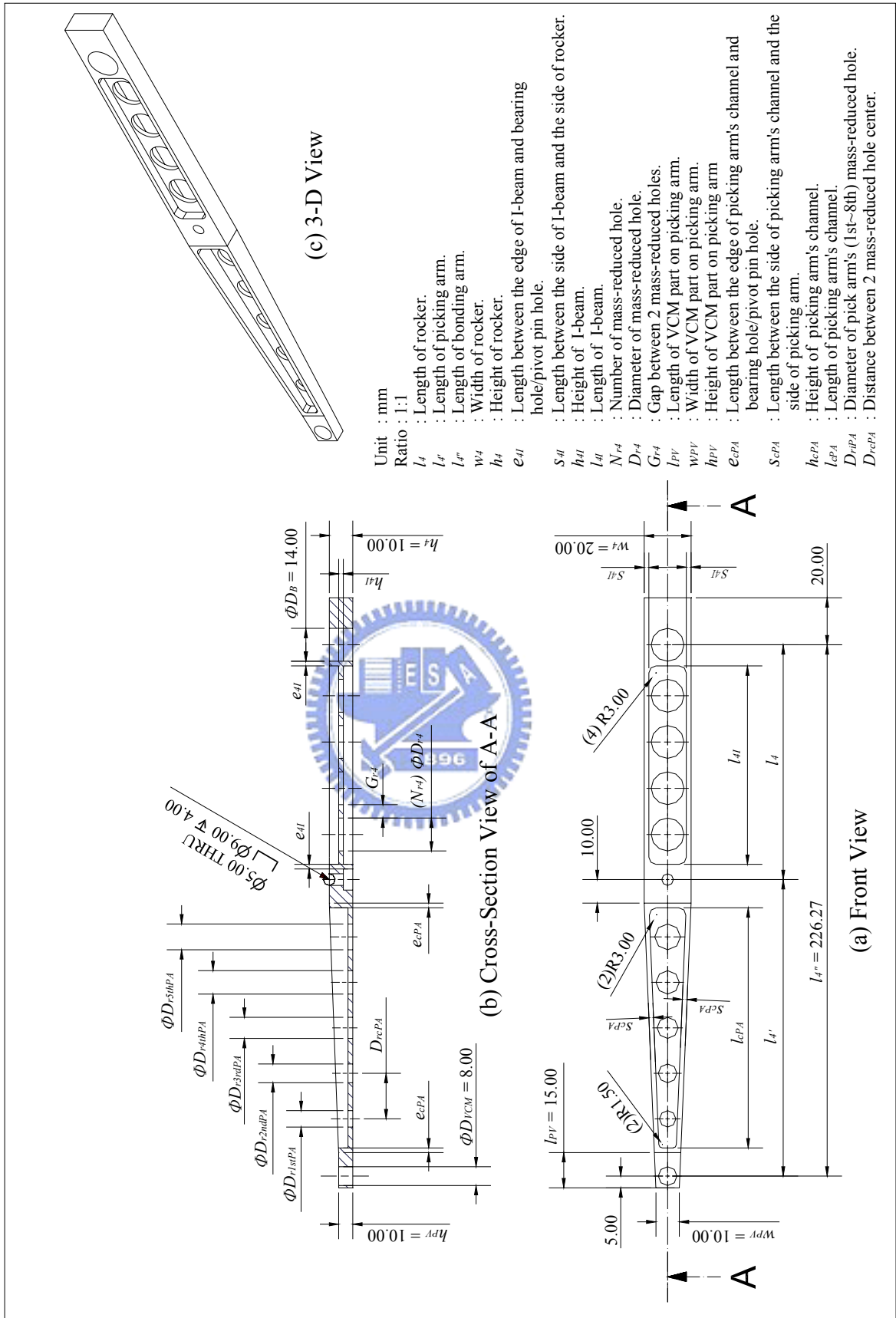


Fig.4.15 Schematic view of the present design- bonding arm

In order to obtain a good strength and less mass for the bar structure which can achieve a better performance, the shapes of the cross-section of crank, coupler and rocker are like an I-beam, and the shape of the picking arm is like a channel. Besides, some mass-reduced holes are also proposed in the bars.

Some parameters which are used to change the structures of bars are variable in some specified values, as listed in Table 4.5. The numbers of mass-reduced holes for each bar are calculated due to the length of the I-beam/channel, which can be referred to the calculation procedures shown in Figs. 4.16 and 4.17.

Table 4.5 Parameters which vary in some specified values

	Values (mm)
s_{iI}	1.0 / 1.5 / 2.0
e_{iI}	1.0 / 1.5 / 2.0
h_{iI}	1.0 / 1.5 / 2.0
D_{ri}	14.0 / 16.0 / 17.0
G_{ri}	3.0 / 5.0
s_{cp}	1.0 / 1.5 / 2.0
e_{cp}	1.0 / 1.5 / 2.0
h_{cp}	1.0 / 1.5 / 2.0
D_{rPA}	14.0
G_{rPA}	3.0 / 5.0

Note: $i=2$ (crank), 3(coupler), 4(rocker);
PA= picking arm.

variables : $l_i, l_{il}, s_{il}, N_{ri}, D_{ri}, G_{ri}, G_{ti}, D_{rci}$;
 $i=2$ (crank), 3 (coupler), 4 (rocker)

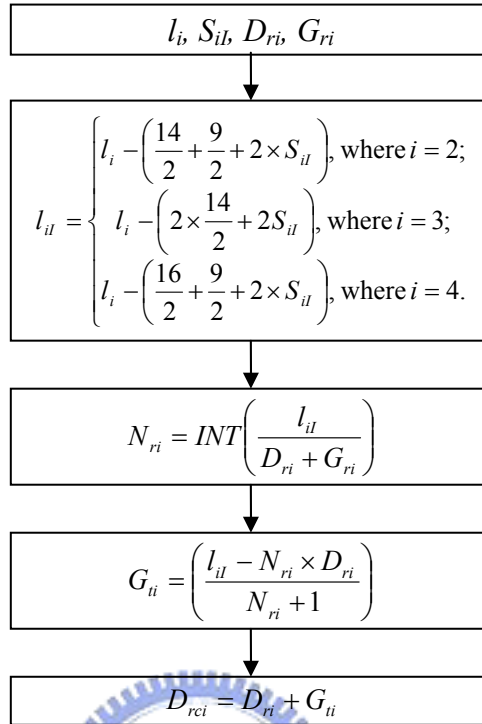


Fig.4.16 Procedures of building mass-reduced holes on the I-beam of crank, coupler, and rocker

variables : $l_4, l_{cp}, s_{cp}, N_{rPA}, D_{rPA}, G_{rPA}, D_{rcPA}$

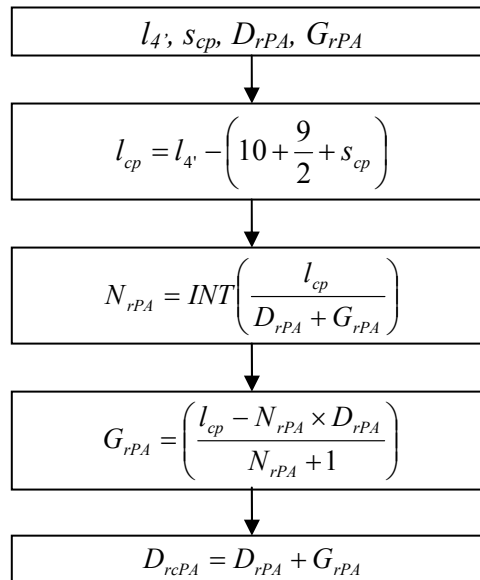


Fig.4.17 Procedures of building mass-reduced holes on the channel of picking arm

4.5 Sensitivity of Design Variables

Once the model of pick and place mechanism is created, the processes of analysis and optimization can be proceeded. Sensitivity analysis is performed to find out the effects of design variables on cost function in the optimization process.

In the sensitivity analysis, the variables are l_1 , l_4 and θ_4 , while the targets are the torque driven by motor and the crank rotation angle from pick to place position. The VCM's mass is set as 20g, the principle lengths of bars are set as the same to the design of ITRI case, that is:

$$l_1 = 85mm, \quad (41)$$

$$l_4 = 98mm, \quad (42)$$

$$\text{and } \theta_4 = 60^\circ. \quad (43)$$

The main parameters for the bars for the initial design of this study are listed in Table 4.6, where the model is shown in Fig.4.18.

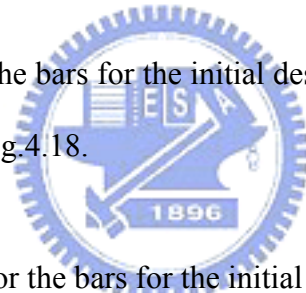


Table 4.6 Main parameters for the bars for the initial design of this study

Parameter	Value (mm)	Parameter	Value (mm)
w_2	18.0	s_{4I}	2.0
h_2	6.0	e_{4I}	2.0
w_3	18.0	h_{4I}	2.0
h_3	6.0	s_{cPA}	2.0
w_4	20.0	e_{cPA}	2.0
h_4	10.0	h_{cPA}	2.0
w_{PV}	10.0	D_{r2}	14.0
h_{PV}	6.0	G_{r2}	5.0
s_{2I}	2.0	D_{r3}	14.0
e_{2I}	2.0	G_{r3}	5.0
h_{2I}	2.0	D_{r4}	14.0
s_{3I}	2.0	G_{r4}	5.0
e_{3I}	2.0	D_{rPA}	14.0
h_{3I}	2.0	G_{rPA}	5.0

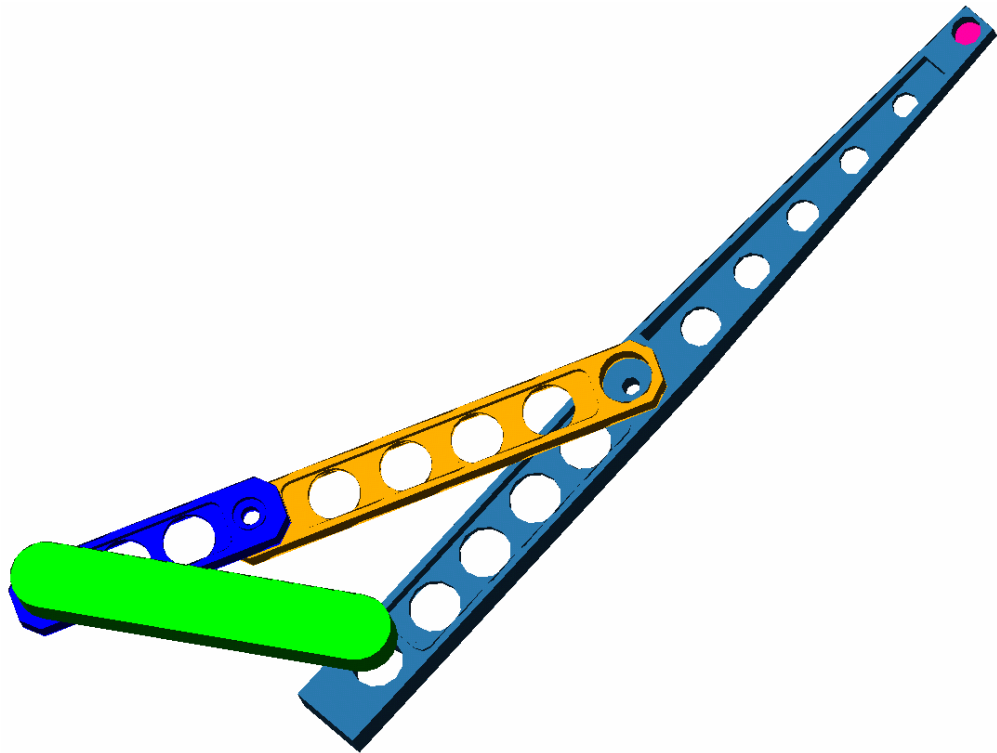


Fig.4.18 Initial chip's pick and place mechanism in the present design

Five values of design variables are chosen to check the sensitivity on the torque and crank rotation angle, which are listed in Table 4.7. The results of sensitivities corresponding to the torque driven by motor and crank rotation angle are shown in Figs.4.19 and 4.20. It is found that the length of crank, l_1 , is very sensitive to the torque driven by motor and also to the crank rotation angle, while the torque driven by motor is inverse proportional to the crank rotation angle.

Table 4.7 Values of the principle design variables used to check the sensitivity

	l_1 (mm)	l_4 (mm)	θ_4 (deg.)
1	50.00	55.00	35.00
2	62.50	66.25	45.00
3	75.00	77.50	55.00
4	87.50	88.75	65.00
5	100.00	100.00	75.00

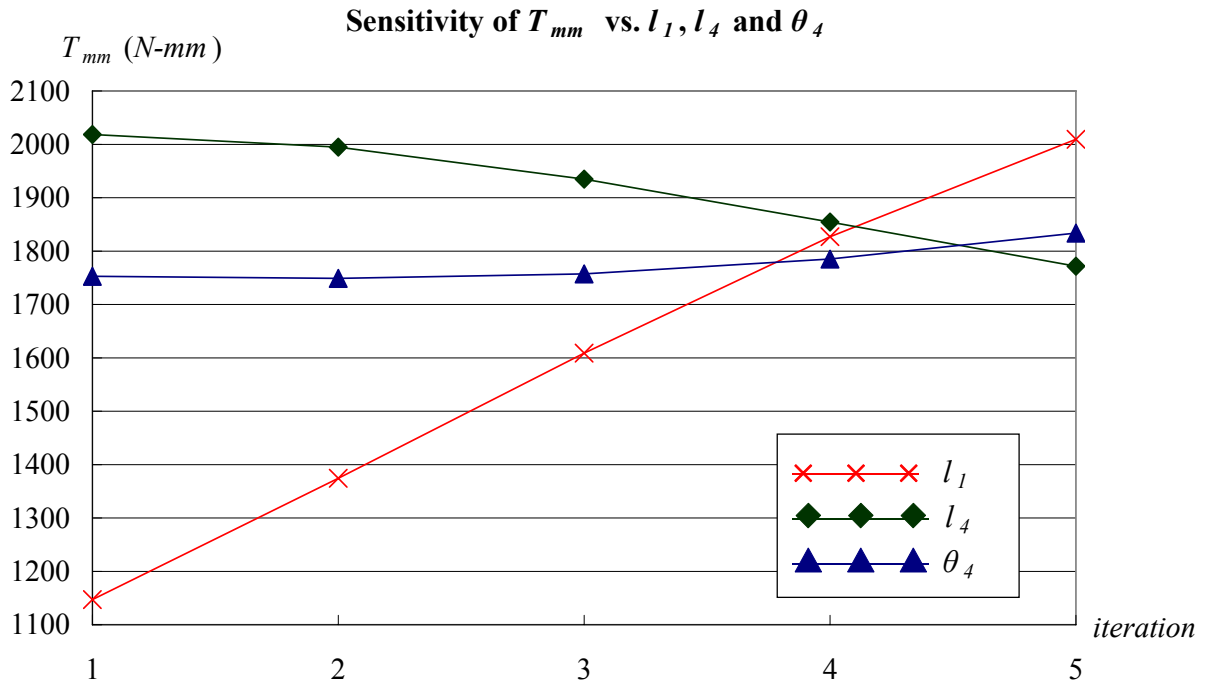


Fig.4.19 Sensitivity of max. torque driven by motor vs. design variables (l_1, l_4, θ_4)

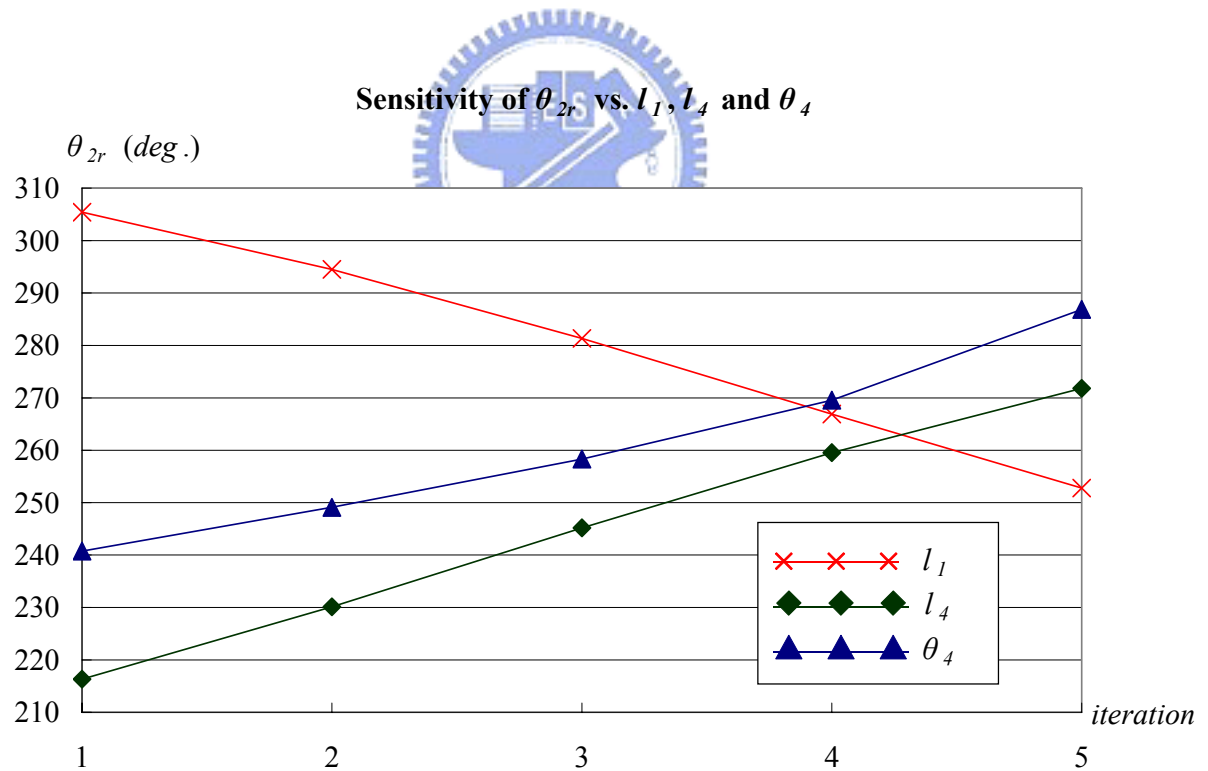


Fig.4.20 Sensitivity of crank rotation angle vs. design variables (l_1, l_4, θ_4)

Another issue which may affect the performance of motor is the mass of VCM. A sensitivity analysis is performed in order to compare the effects of different VCM's masses on

the maximum torque driven by motor, and the results are shown in Fig.4.21. The analysis results reveal that a lighter mass of VCM receives a better performance (i.e. a smaller driven torque is required for the motor), and a smaller crank rotation angle can be achieved.

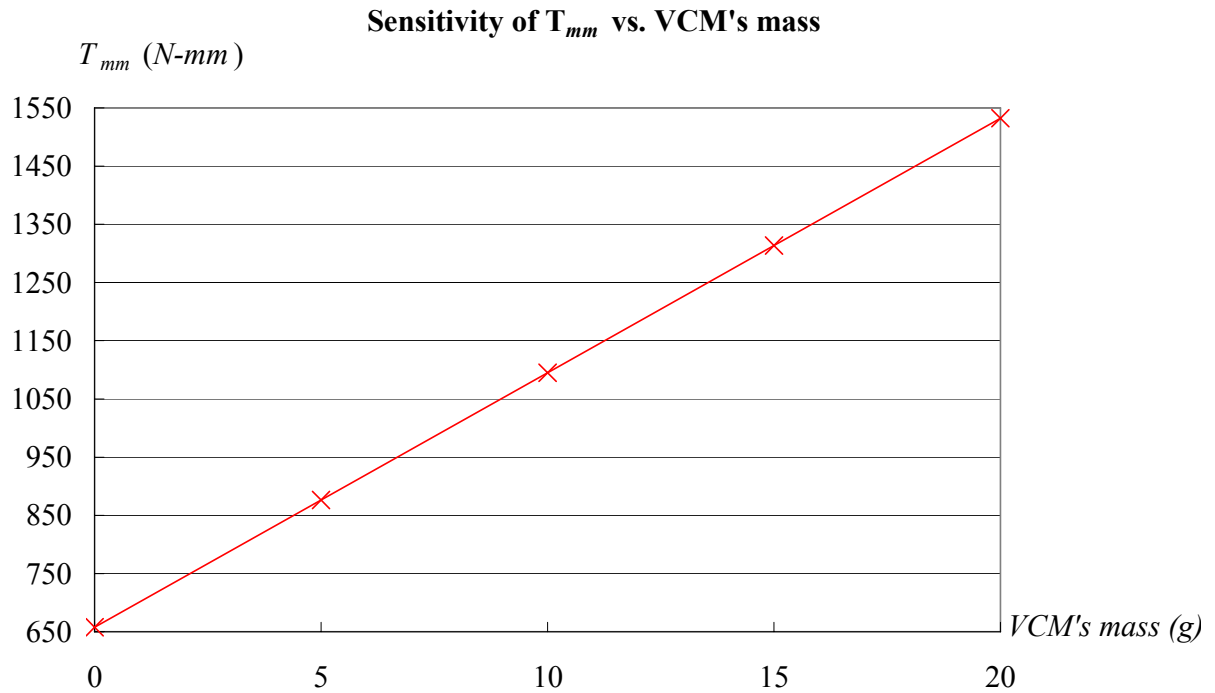


Fig.4.21 Sensitivity of max. torque driven by motor vs. VCM's mass

4.6 Result of the Present Design

As the input mode of motor is symmetric to the pick-to-place and place-to-pick actions, which causes the forces, torques, angular velocities etc. also symmetric, therefore, only the investigation on half a cycle is enough. The half-cycle of pick-to-place action is chosen here.

Six cases will be run based on the procedures shown in Fig.4.11, where the parameter values are listed in Table 4.8.

Table 4.8 Parameters changed in the present design (all units are in mm)

	Case 1	Case 2	Case 3	Case 4	Case 5	Case 6
$s_{2I} / e_{2I} / h_{2I}$	2.0	1.5	1.5	1.0	1.0	1.0
D_{r2}	14.0	14.0	14.0	14.0	16.0	16.0
G_{r2}	5.0	5.0	3.0	3.0	3.0	3.0
$s_{3I} / e_{3I} / h_{3I}$	2.0	1.5	1.5	1.0	1.0	1.0
D_{r3}	14.0	14.0	14.0	14.0	16.0	16.0
G_{r3}	5.0	5.0	3.0	3.0	3.0	3.0
$s_{4I} / e_{4I} / h_{4I}$	2.0	1.5	1.5	1.0	1.0	1.0
D_{r4}	14.0	14.0	14.0	14.0	16.0	17.0
G_{r4}	5.0	5.0	3.0	3.0	3.0	3.0
$s_{cPA} / e_{cPA} / h_{cPA}$	2.0	1.5	1.5	1.0	1.0	1.0
D_{rPA}	14.0	14.0	14.0	14.0	14.0	14.0
G_{rPA}	5.0	5.0	3.0	3.0	3.0	3.0
D_{r1stPA}	7.0	7.0	7.0	7.0	9.0	9.0
D_{r2ndPA}	8.0	8.0	8.0	8.0	10.0	10.0
D_{r3rdPA}	9.0	9.0	9.0	9.0	11.0	11.0
D_{r4thPA}	10.0	10.0	10.0	10.0	12.0	12.0
D_{r5thPA}	11.0	11.0	11.0	11.0	13.0	13.0
D_{r6thPA}	12.0	12.0	12.0	12.0	14.0	14.0
D_{r7thPA}	13.0	13.0	13.0	13.0	15.0	15.0
D_{r8thPA}	14.0	14.0	14.0	14.0	16.0	16.0

In order to achieve the shortest time for pick and place action, and to protect the motor; the optimization in the present design is to minimize the crank rotation angle, while the torque driven by motor is still in an acceptable range, which is chosen as 90% of the rated torque.

The above engineering problem can be expressed as follows:

$$\text{Minimize } \theta_2(l_1, l_4, \theta_4),$$

$$\text{Subject to } T_{mm}(l_1, l_4, \theta_4) \leq 0.9 \times 1300(N - mm). \quad (44)$$

As the optimization problem in the present design is a nonlinear constrained multivariable problem, the sequential quadratic programming (SQP) method is chosen as the

optimization algorithm.

The Nastran FEA settings for each case are shown in Table 4.9. Variations on design variables, cost functions and constraints in case 1 to 6 are shown in Figs.4.22 to 4.27.

Summary results for the cases in the present design are shown in Table 4.10.

Table 4.9 FEA setting in the present design

		Mesh Size (mm)	Nodes	Elements			Mesh Size (mm)	Nodes	Elements
Case 1	Crank	2.5	3186	1644	Case 4	Crank	2.5	3170	1624
	Coupler	2.5	5881	2784		Coupler	2.5	4674	2160
	Bonding Arm	2.5	17317	8812		Bonding Arm	2.5	17008	8493
Case 2	Crank	2.5	3376	1740	Case 5	Crank	2.5	3287	1689
	Coupler	2.5	5375	2507		Coupler	2.5	4506	2044
	Bonding Arm	2.5	16760	8411		Bonding Arm	2.5	16501	8211
Case 3	Crank	2.5	3410	1761	Case 6	Crank	2.5	3284	1688
	Coupler	2.5	5107	2338		Coupler	2.5	4513	2049
	Bonding Arm	2.5	16721	8397		Bonding Arm	2.5	16690	8325

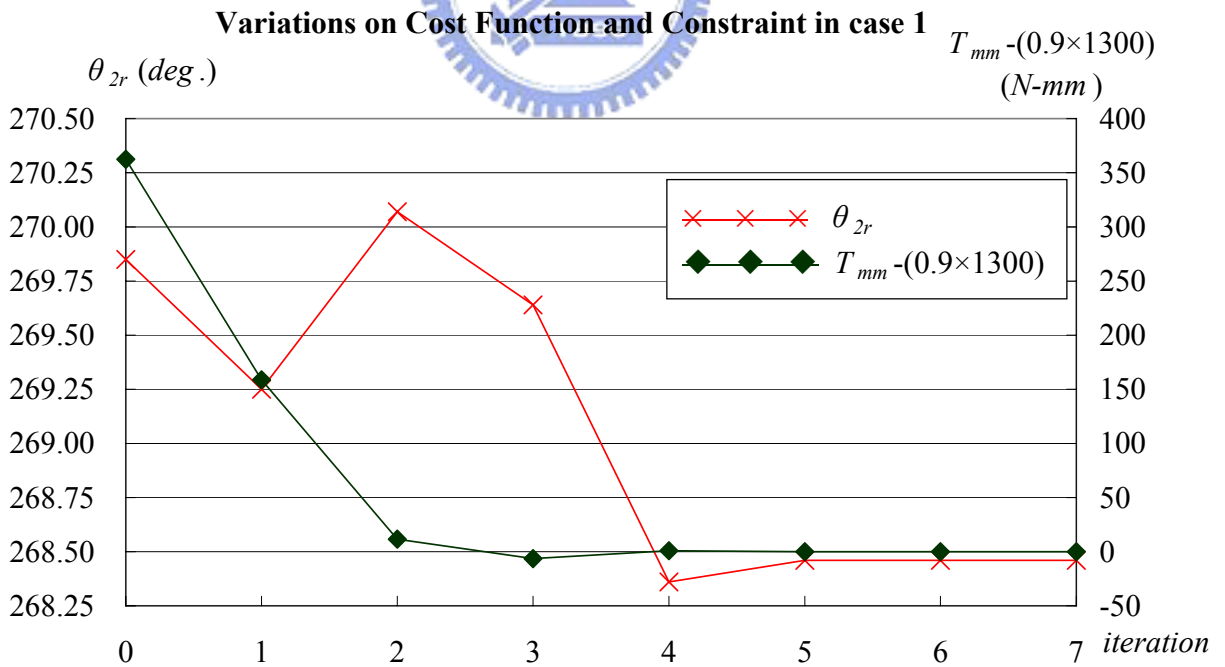
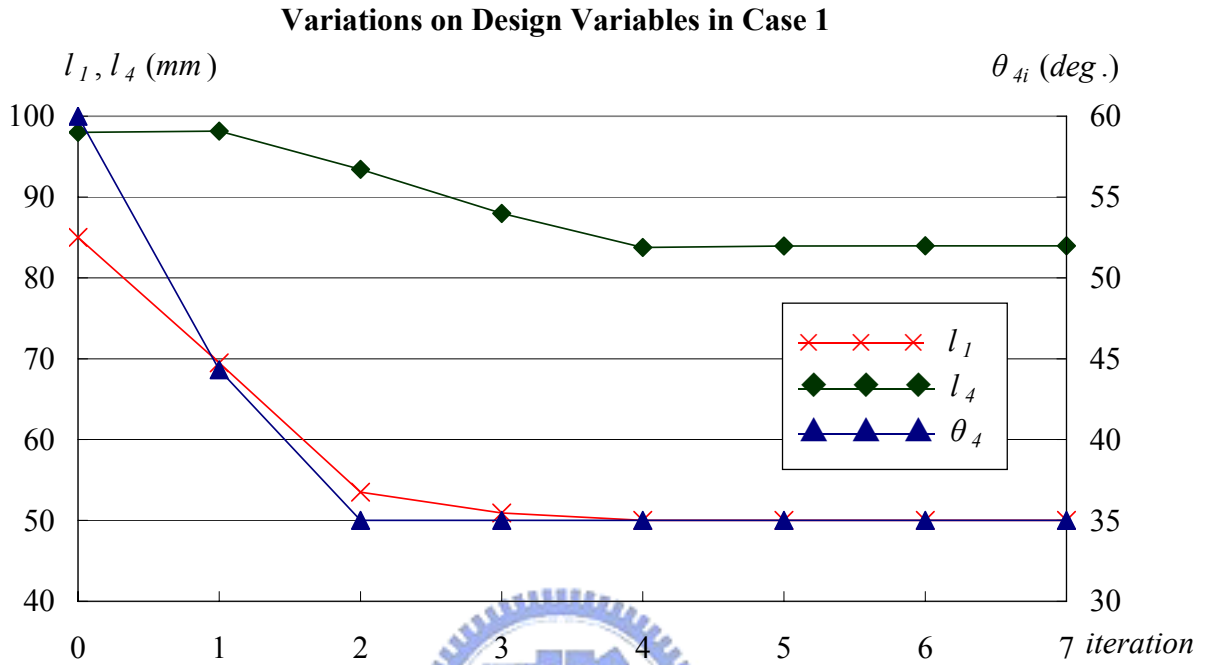


Fig.4.22 Variations on design variables, cost function and constraint in case 1

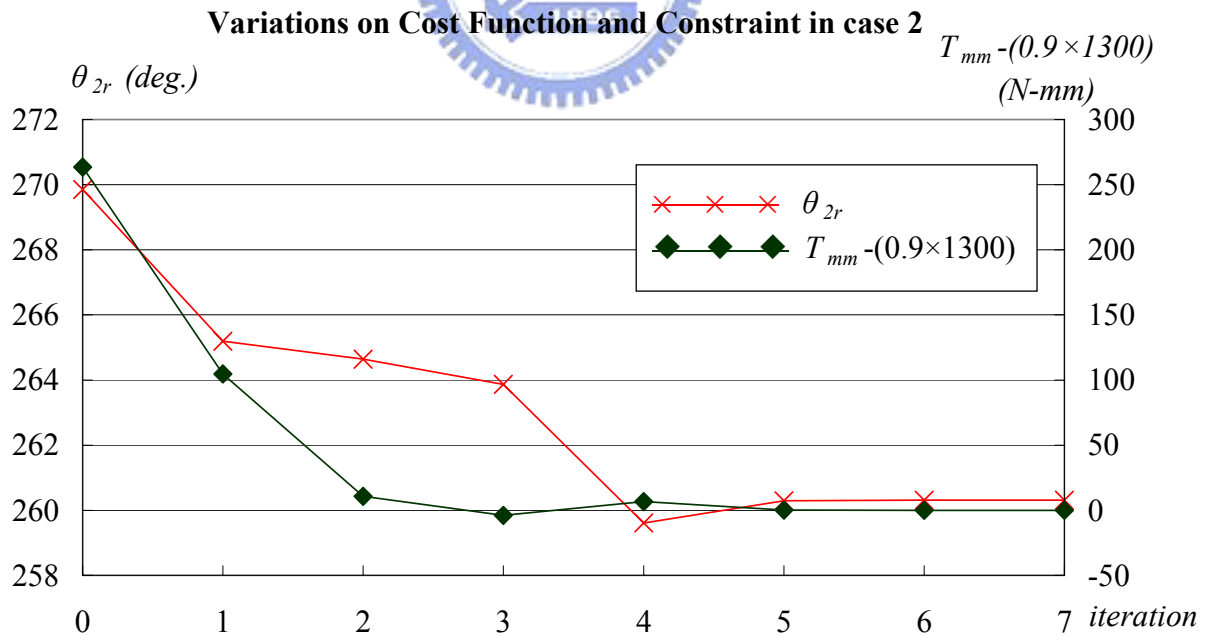
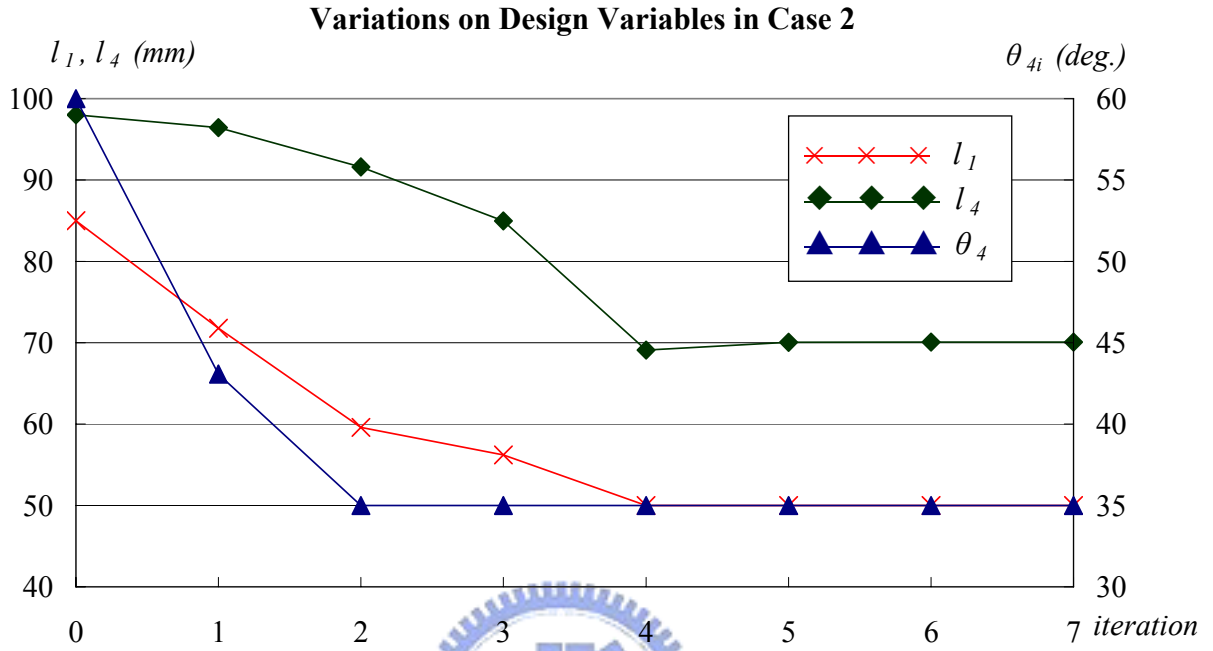


Fig.4.23 Variations on design variables, cost function and constraint in case 2

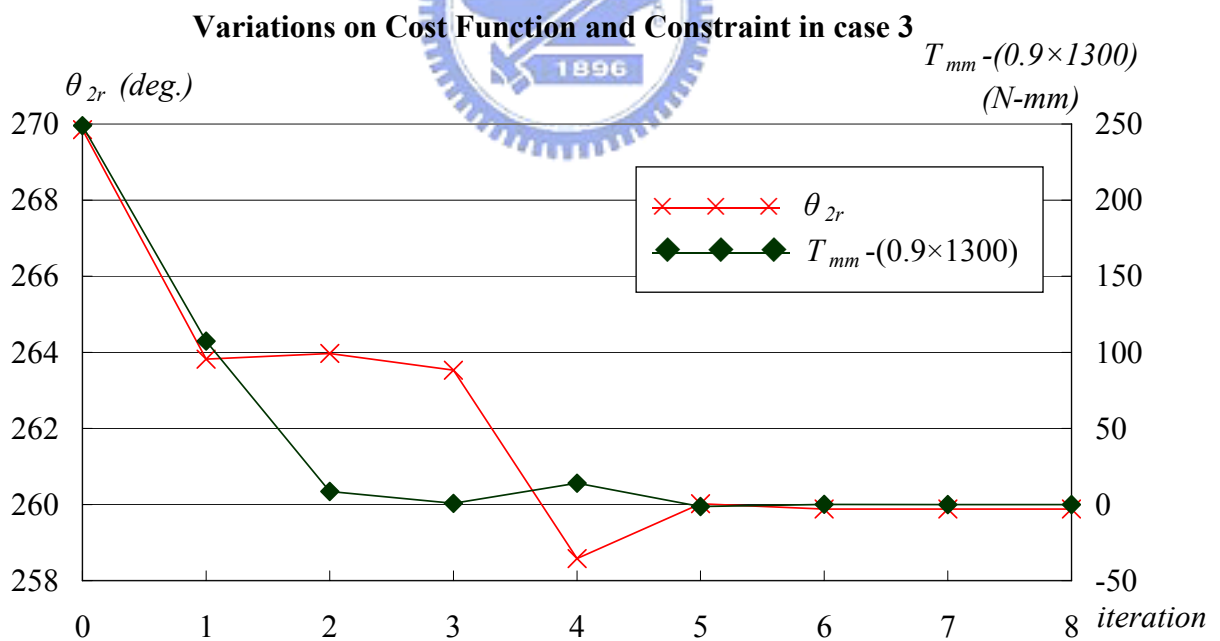
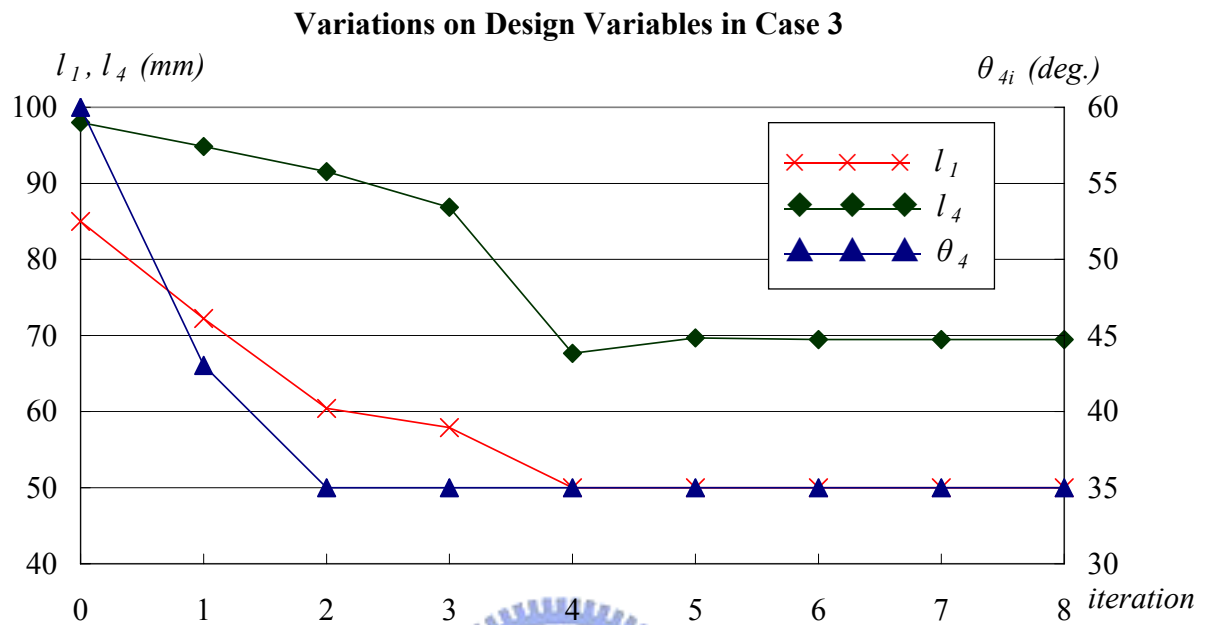


Fig.4.24 Variations on design variables, cost function and constraint in case 3

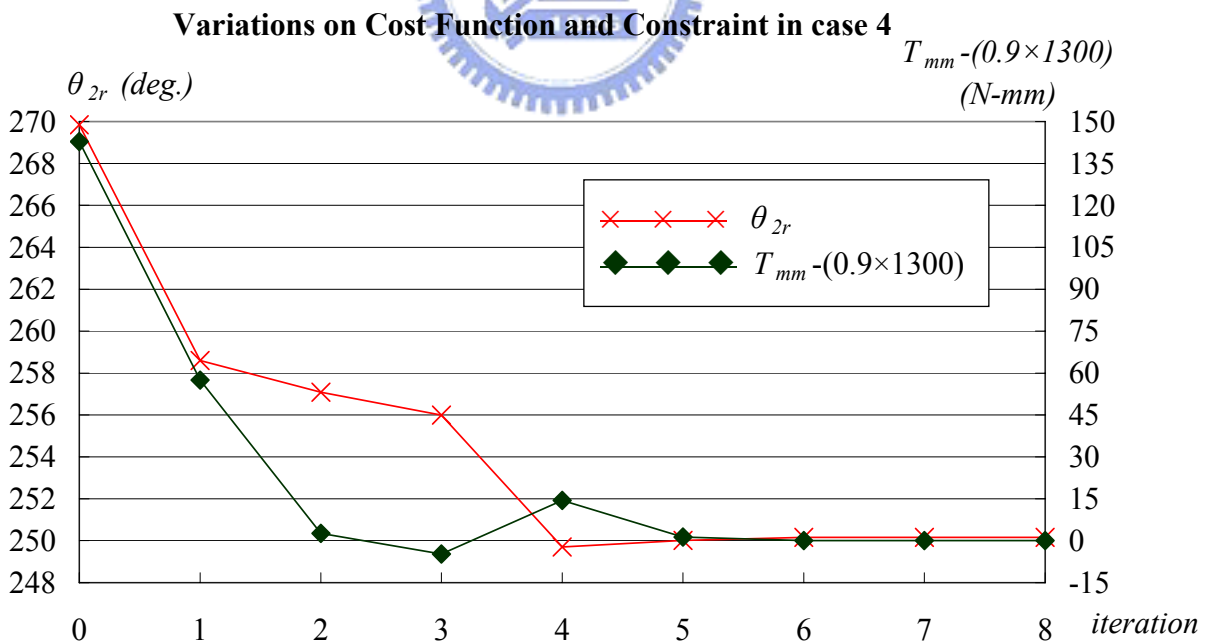
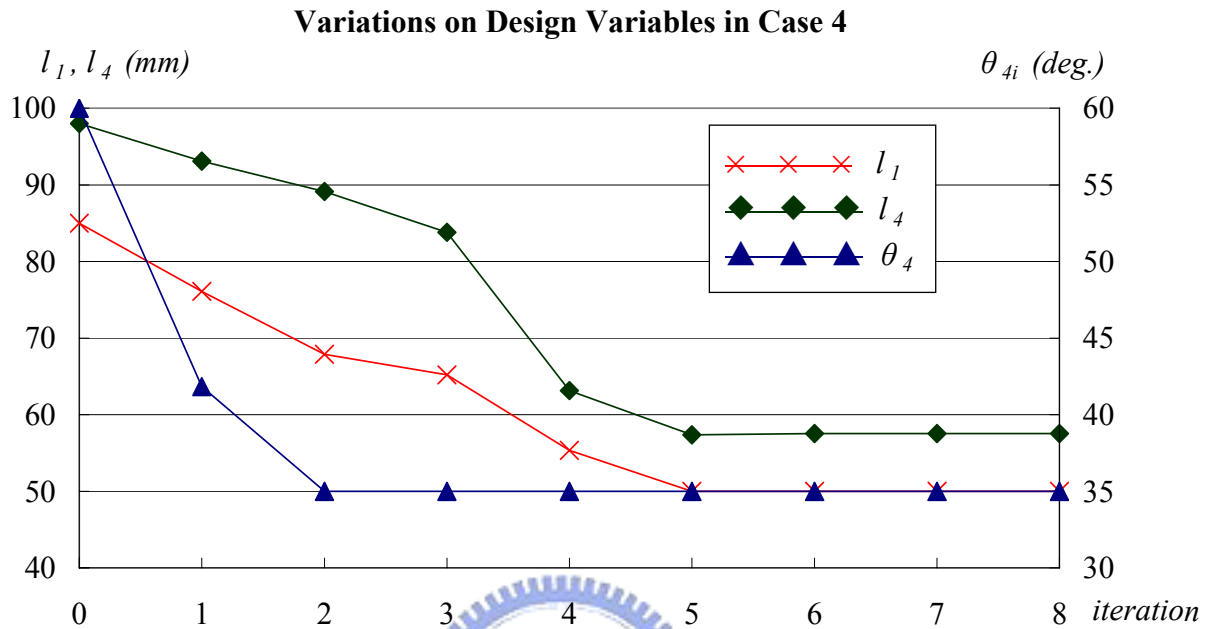


Fig.4.25 Variations on design variables, cost function and constraint in case 4

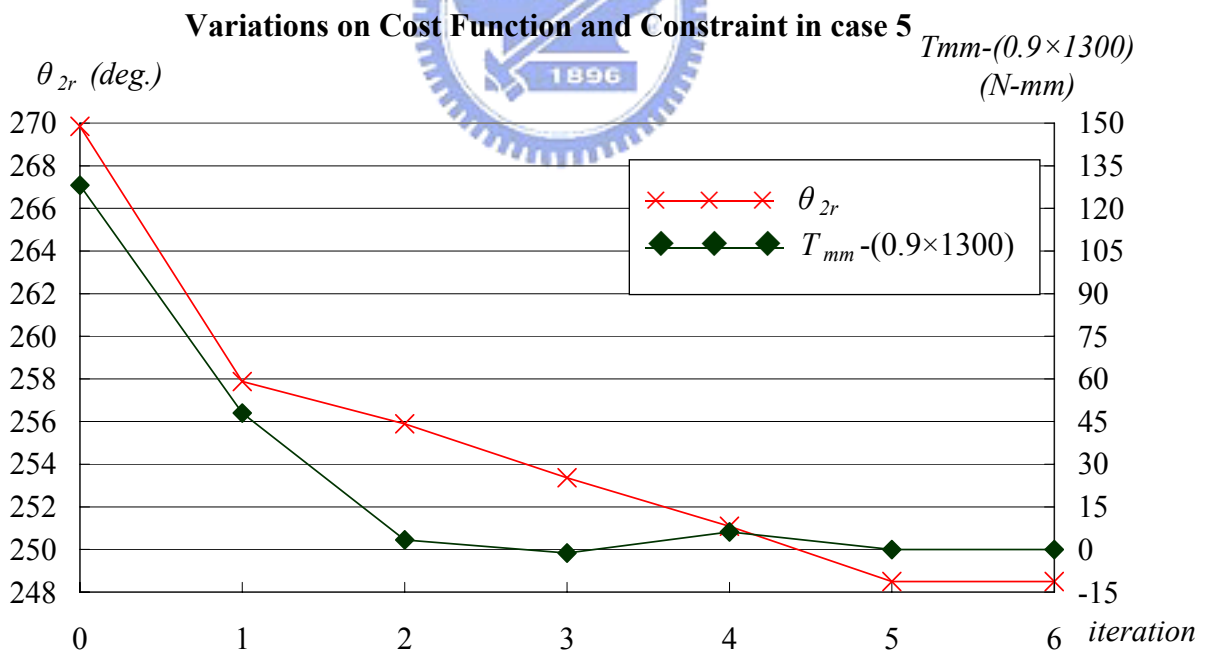
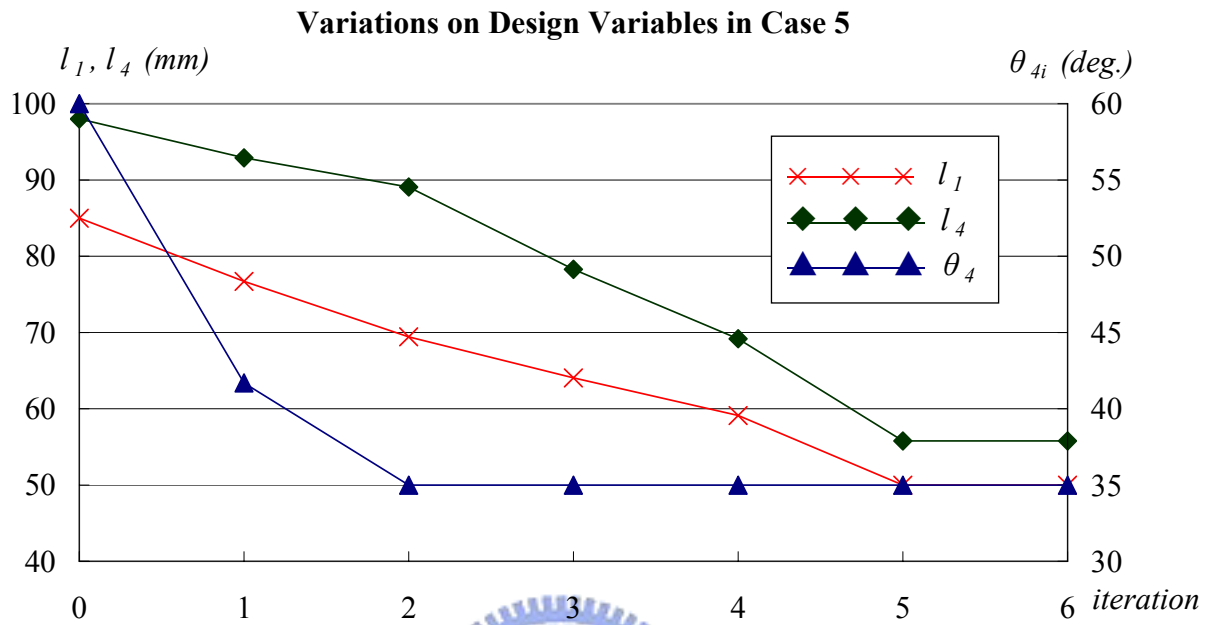


Fig.4.26 Variations on design variables, cost function and constraint in case 5

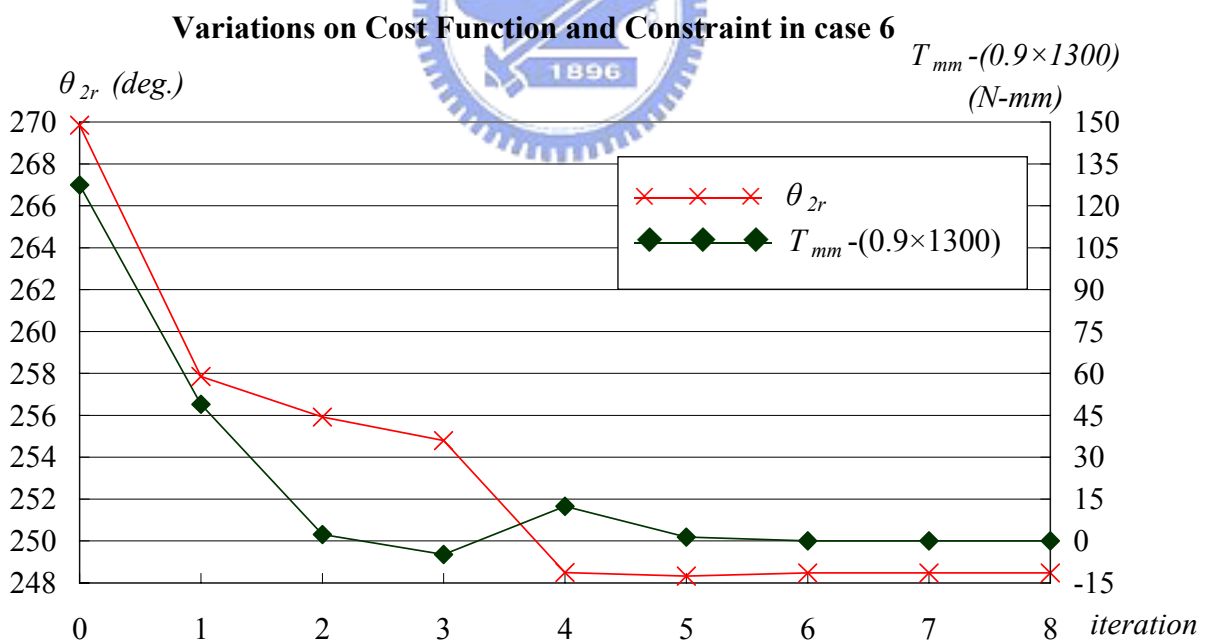
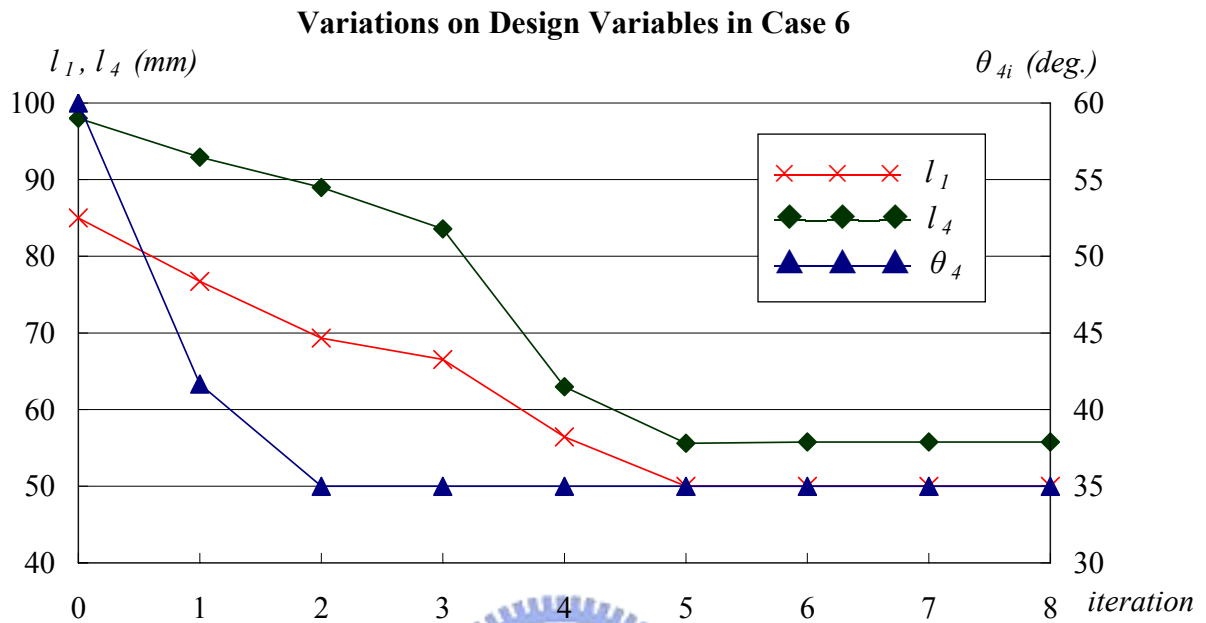


Fig.4.27 Variations on design variables, cost function and constraint in case 6

Table 4.10 Summary results for the cases in the present design

		Case 1	Case 2	Case 3	Case 4	Case 5	Case 6	
Optimization of mechanism	Optimization iteration	7	7	8	8	6	8	
	Objective θ_{2r} (deg.)	initial	269.848	269.848	269.848	269.848	269.848	269.848
		final	268.462	260.310	259.883	250.163	248.503	248.485
	Constraint T_{mm} -1170 (N-mm)	initial	362.370	263.550	248.940	142.850	128.140	127.450
		final	-0.002	-0.002	-0.037	-0.006	-0.002	-0.002
	l_1 (mm)	initial	85.000	85.000	85.000	85.000	85.000	85.000
		final	50.000	50.000	50.000	50.000	50.000	50.000
l_4 (mm)	initial	98.000	98.000	98.000	98.000	98.000	98.000	
	final	83.956	70.084	69.470	57.532	55.792	55.772	
θ_4 (deg)	initial	60.000	60.000	60.000	60.000	60.000	60.000	
	final	35.000	35.000	35.000	35.000	35.000	35.000	
FEA Checking	Max. Stress of Crank (MPa)	2.5×10^7	3.58×10^7	3.51×10^7	5.59×10^7	6.06×10^7	6.08×10^7	
	Min. Safety factor	20.2	14.0	14.3	9	8.3	8.28	
	Max. Stress of Coupler (MPa)	5.48×10^7	7.79×10^7	8.05×10^7	1.3×10^8	1.43×10^8	1.43×10^8	
	Min. Safety factor	9.18	6.45	6.24	3.88	3.53	3.53	
	Max. Stress of Bonding Arm (MPa)	6.77×10^7	1.01×10^8	1.03×10^8	1.57×10^8	1.63×10^8	1.65×10^8	
	Min. Safety factor	7.43	5.02	4.9	3.2	3.08	3.04	
End Time (seconds)		0.1128	0.1108	0.1108	0.1084	0.1080	0.1080	

Based on the results listed above, it is clear that case 6 is the best which satisfies the requirements in the present design.

4.7 Results of the Optimal Pick and Place Mechanism for Case 6

In this section, an advanced investigation on the mechanism and finite element analysis of case 6 is performed and a more detail simulation result is also shown. The optimal model is firstly shown in Fig.4.28, while the dynamic simulation results are shown in Table 4.11, and

Figs. 4.29 to 4.32

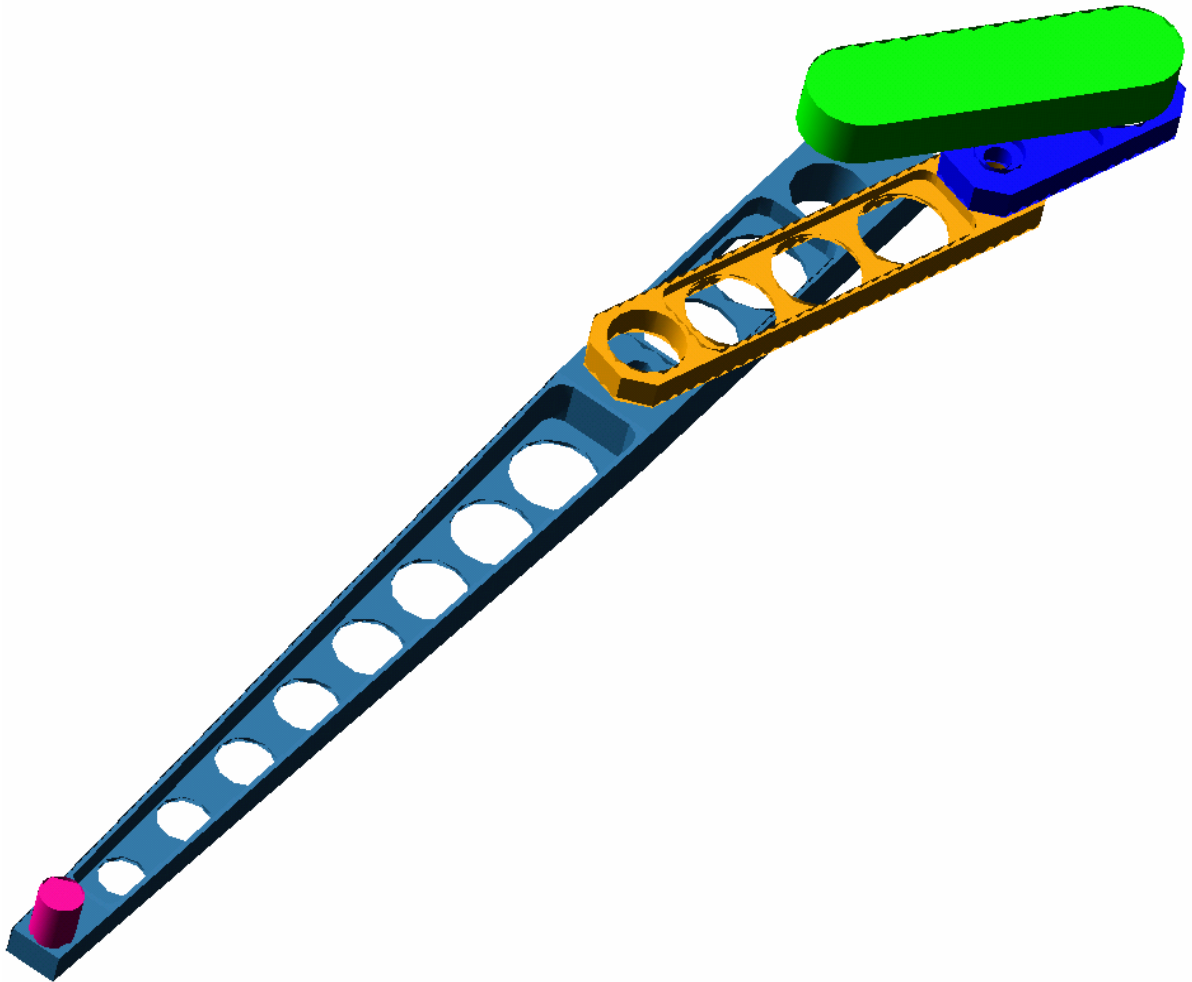


Fig.4.28 The optimal chip's pick and place mechanism in the present design (Case 6)

Table 4.11 Simulation results of the optimal chip's pick and place mechanism in the present design (Case 6) by applying computer software ADAMS

	Time (sec.)	Absolute Extreme Value
T_{mm}	0.0268	1170.001 (N-mm)
T_{sm}	0.0240	2646.613 (N-mm)
F_{sm}	0.0248	13.103 (N)

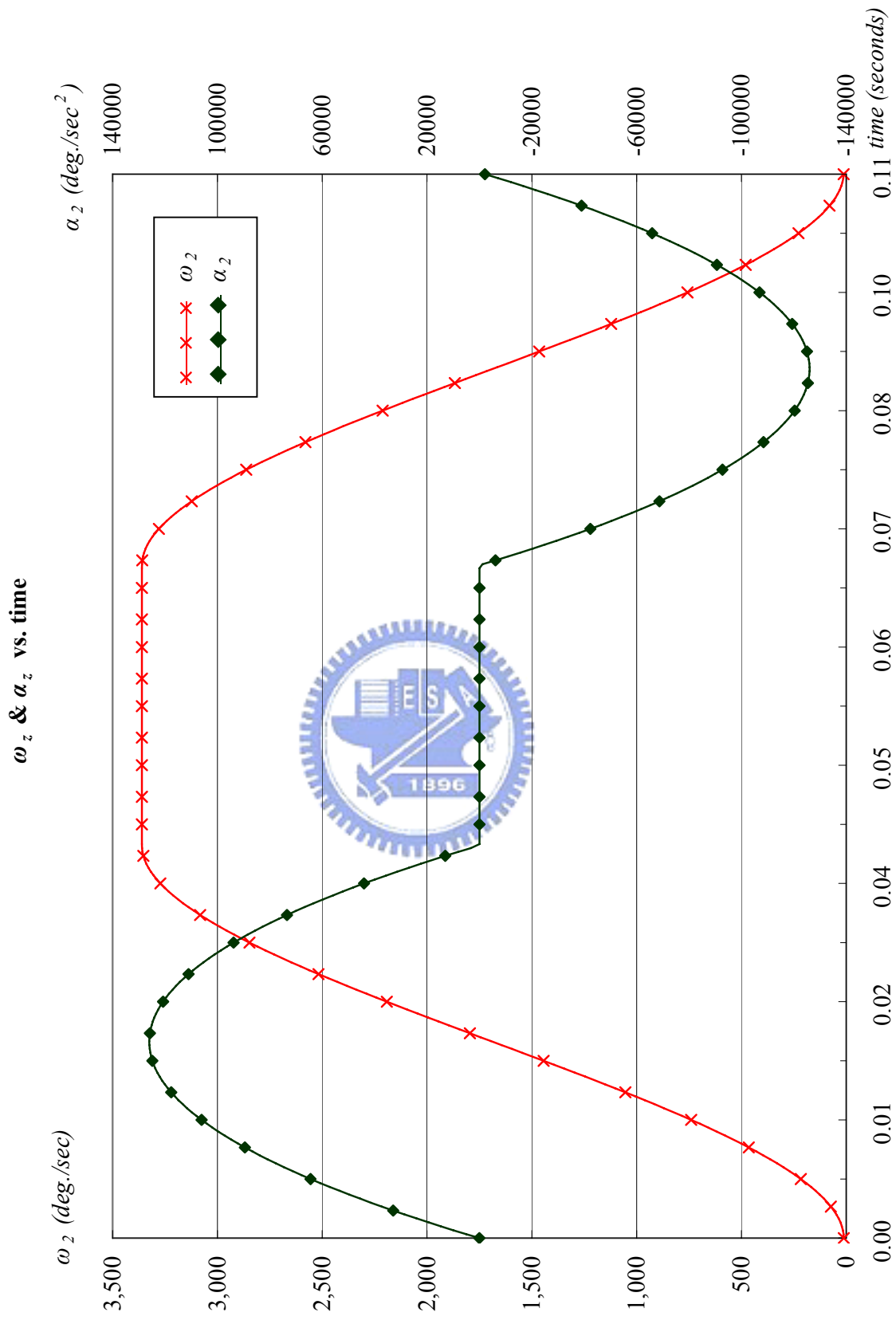


Fig.4.29 Angular velocity and angular acceleration of crank for the optimal chip's pick and place mechanism in the present design (Case 6)

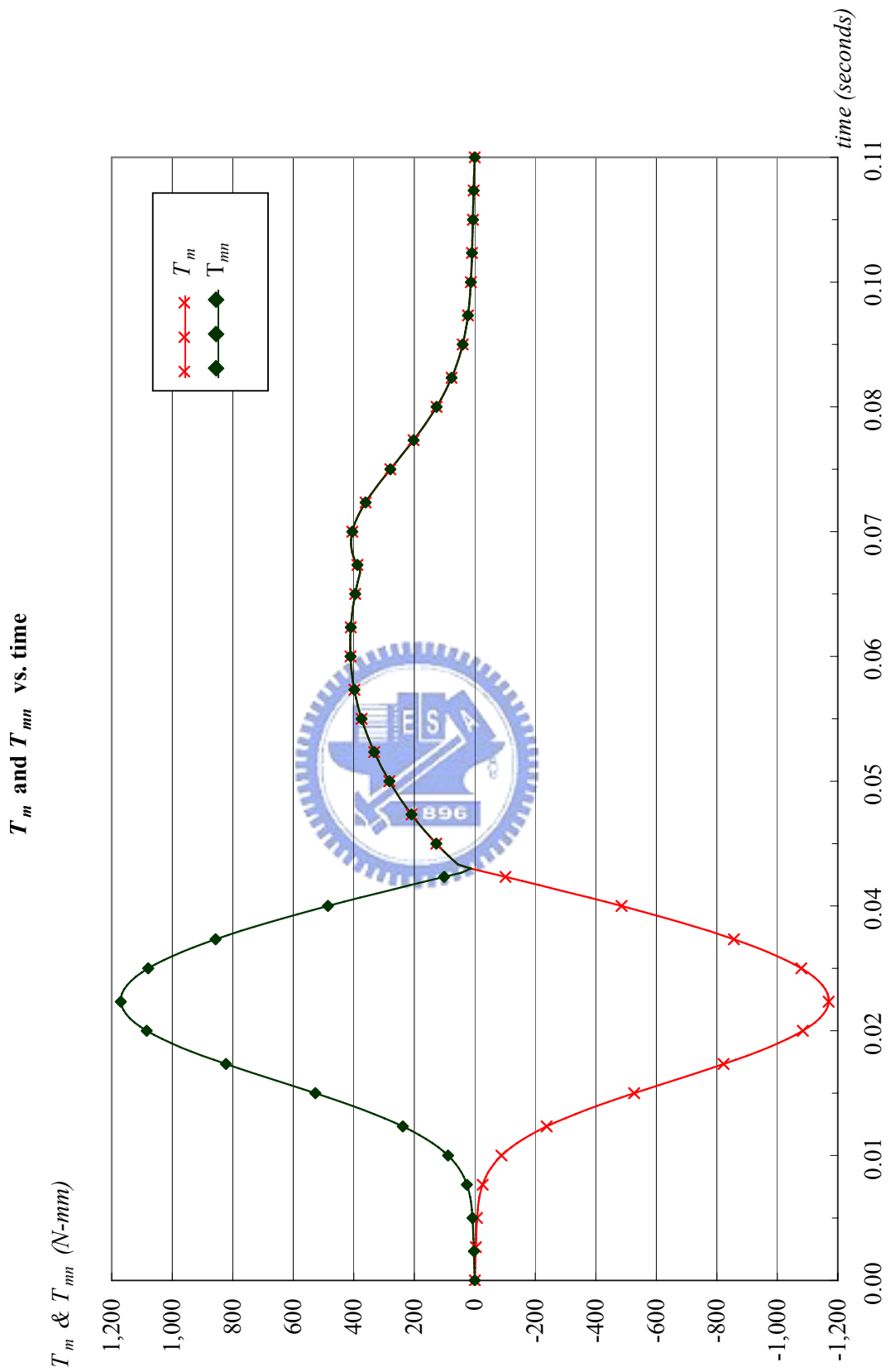


Fig.4.30 Torque driven by motor of the optimal chip's pick and place mechanism in the present design (Case 6)

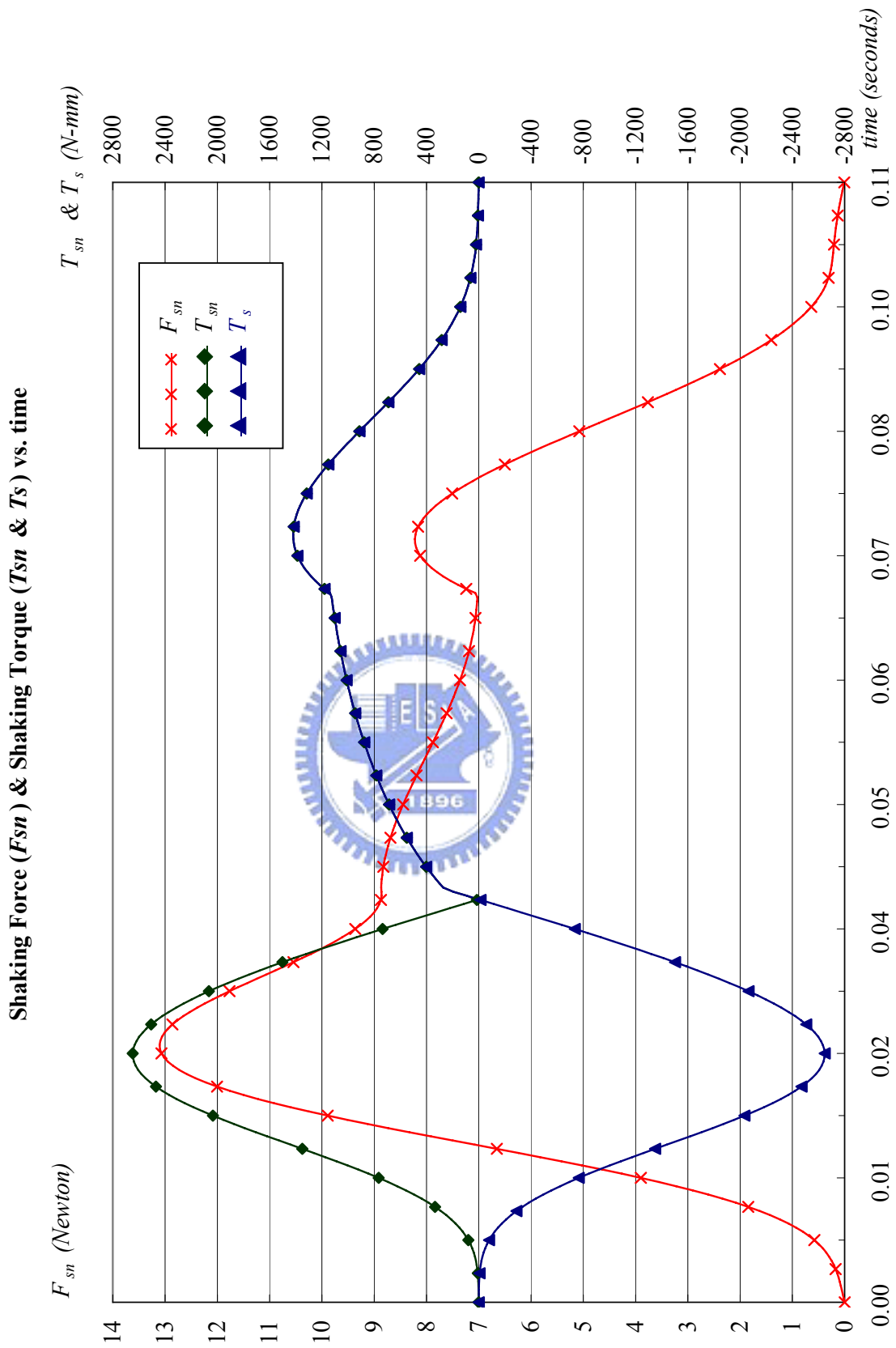


Fig.4.31 Shaking force and shaking torque for the optimal chip's pick and place mechanism in the present design (Case 6)

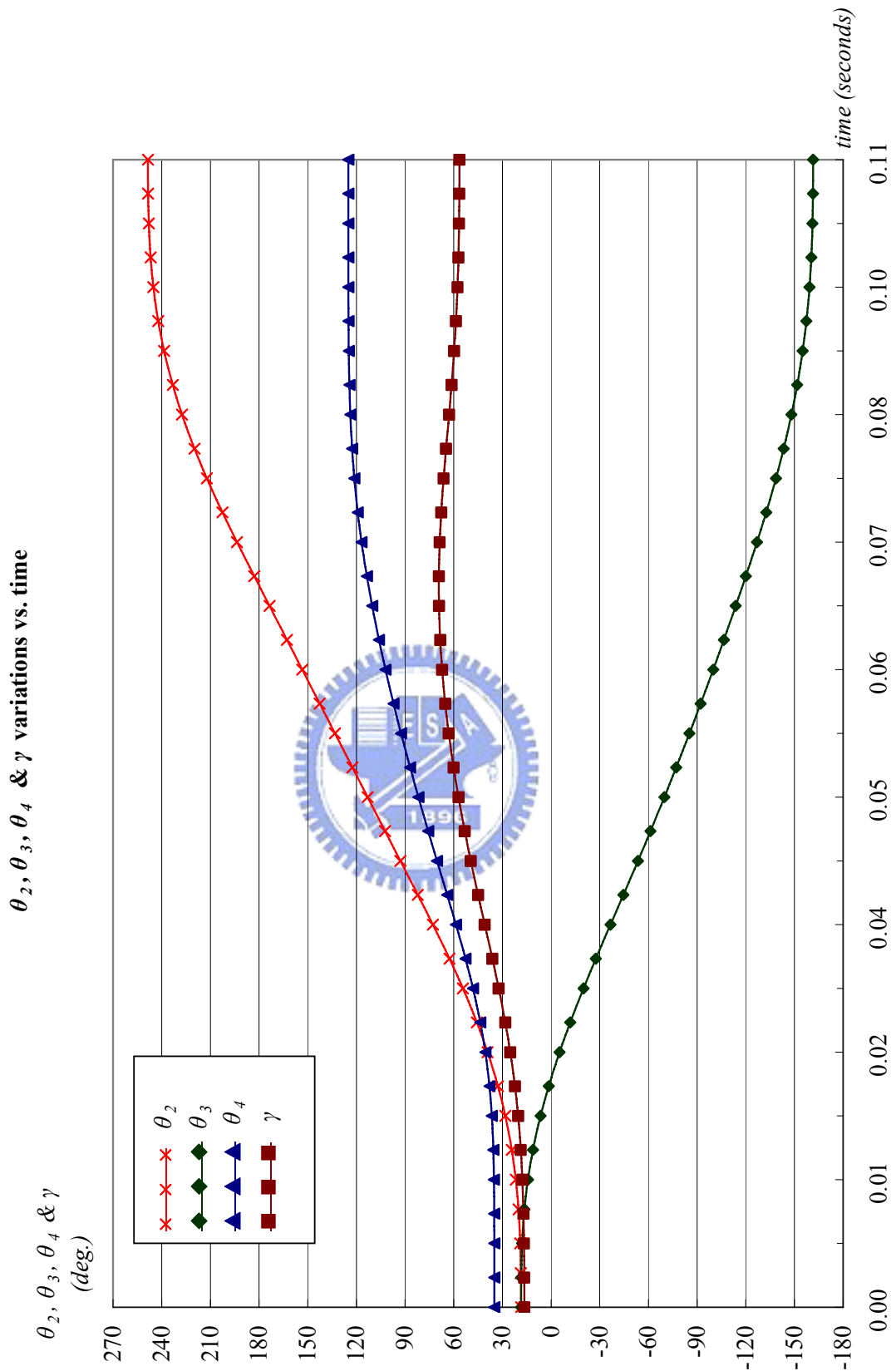
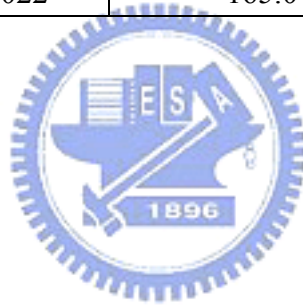


Fig.4.32 Angular ($\theta_2, \theta_3, \theta_4, \gamma$) variations of the optimal chip's pick and place mechanism in the present design (Case 6)

Table 4.12 and Fig.4.33 show the stress distributions of FEA simulation results by applying computer software Nastran, while Figs. 4.34 to 4.36 show the maximum stresses occur on crank, coupler and bonding arm of the optimal pick and place mechanism for Case 6.

Table 4.12 FEA results of the optimal pick and place mechanism in the present design (Case 6)

	Time (sec.)	Max. Stress (MPa)	Min. Safety Factor
Crank	0.022	60.7	8.28
Coupler	0.022	143.0	3.53
Bonding Arm	0.022	165.0	3.04



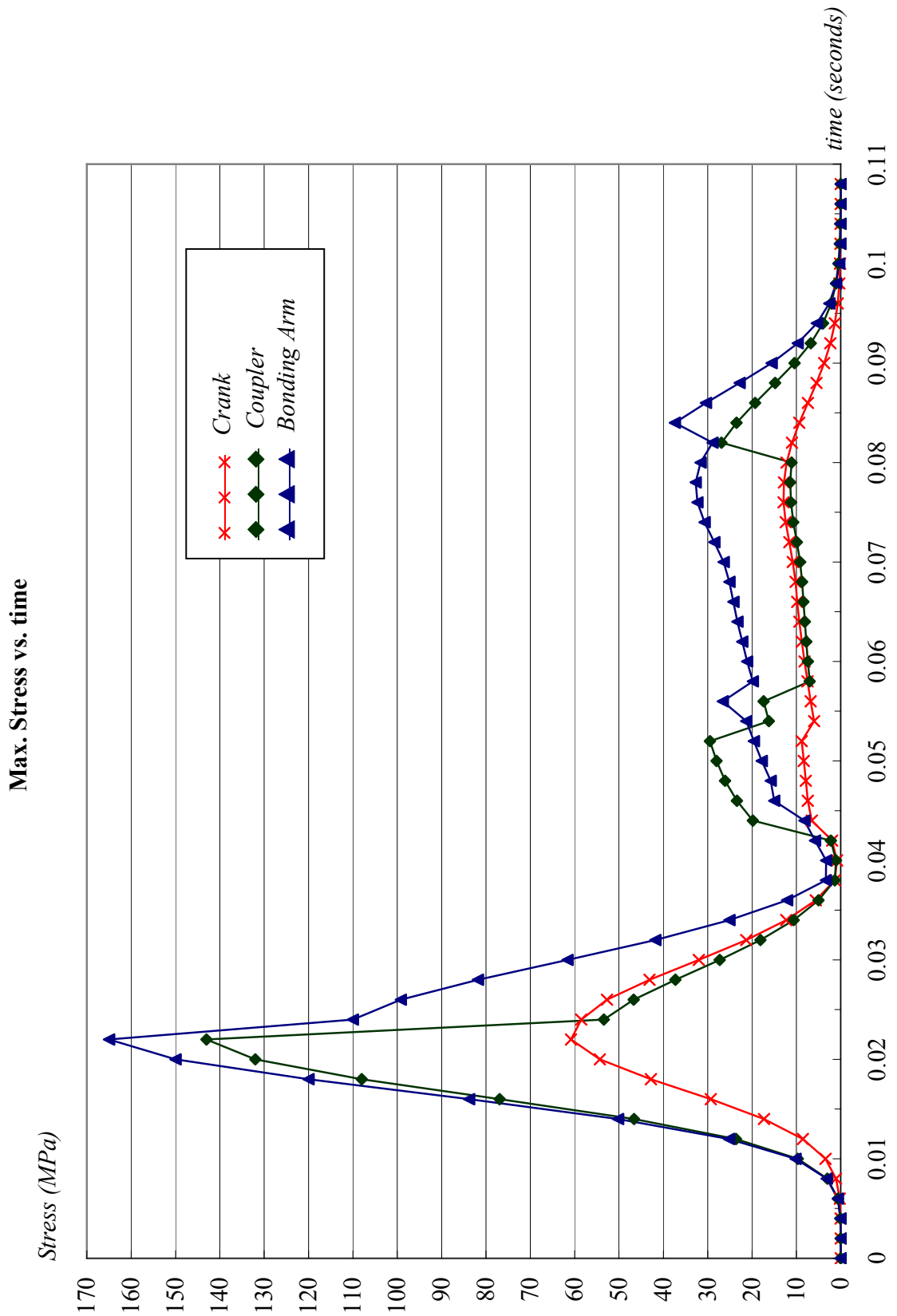


Fig.4.33 Maximum stress of the optimal chip's pick and place mechanism in the present design (Case 6)

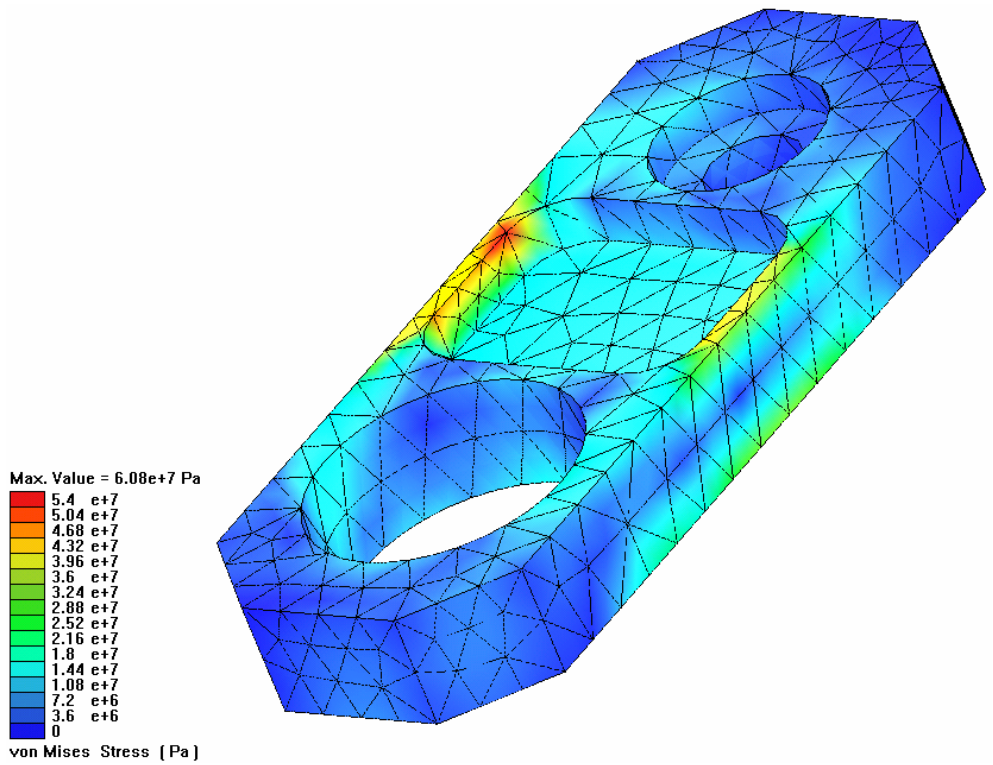


Fig.4.34 Stress distributions for the crank of the optimal chip's pick and place mechanism in the present design (Case 6) at 0.022 seconds

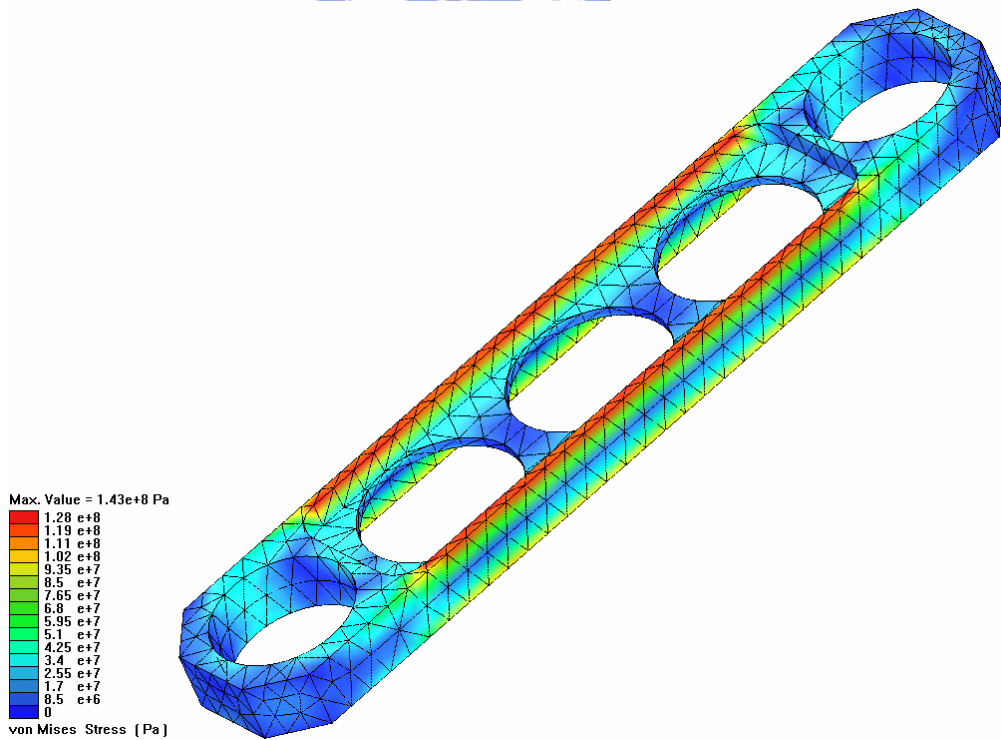


Fig.4.35 Stress distributions for the coupler of the optimal chip's pick and place mechanism in the present design (Case 6) at 0.022 seconds

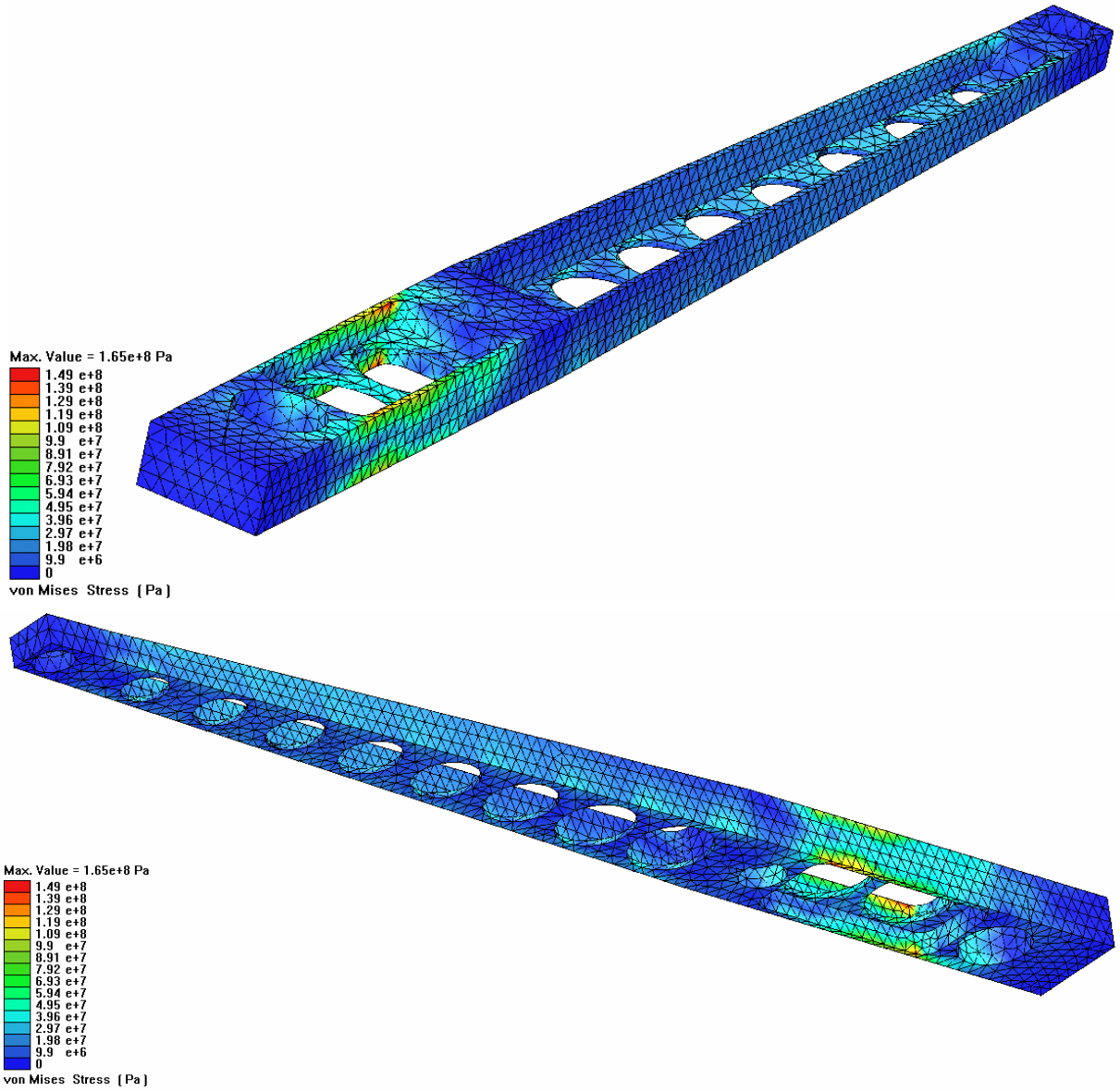


Fig.4.36 Stress distributions for the bonding arm of the optimal chip's pick and place mechanism in the present design - bonding arm (Case 6) at 0.022 seconds

Chapter 5 Conclusions and Future Work

In this thesis, a crank-rocker mechanism is designed and used as a chip's pick and place mechanism. Computer software, ADAMS, is used to analyze the dynamic performance, and to find an optimized model for the chip's pick and place mechanism. Computer software Nastran is used to perform the FEA analysis in order to find the stress distribution in each bar and to calculate the safety factors. An optimal design for the pick and place mechanism which satisfy the engineering requirements is found in this study.

5.1 Conclusions

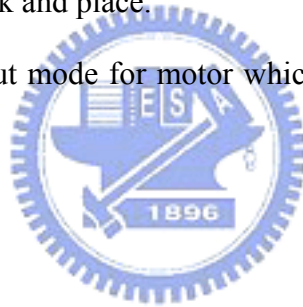
Based on previous investigation and analysis, some conclusions have been made as follows:

1. The length of base (l_1) of the four-bar linkage is the most sensitive design variable to the maximum torque driven by motor and crank rotation angle, while the effects of another two main design variables (l_4 and θ_4) are small.
2. The mass of VCM affects the performance of motor; once the mass of VCM is reduced, the performance of motor can be promoted, and a shorter time for pick and place action can also be achieved.
3. By the constraints of the present design as listed in Chapter 3, the optimal pick and place mechanism can achieve a half-cycle time of 0.108 seconds, and the maximum torque driven by the motor can be ensured in the allowable range (90% of the rated torque of motor).
4. The input mode of motor is set to symmetry for the pick-to-place and place-to-pick actions, therefore, all the results obtained are also symmetric, this causes the analysis in the present research much simpler.

5.2 Future Works

In the present research, a crank-rocker mechanism is designed as a chip's pick and place mechanism. Although some analyses have been carried out, nevertheless some works can also be investigated in the future are listed as follow:

1. The effects of vibration on the crank-rocker mechanism can be considered into the design process, and a better chip's pick and place mechanism can be found.
2. By the reduction of the mass of VCM, both the maximum torque driven by motor and the time of pick and place action can be reduced.
3. A crank-rocker mechanism which has a full-rotation action can be designed in order to carry out the action of pick and place.
4. Designing an optimal input mode for motor which may decrease the cycle time of pick and place action.



Reference

- [1] Esec, SA (Cham, CH), “Method and Apparatus for Loading Metal Leadframes with Electronic Components”, US Patent 5,163,222, Nov.17, 1992.
- [2] Esec, SA (Cham, CH), “Semiconductor mounting apparatus with a chip gripper travelling back and forth”, US Patent 6,185,815, Feb. 13, 2001.
- [3] ESEC, SA (Cham, CH), “Linear Guide with an Air Bearing Having Provision for Heating a Support Element of the Linear Guide to Maintain Fluid Gap”, US Patent 6,571,461, Jun. 3, 2003.
- [4] ASM Assembly Automation Limited (Kwai Chung, HK), “High speed pick and place apparatus”, US Patent 6758113, Jul. 6, 2004.
- [5] Alphasem AG (Andhauserstrasse, CH), “Method and device for receiving, orientating and assembling of components”, US Patent 6,171,049, Jan. 9, 2001.
- [6] Samsung Electronics Co., Ltd. (Suwon, KR), “Die bonding apparatus with a revolving pick-up tool”, US Patent 5,765,277, Jun. 16, 1998.
- [7] Industrial Technology Research Intitute. (Hsinchu, TW), “Device for fast taking out and putting in”, US Patent 6,505,528, Jan. 14, 2003.
- [8] Matsushita Electric Industrial Co., Ltd. (Osaka, JP), “Industrial use robot with horizontal multiple articulated arms with means to minimize or eliminate interference among driving portions”, US Patent 5,151,007, Sep. 29, 1992.

- [9] Kawasaki Jukogyo Kabushiki Kaisha (Hyogo, JP), “Robot”, US Patent 6,748,819, Jun. 15, 2004.
- [10] The USA as represented by the Secretary of the Navy (Washington, DC), “Scara type robot with counterbalanced arms”, US Patent 6,354,167, Mar. 12, 2002.
- [11] J. Rastegar and L. Yuan, A Systematic Method for Kinematics Synthesis of High-Speed Mechanisms with Optimally Integrated Smart Materials, Transactions of the ASME, Vol. 124, pp. 14-20, Mar. 2002.
- [12] Jon C Kieffer and Aidan J Cahill, Fast Pick and Place at Robot Singularities, IEEE International Conference on Robotics and Automation, pp. 2236-2241, 1995.
- [13] Jacques Coderre (Universal Instruments Corporation) and Robert Peter (Alphasem), Step-by-Step Die Placement, White Papers and Technical Reports of Universal Instruments Corporation, 2001.
- [14] Chen-Ming Yang and Ting-Yu Chen, Multidisciplinary Design Optimization of Structures and Mechanism, Master Thesis of National ChungHsing University (in Chinese), 1999.
- [15] Robert L. Norton, Design of Machinery—An introduction to the Synthesis and Analysis of Mechanisms of Machines, 2nd ed., McGraw Hill, New York, 1999.
- [16] Joseph E. Shigley and Charles R. Mischke, Mechanical Engineering Design, 6th ed., McGraw Hill, New York, 2001.

- [17] Dale O. Anderson, Safety Factor, Lecture note, Louisiana Tech University, 2001.
- [18] Panasonic, Minas A Series Digital AC Servo Motor and Amplifier Catalog, January 2001.
- [19] NTN, Ball and Roller Bearings Guidelines, Catalog number 2202-VII/E, 2002.
- [20] MISUMI, Precision Pivot Pins Catalog, 2004.
- [21] Origin, Angular Contact Bearing Catalog, (in Japanese), 2000.
- [22] NSK Corporation, Angular Contact Bearing Catalog, 2004.
- [23] 和椿事業股份有限公司, 個人電腦用馬達數值控制卡 MC8040A/MC8020A 操作說明書, 1996.
- [24] Aluminum property, Material Property Data, available on the webpage <http://www.matweb.com/search/SpecificMaterial.asp?bassnum=MA7075T6>, last visited on May 9, 2005.
- [25] 黃錦煌、鍾光鴻, MSC. Visual Nastran Desktop 機構模擬, 全華科技圖書股份有限公司, 台北, 2002.10.
- [26] 傅增棣, 電腦輔助工程設計—ADAMS 基楚應用手冊, 高立圖書有限公司, 台北, 2004.10.